UNIVERSITY OF CALIFORNIA SAN DIEGO

Cell Membrane-Coated Nanoparticles for Immune Modulation

A dissertation submitted in partial satisfaction of the
requirements for the degree
Doctor of Philosophy

in

NanoEngineering

by

Ashley Kroll

Committee in charge:

Professor Liangfang Zhang, Chair
Professor Jack Bui
Professor Shaochen Chen
Professor Yi Chen
Professor Dong-Er Zhang

2019

The Dissertation of Ashley Kroll is approved, and it is acceptable in quality and form for publication on microfilm and electronically:

_____

_____

_____

_____

_____

Chair

University of California San Diego

2019

DEDICATION

This dissertation is dedicated to my family: Garth Kroll, Linda Kroll, Austin Kroll, Lauren Kroll-Wheeler, Shawn Kroll-Wheeler, and Cassie Kroll-Wheeler. Their constant support and check-ins kept me sane throughout my entire academic career.

This dissertation is also dedicated to my partner, Rachel, who has been incredibly supportive with many late-night pick-ups and interrupted weekends, and has listened to my practice presentations so often she could probably defend her own Ph.D. I am forever grateful.

EPIGRAPH

"Everybody is a genius. But if you judge a fish by its ability to climb a tree, it will live its whole life believing that it is stupid"

Albert Einstein

TABLE OF CONTENTS

LIST OF FIGURES

ACKNOWLEDGEMENTS

First and foremost, I would like to thank my PhD advisor, Professor Liangfang Zhang for his guidance and support in every step of my graduate journey. His constant belief in my success has led to many amazing opportunities that have greatly enhanced my life and career. I will always strive to emulate his work ethic, kindness, integrity, and vision.

I would also like to thank my mentor, Ronnie Fang, to whom I owe much of my success. Working with him has undoubtedly had the biggest impact on my development as a scientist, and I will always be inspired by his methodology and mentorship practices. I am also lucky enough to call him my close friend, and his friendship has brought much thought and laughter into my life.

I also thank my closest friends, Yao Jiang, XiaoLi Wei, and Jiarong Zhou, for always brightening my days and sharing both triumphs and struggles. I especially want to thank Jiarong Zhou for being an excellent scientific partner and for doing all the math.

I am also thankful to have had two labmates, Diana Dehaini and Yue Zhang, enter the lab at the same time as me, and I was lucky to have their company throughout classes, exams, and so many life changes together. In addition, I want to acknowledge all of the wonderful labmates I've encountered during my time in the Zhang lab, including Joon Ho Park, Maya Holay. Oliver Zhang, Joe Chen, Hua Gong, Dr. Weiwei Gao, and many others, who are always expanding my horizons and helping me think outside the box. Not to be forgotten, I want to acknowledge

the alumni of our lab, from whom I have gained much wisdom and guidance: Kun Thamphiwatana, Brian Luk, Keep Angsantikul, Danni Ran, Man Ying, Jie Gao, and Fei Wang. Finally, I want to thank the undergraduate lab members for putting up with me and giving me a valuable opportunity to teach: Matthew Yu, Nishta Krishnan, Sanam Chekuri, John Ventura, Crystal Xiao, and Igor Landa.

In addition, I would like to thank the National Science Foundation, the National Institute of Health, and the UCSD Nanoengineering Department for providing funding for my graduate studies. I would also like to thank the Siebel Foundation and the ARCS Foundation for recognizing my work and granting me very generous financial awards to supplement my studies throughout my graduate school career.

Last, but not least, I would like to thank UC San Diego. In particular, the NanoEngineering department faculty and staff, as well as the Graduate Division staff, has consistently supported me and has been so helpful and friendly

Chapter 1, in full, is a reprint of the material as it appears in *Advanced Biosystems*, 2019, Ashley Kroll, Yao Jiang, Jiarong Zhou, Maya Holay, Ronnie Fang and Liangfang Zhang. The dissertation author was the primary author of this paper.

Chapter 2, in full, is a reprint of the material as it appears in *Advanced Materials*, 2017, Ashley Kroll, Ronnie Fang, Yao Jiang, Jiarong Zhou, Xiaoli Wei, Chun Lai Yu, Jie Gao, Brian Luk, Diana Dehaini, Weiwei Gao and Liangfang Zhang. The dissertation author was a primary investigator and author of this

material.

Chapter 3, in full, is a reprint of the material as it appears in *Advanced Functional Materials*, 2016, Fei Wang, Ronnie Fang, Brian Luk, Che-Ming Hu, Soracha Thamphiwatana, Diana Dehaini, Pavimol Angsantikul, Ashley Kroll, Zhiqing Pang, Weiwei Gao, Weiyue Lu and Liangfang Zhang, and *Advanced Materials*, 2017, Xiaoli Wei, Jie Gao, Fei Wang, Man Ying, Pavimol Angsantikul, Ashley Kroll, Jiarong Zhou, Weiwei Gao, Weiyue Lu, Ronnie Fang and Liangfang Zhang. The dissertation author was a major contributor and co-author of these papers.

Chapter 4, in full, is a reprint of the material as it appears in *Biomaterials*, 2016, Xiaoli Wei, Jie Gao, Ronnie Fang, Brian Luk, Ashley Kroll, Diana Dehaini, Jiarong Zhou, Hyeon Woo Kim, Weiwei Gao, Weiyue Lu and Liangfang Zhang. The dissertation author was a major contributor and co-author of these papers.

VITA

2014 B.S. in Nanoengineering, University of California San Diego, USA

2016 M.S. in Nanoengineering, University of California San Diego, USA

2019 Ph.D. in Nanoengineering, University of California San Diego, USA

PUBLICATIONS

1. Kroll, A.; Jiang, Y.; Zhou, J.; Holay, M.; Fang, R.; Zhang, L. (2019). "Biomimetic nanoparticle vaccines for cancer therapy". *Advanced Biosystems 3*, 1800219.

2. Fang, R.; Kroll, A.; Gao, W.; Zhang, L. (2018). "Cell Membrane Coating Nanotechnology". *Advanced Materials*, 1706759.

3. Wei, X.; Ying, M.; Dehaini, D.; Su, Y.; Kroll, A.; Zhou, J.; Gao, W.; Fang, R.; Chien, S.; Zhang, L. (2018). "Nanoparticle functionalization with platelet membrane enables multi-factored biological targeting and detection of atherosclerosis". *ACS Nano, 12*, 109-116.

4. Kroll, A.; Fang, R.; Jiang, Y.; Zhou, J.; Wei, X.; Yu, C-L.; Gao, J.; Luk, B.; Dehaini, D.; Gao, W.; Zhang, L. (2017). "Nanoparticulate delivery of cancer cell membrane elicits multi-antigenic antitumor immunity". *Advanced Materials*, *29*, 1703969.
   Highlighted: *Science Translational Medicine* 2017, *9(417)*, eaar2438.

5. Wei, X.; Gao, J.; Wang, F.; Ying, M.; Angsantikul, P.; Kroll, A.; Zhou, J.; Gao, W.; Lu, W.; Fang, R.; Zhang, L. (2017). "*In situ* capture of bacterial toxins for antivirulence vaccination". *Advanced Materials*, *29*, 1701644.

6. Dehaini, D.; Wei, X.; Fang, R.; Masson, S.; Angsantikul, P.; Luk, B.; Zhang, Y.; Ying, M.; Jiang, Y.; Kroll, A.; Gao, W.; Zhang, L. (2017). "Erythrocyte-platelet hybrid membrane coating for enhanced nanoparticle functionalization". *Advanced Materials, 29*, 1606209.

7. Kroll, A.; Fang, R.; Zhang, L. (2017) "Biointerfacing and applications of cell membrane-coated nanoparticles". *Bioconjugate Chemistry*, *28*, 23-32.

8. Wei, X.; Gao, J.; Fang, R.; Luk, B.; Kroll, A.; Dehaini, D.; Zhou, J.; Kim, H.W.; Gao, W.; Lu, W.; Zhang, L. (2016). "Nanoparticles camouflaged in

platelet membrane coating as an antibody decoy for the treatment of immune thrombocytopenia". *Biomaterials*, *111*¸116-123.

9. Dehaini, D.; Fang, R.; Luk, B.; Pang, Z.; Hu, C-M; Kroll, A.; Yu, C. L.; Gao, W.; Zhang, L. (2016). "Ultra-small lipid polymer hybrid nanoparticle for tumor-penetrating drug delivery". *Nanoscale*, *8,* 14411-14419.

10. Wang, F.; Fang, R.; Luk, B.; Hu, C-M.; Thamphiwatana, S.; Dehaini, D.; Angsantikul, P.; Kroll, A.; Pang, Z.; Gao, W.; Lu, W.; Zhang, L. (2016) "Nanoparticle-based anti-virulence vaccine for the management of methicillin-resistant Staphylococcus aureus skin infection". *Advanced Functional Materials*, *26*, 1628-1635.

11. Fang, R.; Kroll, A.; Zhang, L. (2015). "Nanoparticle-based manipulation of antigen-presenting cells for cancer immunotherapy". *Small*, *11*(41), 5483-5496.

12. Hu, C-M.; Fang, R.; Wang, K-C.; Luk, B.; Thamphiwatana, S.; Dehaini, D.; Nguyen, P.; Angsantikul, P.; Wen, C.; Kroll, A.; Carpenter, C.; Ramesh, M.; Qu, V.; Patel, S.; Zhu, J.; Shi, W.; Hofman, F.; Chen, T.; Gao, W.; Zhang, K.; Chien, S.; Zhang, L. (2015). "Nanoparticle biointerfacing by human platelet membrane cloaking". *Nature*, *526*(7571), 118-121.

13. Wong, Y.L.; Anzola, J.V.; Davis, R.L.; Yoon, M.; Motamedi, A.; Kroll, A.; Seo, J.P.; Hsia, J.E.; Kim, S.K.; Mitchell, J.W.; Mitchell, B.J.; Desai, A.; Gahman, T.C.; Shiau, A.K.; Oegema, K. (2015). "Reversible centriole depletion with an inhibitor of Polo-like kinase 4". *Science*, *348*(6239), 1155-1160.

ABSTRACT OF THE DISSERTATION

Cell Membrane-Coated Nanoparticles for Immune Modulation

by

Ashley Kroll

Doctor of Philosophy in NanoEngineering

University of California San Diego, 2019

Professor Liangfang Zhang, Chair

Nanotechnology is an exciting scientific area that is changing the way we design and administer medicines. One avenue in which nanomedicine can have a large impact is through immune modulation and "nano-immunoengineering". Nanoparticle size, design freedoms, and unique cell-particle interactions can be taken advantage of to influence the immune system in new and efficacious ways.

This dissertation will demonstrate how cell membrane coating can be merged with nanoparticle design to facilitate immune modulation for the improvement of a variety of pathological conditions. The rationale for cell membrane coating and the use of nanoparticles in immune modulation will be discussed in the first chapter of the dissertation.

The second portion of the dissertation will focus on the design of cancer cell membrane-coated nanoparticles for anticancer vaccination. The nanovaccine is designed to include multi-antigenic cancer cell membranes wrapped around an immune-stimulating nanoparticle core. The codelivery of both components to the lymphatic system then directs the formation of a strong and specific anticancer immunity. The third portion of the dissertation will concentrate on the development of erythrocyte membrane-coated nanoparticles for antivirulence vaccination. Membrane-disrupting pore-forming toxins naturally embed into the red blood cell membrane coating of the nanoparticles. The nanoparticle-bound toxins are then safely delivered to immune cells for antigenic processing, driving the generation of potent anti-toxin antibodies and immunity. Finally, the fourth section of this dissertation will focus on the use of platelet membrane-coated "nanosponges" as a therapy for clearing autoantibodies. The platelet membrane coating on the nanoparticle accurately mimics the surface of a real platelet to enable the absorption of anti-platelet antibodies. The bound antibodies are then rendered harmless to real platelets and are cleared in a nanoparticle form, ultimately reducing autoimmune disease symptoms.

This dissertation will serve as an example of rationally engineering cell membrane-coated nanoparticles to enhance the ability of the immune system to resolve different immunological challenges. By harnessing these tools, cell membrane-coated nanoparticles can have a great impact in the field of immunotherapy, and have much potential to be expanded upon for new therapeutic and prophylactic modalities.

Chapter 1

Introduction

1.1 Introduction

Our immune system is a complex network of cells, proteins, and physical barriers that work together to keep the human body free from disease. When mobilized correctly, it has the ability to seek out and eliminate foreign invaders with exquisite specificity. Malfunctioning or underperforming immunity is often the root cause of many disease states. For example, an overactive immune system can result in autoimmunity, which is characterized by proinflammatory states and leads to the destruction of healthy tissue [1, 2]. On the other hand, an underactive immune system can lead to enhanced susceptibility to infection, which is becoming increasingly dangerous given the rise of antibiotic resistance [3]. With regards to tumorigenesis, it has been shown that the immune system is integral in helping to prevent the proliferation of malignant cells [4]. It is now known that for tumors to successfully grow, cancerous cells must generally go through a prolonged evolutionary process in order to develop mechanisms for immune evasion [5]. Tumors can manipulate the surrounding microenvironment to support growth and suppress host immune responses using cytokine and growth factor secretion [6], extracellular matrix restructuring [7], and cellular signaling [8, 9]. It is for this reason that an intense amount of research has been focused on leveraging the immune system to fight off cancer [10]. In general, cancer immunotherapies seek to train, augment, or supplement the body's own ability to eliminate malignant growths. There are numerous classes of immunotherapy, and they can act on

different stages of immunity, ranging from initial antigen presentation up to the final effector stages [11, 12]. Depending on the specific type of cancer being treated, early returns have thus far been promising, and a number of immunotherapies have proven to be highly potent in scenarios where the previous clinical standard of care had little effect [13-15].

Anticancer vaccination is a class of cancer immunotherapy that focuses largely on training the immune system to recognize and mount a response against tumors in an antigen-specific manner [12, 16]. Over the course of recent human history, vaccines have represented an attractive means of managing the spread of disease, as most are easy to administer and can promote the development of sterilizing immunity [17]. Particularly in the case infectious diseases, vaccination has proven to be highly effective, having likely helped to prevent millions of deaths as a result of large-scale prophylaxis campaigns [18]. Despite the favorable history of antibacterial and antiviral vaccines, anticancer vaccination unfortunately has not achieved the same level of success [19, 20]. Unlike with those against pathogens, there are additional hurdles that must be overcome in order for vaccines against tumors to be effective. One of the main challenges comes from the fact that most tumors are lowly immunogenic and originate from one's own healthy cells. As such, it is incredibly difficult for the immune system to correctly identify malignant tissue. Additionally, vaccines against established tumors must be administered therapeutically, requiring the need for formulations that are highly potent in addition to being tumor-specific. This has oftentimes necessitated the use of

complex strategies for immune system manipulation [19-21], many of which are lowly viable in a clinical setting given poor cost-to-benefit ratios. In 2010, the United States Food and Drug Administration approved the first and only therapeutic anticancer vaccine, sipuleucel-T [22]. This autologous cell-based therapy trains patient-derived immune cells against a common prostate cancer antigen before reinfusion of the cells back into the patient. The treatment has been shown to marginally increase patient survival time, but the complex logistics and high cost of manufacturing a personalized cell-based vaccine have limited its commercial viability.

To address the hurdles faced by traditional vaccination schemes against cancer, many researchers have turned toward nanotechnology to help guide the design of nanovaccines capable of producing potent, specific, and durable antitumor responses [23, 24]. Compared with traditional vaccines, those manufactured at the nanoscale have unique physical and material properties that make them better suited for immune manipulation. Through purposeful engineering, nanovaccines can be formulated with antigen and adjuvant payloads in a manner that maximizes immune responses through efficient delivery to specific cellular subsets. Ultimately, the goal is to leverage such platforms for the controlled programing of endogenous immunity to reverse tumor burden. In this review, we start by covering some basic background information regarding anticancer vaccines and the current state of traditional platforms. We then discuss developments in the field of anticancer nanovaccines, focusing on platforms for both nonspecific and

antigen-specific immune modulation. Finally, we introduce an emerging class of biomimetic nanoparticles based on cell membrane coating nanotechnology. This top-down strategy directly leverages nature's own design principles as a means of fabricating multifunctional and multiantigenic nanosystems, which have the potential to play an important role in the future of anticancer vaccination.

1.2 Background on Anticancer Vaccination

1.2.1 Cancer Immunology and Immunotherapy

Cancer is generally characterized by an accumulation of mutations that allows for uncontrolled cell proliferation. As tumors grow, they are in a constant battle with the immune system and must evolve mechanisms for escape over time [5]. Due to the random nature of the mutations that lead to malignancy, phenotypes can vary greatly among different cancers, as well as among cells within the same tumor. This heterogeneity not only serves as a challenge for traditional cancer therapeutics, but also acts as an immune evasion mechanism, increasing the likelihood of some mutant cell populations remaining undetected [20, 25]. Another immune escape mechanism occurs through antigen shedding [26]. As part of their normal growth, cells generate a large amount of waste products, and these unwanted products are commonly secreted through membrane vesicles. When released in large abundance, this process can also deplete the parent cell of tumor-

specific antigens, thus enabling the altered cancer cells to avoid destruction by cytotoxic T cells. Furthermore, shed antigens released into the bloodstream can act as decoys for neutralizing cancer-specific antibodies. Solid tumors can employ additional means of escape, whereby their local microenvironments are remodeled to promote immune tolerance [27].

A better understanding of how cancer interacts with the immune system has allowed for the development of new and effective therapeutics. The goal of cancer immunotherapies is to leverage a patient's own immune system to eradicate tumors in a highly specific and relatively safe manner [28]. One example is through an overall activation of the immune system by administering proinflammatory cytokines, which are immunomodulatory molecules released by activated immune cells [29, 30]. Although the immune stimulation caused by these molecules is nonspecific, an overall boost in immunity can sometimes strengthen immune cells enough to overcome tumor suppression. More specific, tumor-targeted approaches can be achieved using genetically engineered chimeric antigen receptors (CAR) on T cells [31, 32]. In CAR T cell therapy, T lymphocytes are isolated from a patient or a donor through leukapheresis [33]. The cells are then genetically modified to express a receptor that can recognize tumor-associated antigens, leading to elimination of the corresponding cells. Altered T cells are purified, expanded *ex vivo*, and finally infused back into patients for treatment. For some cancer types, this CAR approach has displayed striking efficacy in the clinic.

Antibodies have also been widely used to elicit antitumor immunity. For example, tumor-targeted monoclonal antibodies that recognize tumor antigens can opsonize cancer cells and trigger antibody-dependent, cell-mediated cytotoxicity [34]. Furthermore, by conjugating antibodies with chemotherapeutics, these cytotoxic cargos can be more accurately targeted to the tumor site and induce immunogenic cell death [35]. More recently, antibody-based checkpoint inhibitors have been used to directly modulate the function of specific immune cell subsets [36]. Immune checkpoints involve inhibitory receptors such as programed cell death protein 1 (PD1) and cytotoxic T lymphocyte–associated protein 4 (CTLA4) that regulate T cells. By presenting the corresponding ligands, the cytotoxic activity of T cells can be inhibited by tumor cells and regulatory immune cells. In checkpoint blockade therapy, antibodies target and block these receptor binding sites, thus removing the inhibitory signals on the T lymphocytes and unleashing their full potential for eliminating cancer cells. Despite their ability to elicit strong antitumor responses, efficacy of checkpoint blockades can vary greatly by patient [37]. This discrepancy may be explained by the fact that the therapy generally relies on the presence of preexisting tumor-targeted T cells [38]. For this reason, checkpoint blockades are being actively explored for use in combination with other therapies such as anticancer vaccination, which can help to generate new T cell populations [39, 40].

1.2.2 Current State of Cancer Vaccines

Cancer vaccines introduce tumor-relevant antigenic material in a manner that leads to downstream mobilization of the immune system [28]. As the most immunogenic mutations have likely already been selected out by the time cancer is detected [5], the presence of tumor antigens alone is usually not sufficient to drive proper immune stimulation. As such, tumor antigens are almost always combined with an adjuvant in order to enhance the immune response [41]. In the basic process, delivered antigens are taken up by professional antigen-presenting cells (APCs), such as dendritic cells, which process and break down the antigens, followed by presentation of the peptide fragments via major histocompatibility complexes (MHCs) [42]. With the help of the adjuvant, the APCs mature, enabling engagement and activation of cancer-relevant T cells. Finally, the activated T cells can help to promote tumor elimination, either by further propagating immune activation or by directly seeking out and destroying the cancer cells.

Antigenic delivery to the immune system can be achieved in multiple ways. The most straightforward is the direct administration of tumor antigens. In single-antigen approaches, a tumor antigen overexpressed on cancer cells is administered parenterally [43]. This has been shown to elicit a robust immune response against the target antigen, especially in combination with an adjuvant; however, this approach may ultimately be thwarted by tumor heterogeneity. Whole cell preparations are another source of antigenic material that can theoretically be used

to vaccinate against the full breadth of tumor antigens [44]. However, this strategy often suffers from inadequate antitumor immune responses due to the interference from irrelevant proteins. In response to the often weak immunity generated by the above approaches, dendritic cells can be pulsed with an antigen and stimulated *ex vivo* [21]. Once this process is completed, the cells are then injected back into the patient in a process similar to CAR T cell therapy. The manipulated dendritic cells can subsequently migrate to the body's immune centers, where they train endogenous T cells. In a final method, antigenic uptake can happen *in situ* at the tumor site, taking advantage of processes such as immunogenic cell death, which provide autologous tumor antigens under an immunostimulatory context [45]. *In situ* vaccinations can also be achieved with oncolytic viruses that selectively infect and destroy cancer cells [46].

In April of 2010, the United States Food and Drug Administration gave its first approval to a therapeutic anticancer vaccine, sipuleucel-T, for the treatment of prostate cancer [47]. In this therapy, patient-derived dendritic cells are pulsed with prostatic acid phosphatase, which is expressed in a significant number of patients with prostate cancer [48]. After exposure to the antigen, along with granulocyte-macrophage colony-stimulating factor, the activated dendritic cells are introduced back into the patient. It was demonstrated in a clinical trial that sipuleucel-T was able to extend median survival by 4.1 months, which paved the way for its eventual approval [47]. The successful translation of this treatment has motivated the further clinical exploration of anticancer vaccine formulations, and a search on

ClinicalTrials.gov yields over 200 results for active trials. Examples of current clinical studies include dendritic cell therapies for glioblastoma (NCT01808820), oncolytic viruses for ovarian cancer (NCT00408590), peptide vaccines for recurrent glioblastoma (NCT02754362), and whole cell vaccines for breast cancer (NCT00317603).

Although cancer vaccines have had some success in the clinic, their limited ability to produce strong antitumor responses has hindered their widespread adoption. Despite its regulatory approval, the long-term financial viability of sipuleucel-T has come into question. The labor-intensive processes involved in its manufacture necessitate its high cost, which may be hard to justify given that the treatment only modestly prolongs median survival. Single-antigen peptide vaccines are able to elicit potent immune responses against the tumor cells that display the relevant antigenic epitopes; however, due to the heterogeneity of cancers, antigen-negative cells can eventually escape detection and proliferate without competition [20]. This approach is also not universal, and personalized identification and manufacture of vaccines based on tumor-specific neoantigens may not yet be viable on a large scale [49, 50]. Whole cell vaccination with tumor lysates has the potential to elicit multiantigenic immunity, but the final immune response is often dampened by the presence of extraneous proteins [44]. This underscores the fact that, even when delivering the correct antigenic material, current vaccination strategies may not have sufficient immunostimulatory capacity to overcome the tolerogenic tumor microenvironment.

1.2.3 Advantages of Nanovaccines

Nanotechnology offers many opportunities for improving the treatment efficacy of cancer vaccine formulations compared to traditional strategies (Figure 1.1). A major advantage is the ability to formulate the antigen and adjuvant components together in a manner that maximizes immune stimulation [51]. Flexibility in nanoparticle synthesis methods and material choice allows for the incorporation of different classes of molecules, such as proteins, polysaccharides, nucleic acids, lipids, proteins, and polymers. For example, electrostatic interactions can be used to bind nanoparticles and payloads with opposite charges together [52], or lipid-based cargoes can be incorporated into the bilayer of liposomes through an insertion technique [53, 54]. Cargoes can also be encapsulated through chemical conjugation [55], or they can be decorated onto the nanoparticle surface [56]. Oftentimes, the nanocarriers themselves can also be fabricated using biologically active vaccine components. For example, it has been demonstrated that both calcium phosphate [57], a mineral-based adjuvant, and certain antigen proteins [58] can be made into nanoparticulate form.

Loading of antigen and adjuvant into nanoparticles can serve a variety of purposes. Encapsulation of vaccine components has been shown to increase immunogenicity by protecting the integrity of the molecules from enzymes in the body, such as nucleases, proteases, and phosphatases [59]. Nanoparticulate delivery not only protects the adjuvant from degradation, but can also protect the

body from the systemic toxicity of the adjuvants, which can cause side effects such as fever, lethargy, diarrhea, and nausea [60]. Nanoencapsulation can also be used to enhance immune responses by providing extended release properties. Certain gel-like or polymeric nanoparticle platforms can act as depots, slowly releasing adjuvants and antigens over a long period of time [61]. Finally, there are a wide range of techniques available for loading both antigens and adjuvants into the same nanocarrier, which has been shown to dramatically increase antigen-specific immune responses by unifying the pharmacokinetics of the coencapsulated payloads [51].

In terms of payload delivery, nanoparticles can be designed to better target immune cells and immune-rich organs. At their size range, nanoparticulate vaccine formulations more easily drain into the lymphatic system after administration, enabling efficient delivery to the lymph nodes [62, 63], which contain high densities of immune cells. The localization of the nanoparticles can be further improved by modifying their outer layer to display ligands specific to immune cell surface receptors [64, 65]. Nanoformulations can also be designed to promote intracellular localization in a manner that maximizes the biological activity of the payloads. For example, nucleotide-binding oligomerization domain–like agonists and small interfering RNA (siRNA) can be delivered directly to the cytosol using nanoparticles designed to penetrate through cell membranes [66], and toll-like receptors (TLRs) can be engaged by various agonists when delivered into cells via an endosomal pathway [67]. Overall, careful choices in the use of materials,

loading methods, and synthesis techniques for nanoparticle-based formulations can all lead to improved vaccine efficacy.

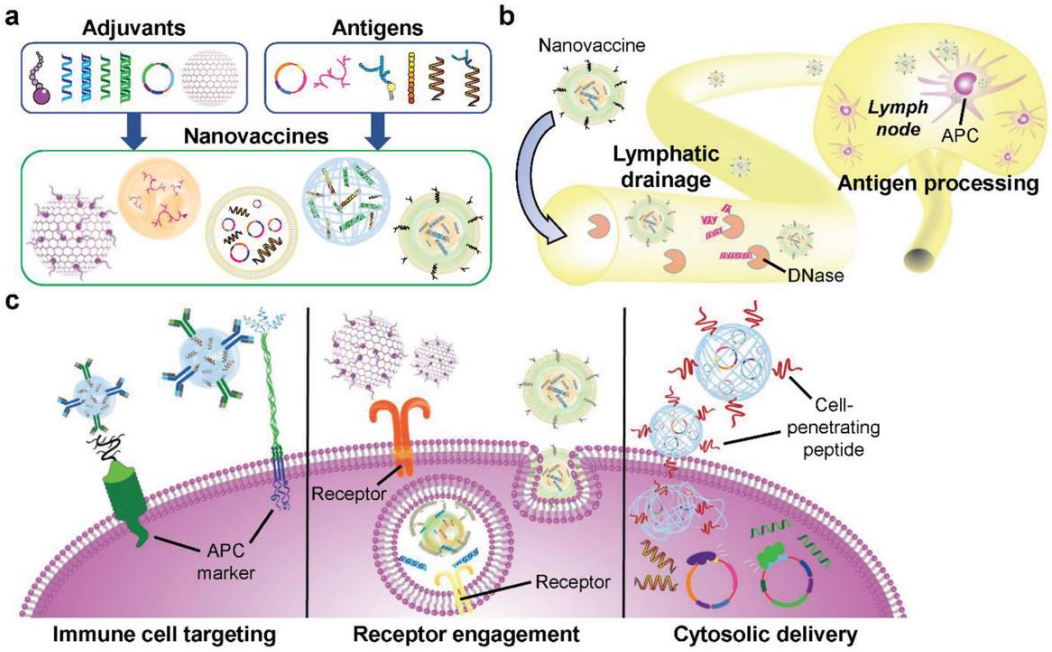

Figure 1.1: Advantages of nanoparticles for vaccine design. a) Various combinations of adjuvants and antigens can be formulated using nanoparticle platforms such as liposomes, emulsions, nanogels, and many others. b) Nanovaccines can access the lymphatic drainage system for lymph node delivery while protecting cargoes from environmental degradation. Once at the lymph nodes, the nanocarriers can deliver their cargoes to antigen-presenting cells (APCs) for immune processing. c) Nanovaccine properties can be tuned to efficiently deliver their cargoes for maximum immune activation. For example, nanoparticles can be modified to target specific subsets of immune cells. They can also be delivered to specific intracellular compartments, where receptors for immune pathways can be triggered.

1.3 Nanoparticle-Based Cancer Vaccines

1.3.1 Nonspecific Modulation

Some immunomodulatory nanoparticle platforms work to nonspecifically boost immune system function. While not strictly considered vaccines, these systems do rely on a patient's own tumor as the source of antigenic material and work by augmenting immune processes such as antigen processing and antigen presentation. This is generally achieved by manipulating the immune system in a way that reduces immunosuppression or activates specific immune cell subsets to potentiate a response against cancer cells. In some cases, these formulations can also be combined with tumor cell killing mechanisms to increase exposure to tumor-associated antigens.

1.3.1.1 Enhancing Physical Proximity of Immune Cells

An intuitive method for boosting antitumor immune activity is to bring the principal immune cells responsible for tumor elimination closer to their target. To achieve this, nanoparticles can be decorated with two different antibodies, one to target and/or activate immune cells, and another to target the tumor cells. By using these bifunctional nanoparticles, nearby immune cells can be targeted to tumors, increasing the chance of exposure to released tumor antigens or apoptotic cancer

cells while enhancing immune stimulation. In a first example, biodegradable poly(lactic acid) nanoparticles were decorated with antibodies against the dendritic cell costimulatory marker CD40, as well as an antibody against human epidermal growth factor receptor 2 (HER2)/neu, a common tumor antigen overexpressed in human breast cancer [68]. The anti-CD40 antibody was found to both bind and activate dendritic cells, inducing a strong proinflammatory immune response that could be directed toward neu^+ tumors. Intratumoral injection of the nanoparticles yielded 100% rejection, while systemic injections resulted in 70% of mice rejecting neu^+ tumors. Importantly, rechallenge of mice that rejected the primary tumor did not lead to any subsequent tumor growth. In another example, polystyrene nanoparticles were conjugated with antibodies against HER2/neu and calreticulin, a protein that facilitates phagocytosis in APCs [69]. Macrophages treated with these multivalent bispecific nano-bioconjugate engagers were able to better take up $HER2^+$ cancer cells and presented tumor-associated antigens via MHC surface complexes. Intratumoral and intravenous injections of the nanoparticles led to higher infiltration of $CD8^+$ T cells and inhibited the growth of HER2-expressing tumors. Upon rechallenge, treated mice rejected $HER2^+$ cancer cells but not $HER2^-$ cells, demonstrating the specificity of the treatment and the durability of the response. Instead of binding APCs to tumor cells, it has also been demonstrated that antigen-specific T cells can be linked to cancer cells in a similar manner [70]. Conjugation of nanoparticles with SIY–MHC complexes effectively enabled binding to 2C T cells, while the inclusion of anti-CD19 allowed for crosslinking

with $CD19^+$ Raji cancer cells. Shortly after intratumoral injection of the nanoparticles, mice were infused with adoptively transferred 2C T cells, which led to significant retardation of tumor growth.

1.3.1.2 Reduction of Immunosuppression

The immunosuppressive tumor microenvironment is a hurdle for most anticancer immunotherapy treatments, as effector cells can be rendered ineffective by inhibitory proteins or anti-inflammatory cytokines. For example, a melanoma-specific peptide vaccine was found to be effective for early stage melanoma, but it failed to demonstrate efficacy at later disease stages due to increased levels of immunosuppressive cytokines like tumor growth factor β (TGFβ) in the tumor microenvironment [71]. To address this, a liposome–protamine–hyaluronic acid nanoparticle was designed to deliver siRNA against TGFβ into tumor cells [72]. Injection of the nanoparticles halved the levels of TGFβ in the tumor microenvironment while doubling the efficacy of the vaccine. This improvement was discovered to be caused by an increase in $CD8^+$ T cells in the late stage tumor tissue along with a marked decrease in regulatory T cell levels. Other immunosuppressive efforts focus on the expression of signaling proteins on tumor tissue that interact with immune cells. Well-known pathways such as PD1 can be intercepted using checkpoint blockades, but systemic administration can have toxic side effects, potentially leading to the development of autoimmune diseases and pathological inflammation [73]. In one recent work, platelet-derived

microparticles were used as a carrier for antibodies against programed death-ligand 1 (PDL1) [74]. After tumor resection, residual cancer cells can oftentimes start to regrow the tumor or be released into circulation. These remaining cells can express PDL1 in response to inflammation, making it highly difficult for the immune system to destroy them and prevent tumor recurrence. Due to the abundance of exposed collagen in wound sites, platelet microparticles were chosen as the delivery vehicle for anti-PDL1 given their inherent targeting ability. Intravenous injection of the microparticles immediately after incomplete tumor resections was shown to greatly reduce tumor regrowth and metastasis formation in both B16-F10 melanoma and triple-negative 4T1 breast cancer mouse models. Similarly, immunotherapy mediated by low dose doxorubicin has been shown to have partial efficacy against B-Raf proto-oncogene mutant melanoma, but it failed at long-term efficacy likely due to the emergence of the Wnt family member 5a (Wnt5a) protein on cancer cells. Wnt5a can induce dendritic cell tolerance and cause fibrosis of tumor tissue, as well as prevent T cell infiltration. A lipid–protamine–DNA nanoparticle loaded with plasmid DNA encoding for a Wnt5a trap was able to transiently reduce Wnt5a levels in the tumor microenvironment and significantly boost treatment efficacy using doxorubicin [75].

1.3.1.3 Immune System Activation

The immune system can be boosted through the introduction of immunostimulatory payloads, including pathogen-associated molecular patterns

(PAMPs), costimulatory markers, cytokines, and other signaling proteins. Adjuvant administration has been found to be a powerful nonspecific modulator to aid in cancer immunotherapy. PAMPs such as single-stranded DNA, double-stranded RNA, and lipopolysaccharides are recognized by the TLRs found on immune cells and help to promote downstream inflammatory responses. Many of these PAMPs, such as CpG oligonucleotides (ODNs) recognized by endosomal TLR9, have been extensively used as adjuvants in conjunction with a coinjection of proteins or peptides to promote specific immune responses [76-80]. Other TLR-targeted PAMPs such as monophosphoryl lipid A (MPLA) [81, 82] and imidazoquinoline [83] have been used in nanoparticle formulations as adjuvants, and some PAMPs have even been coloaded together to simultaneously engage multiple different TLRs [84].

Cyclic dinucleotides (CDNs), small nucleic acids characteristic of invading microbes, are a family of type I interferon (IFN)–producing PAMPs. These CDNs are in phase I clinical trials, but they require very high dosages to ensure that adequate amounts can get into the cytosol to interact with their stimulator of interferon genes (STING) receptor. Encapsulation of CDNs into nanoparticles can improve cytosolic delivery and enhance immune responses at lower concentrations. In one work, cyclic diguanylate was encapsulated into polyethylene glycol-functionalized lipid nanoparticles and used to adjuvant soluble ovalbumin (OVA) protein [85]. After vaccination, a significant increase in both $CD8^+$ and $CD4^+$ T cells was observed, and T cells restimulated with OVA produced fivefold increases

in IFNγ and tumor necrosis factor α (TNFα). Further, a CDN-adjuvanted B16-F10 vaccine formulation induced a sevenfold higher frequency of gp100-specific $CD8^+$ T cells and significantly delayed B16-F10 tumor growth. CDNs have also been incorporated into nanoparticles consisting of cationic poly(β-amino ester) (PBAE), a polymer widely used for cytosolic delivery of DNA [86]. Delivery of cyclic diguanylate to THP-1 cells using a PBAE carrier yielded an equivalent amount of IFN regulatory factor 3 activation as free CDN, but at a 100-fold lower dose of adjuvant. When the nanoparticles were given as an intratumoral injection along with anti-PD1 antibodies, complete remission of B16-F10 tumors was seen at an order of magnitude lower CDN dosage than the soluble form.

The repetitive protein structure of viral capsids self-assembled into nanoparticles can also serve as a PAMP. For example, cowpea mosaic virus is a noninfectious agent that self-assembles into hollow, icosahedral 30 nm virus-like particles, which can have strong antitumor immunotherapeutic activity (Figure 1.2) [87, 88]. Inhalation of the virus-like particles by B16-F10 tumor–bearing mice increased tumor-infiltrating neutrophils, activated neutrophils in the lung microenvironment, and elevated levels of neutrophil-secreted cytokines. Significantly delayed tumor growth was seen after injections of the nanoparticles via various routes in multiple different tumor models. In particular, the virus-like particles were able to eliminate primary B16-F10 tumors in half of mice upon intratumoral injection, as well as provide long-term antitumor immunity as shown by rejection of a contralateral B16-F10 rechallenge. Other virus-like particles such

as the papaya mosaic virus [89], influenza virus [90], and tomato yellow leaf curl virus [91] have also shown strong adjuvanting properties that can be taken advantage of for immune modulation.

Cytokines serve a very important role in the adaptive immune system and can also be used for potent immune activation. For instance, mast cells can influence dendritic cell migration to the lymph nodes and upregulate inflammatory responses through the release of granules full of immune mediators like TNF. To mimic this

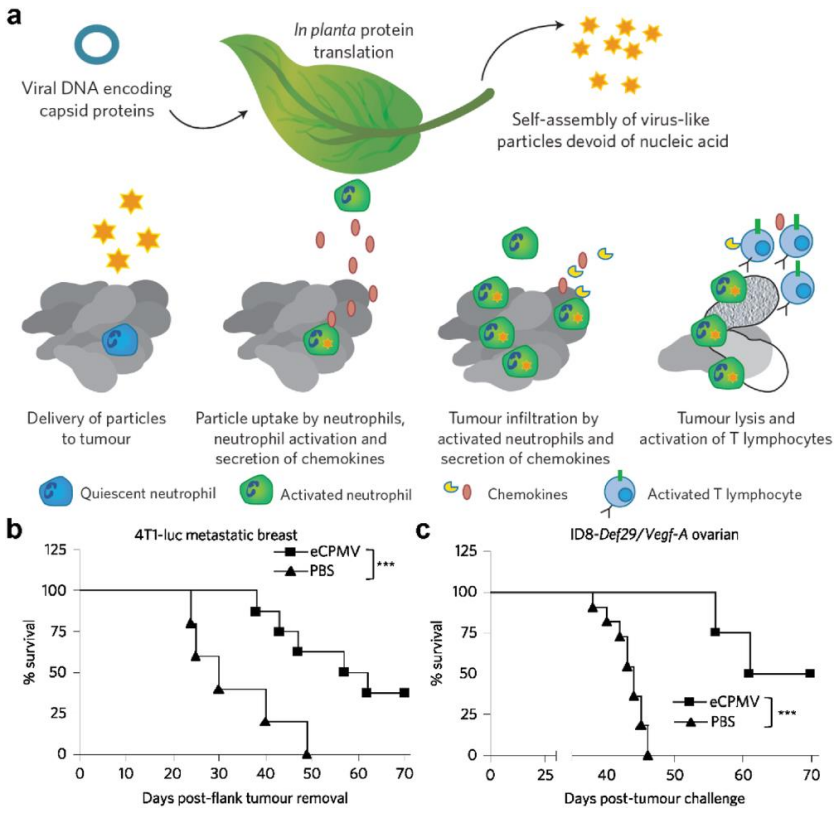

Figure 1.2: Virus-like nanoparticles for *in situ* anticancer vaccination. a) Schematic depicting the synthesis of empty cowpea mosaic virus (eCPMV) nanoparticles and their expected mechanism of action for tumor treatment. b,c) When used to treat tumor-bearing mice, virus-like nanoparticles significantly enhanced survival in both a 4T1-luc metastatic breast cancer model (b) and an ID8-Def29/Vegf-A ovarian cancer model (c). Reproduced with permission Copyright 2016, Springer Nature.

natural boosting of the immune system, synthetic mast cell granules were synthesized by trapping TNF into a nanoparticle matrix of chitosan–heparin [92]. Like real mast cell granules, the particles drained to lymph nodes and promoted germinal center formation. Due to the modular nature of the nanoparticles, TNF could be replaced with interleukin-12 (IL12) to promote polarization of immune cells toward proinflammatory phenotypes, such as IFNγ-secreting T cells. Delivery of IL2, a crucial cytokine for T cell survival and proliferation, has also been explored as a method to enhance T cell–mediated immunotherapy. Hydroxyethyl starch nanocapsules were coupled with IL2 using copper-free click chemistry, and incubation with T cells resulted in a high level of uptake and a fourfold increase in division index compared to unmodified nanocapsules. It has been shown previously that nanoparticles delivering a combination of different classes of immune-activating adjuvants can promote increased therapeutic efficacy [93]. Combinations of cytokines with other molecules, such as PAMPs [94] and costimulatory ligands [95], have also been shown to synergistically activate immune cells.

1.3.1.4 Immune Activation and Immunosuppressive Intervention Combination

Beyond combining different methods of activating immune cells, simultaneous use of immunosuppressive intervention and immune activation can also yield impressive results. For example, combining IL10 siRNA and CpG ODN

into a pathogen-mimicking nanoparticle resulted in a balanced Th1/Th2 cytokine response that improved antitumor efficacy [96]. Immune activating R848 has also been delivered to T cells by encapsulation in nanoparticles that were targeted to T cells expressing PD1 [97]. To enhance costimulation while reducing immunosuppression, dual-targeted nanoparticles have been developed with both agonistic and antagonistic antibodies conjugated onto the same surface. In one case, anti-4-1BB was attached onto particles to activate the 4-1BB costimulation pathway on $CD8^+$ T cells, while the conjugation of anti-PDL1 served to block PDL1 expressed on the surface of cancer cells [98]. Alternatively, nanoparticles decorated with anti-OX40 and anti-PD1 were able to target T cells expressing both receptors, simultaneously activating them and preventing their anergy [99]. In both the cases above, T cells were less inhibited by the immunosuppressive tumor microenvironment, leading to enhanced antitumor efficacy in a variety of mouse cancer models.

1.3.1.5 Combination with Traditional Anticancer Therapies

In the examples discussed thus far, it can be understood that the immunostimulatory nanoparticle platforms relied on the natural immune processing of tumor cells as the source of antigenic material. To facilitate the generation of tumor antigens and downstream immune activation, another strategy is to actively promote the release of material from tumors while concurrently introducing nonspecific immune modulators. For example, administration of the

immunotherapeutic potato virus X alone caused a modest decrease in the growth rate of B16-F10 cancer cells, similar to monotherapy with doxorubicin. However, coadministration of both the components led to a significant improvement in antitumor efficacy [100]. In another work, cytotoxic cationic silica nanoparticles were used to induce necrotic cell death while delivering a STING agonist to the immune cells in the tumor microenvironment [101]. Finally, "sticky" nanoparticles were designed to capture antigens *in situ* before being phagocytosed by immune cells [102]. After administration of anti-PD1 antibodies, primary tumors were irradiated and then injected with the antigen-capturing nanoparticles. Taking advantage of the abscopal effect, protein-loaded nanoparticles could then travel to the lymph nodes to facilitate an adaptive immune response, which led to the eventual destruction of a secondary tumor in 20% of mice.

1.3.2 Specific Modulation

The ultimate goal of vaccination is to stimulate the immune system while simultaneously guiding a specific response against the desired target. For cancer immunotherapy, this target is often a lowly immunogenic antigen that is differentially expressed by tumor cells. As a result, an ideal cancer vaccine requires delivery of the relevant antigens along with a potent immunological adjuvant, which can be used to force the immune system to mount an antitumor response. In recent research, nanotechnology has been employed to further improve the efficacy

of cancer vaccines using several strategies, including inherent nanoparticle adjuvancy, codelivery of antigen and adjuvant, targeted delivery to immune cells, enhanced immune cell uptake and cross-presentation, and cytosolic delivery.

1.3.2.1 Inherent Nanoparticle Adjuvancy

There is a wide variety of materials and structures that can be made into nanoparticles, and one strategy for the formulation of nanovaccines is to carefully choose a material that is naturally immunostimulatory. This can help to streamline nanoparticle fabrication by reducing the complexity of the final formulation. As an example, nanoparticles made of viral capsids naturally activate the immune system, largely due to the conservation of repetitive protein structures or the retention of nucleic acid-based PAMPs. These virus-like particles can engage TLRs in immune cells while delivering an antigenic payload. Even very lowly immunogenic tumor–associated antigens like idiotypic immunoglobulin from B cell lymphomas can elicit a strong humoral response when delivered by nanoparticles made of potato virus X coat proteins [103]. Other gel-like nanoparticles can be made by crosslinking materials that mimic the structure of PAMPs, such as hydrophobic polymers [104], peptides [105, 106], or DNA [107], while also encapsulating antigens. d-tetra-peptide hydrogels in particular show promise as a vaccine adjuvant. Nanoformulations made by mixing irradiated tumor cells with a self-assembling hydrogel made of the d configuration of naphthylacetic acid-modified

GFFY peptide were able to significantly protect mice from both E.G7 and 4T1 tumor challenges [108].

Immune responses to antigens can also be naturally boosted by carefully tuning their release over time. Nanogels are especially adept at this, as protein-to-polymer ratios can be precisely varied to change matrix spacing and cargo release rates [109, 110]. Some formulations have shown impressive sustained protein release, such as a PBAE layer-by-layer microparticle that extended release half-life from 4.9 to 143.9 h [111], or a hyaluronic acid-based nanogel that released proteins for over one week in rats [112]. Antigen delivery can be further improved by modifying nanogels to be retained at the immunization site, promoting sustained release of the payload in the presence of immune cells [113]. Polymeric nanoparticles can also provide sustained protein release profiles, as in the case of a poly(lactic-*co*-glycolic acid) (PLGA)-based formulation that was shown to release OVA protein for over a week [114]. When modified to carry gp100 or B16-F10 lysate, the same particles could produce approximately threefold greater T cell activation compared to equivalent doses of protein in soluble form, and this resulted in superior B16-F10 tumor suppression.

1.3.2.2 Codelivery of Antigen and Adjuvant

In general, delivery of antigens alone is not enough to trigger a strong immune response, requiring the use of an adjuvant to boost immune activation. For example, OVA antigen conjugated to poly(propylene sulfide) nanoparticles showed

no anti-OVA immune response in mice, but high levels of dendritic cell maturation and OVA-specific T cell generation were observed when the same particles were delivered along with an administration of CpG, resulting in protection against influenza–OVA challenge [115]. Furthermore, vaccines generally work the best when the antigen and adjuvant are delivered concurrently to the same APC, which can be readily accomplished using nanoparticle-based systems. This idea was shown systematically with a model cancer vaccine consisting of a polymeric nanoparticle loaded with an OVA peptide and the TLR7/8 agonist R848 [116]. Administration of a nanoparticle encapsulating both the payloads resulted in higher anti-OVA IgG production compared to either component in free form, one component in free form and the other encapsulated, or both the components encapsulated separately. In addition, codelivery of both the components together enhanced downstream T cell–mediated lysis of OVA-expressing cells and elicited increased local cytokine production. Many platforms have been designed for the codelivery of antigen and adjuvant together, including inter-bilayer-crosslinked multilamellar vesicles loaded with OVA antigen inside and MPLA interspersed throughout their lipid bilayers [117]. Immunization with this formulation led to an impressive 28% of $CD8^+$ T cells exhibiting OVA specificity, which was 14 times greater than observed when using soluble OVA and MPLA. These specific T cells also retained their functionality, as shown by high IFNγ production upon restimulation with OVA *ex vivo*.

When vaccinating against a heterogenous target like cancer cells, multiepitope vaccine formulations can be employed to prevent immune escape and tumor recurrence [20]. Modular vaccine designs, exemplified by recent work describing designer nanodisks [118], can help overcome this barrier. Synthetic high-density lipoprotein nanodisks were mixed with cholesterol-modified CpG ODN for immunogenicity and further functionalized with cysteine-modified, tumor-specific neoantigens for specificity. Mice immunized with nanodisks harboring a combination of three antigens experienced an expansion in their pool of antigen-specific $CD8^+$ and $CD4^+$ T cells when compared to those receiving soluble formulations. The multiantigen formulation also showed significantly better control of B16-F10 tumor growth compared to single-antigen or dual-antigen formulations. Impressively, when mice were vaccinated in combination with anti-PD1 and anti-CTLA4, 90% were cured of their tumor burden.

1.3.2.3 Immune Cell Targeting

Due to the easy surface functionalization properties of nanoparticles, the efficacy and efficiency of nanovaccines can be improved by including an immune cell targeting moiety. Vaccine processing mainly takes place in APCs, and thus the most common immune cells targeted are dendritic cells and macrophages. A variety of surface markers can be targeted, such as the C-type lectin mannose receptor (CD206) by the inclusion of mannose on the nanovaccine surface [71, 119, 120]. In one example, the targeting ability of mannose was examined, and it was observed

that functionalization could increase particle uptake into bone marrow–derived dendritic cells [121]. Strong localized signal of a fluorescently labeled targeted nanovaccine was seen in the draining lymph nodes at 24 h, while particles without mannose started to lose signal as early as 12 h after injection. Other surface markers such as CD11c [122], scavenger receptor class B type 1 [123], DEC205 [124, 125], and macrophage galactose-specific C-type lectin [55] have also been commonly targeted.

1.3.2.4 Efficient Cytosolic Entry

Traditional cancer vaccines suffer from difficulty in entering the cytosol of immune cells. Cytosolic entry can help to facilitate the presentation of antigens by MHC-I and subsequent mobilization of $CD8^+$ effector T cells. In addition, there are several maturation pathways and pathogen recognition receptors located in the cytosol that can be leveraged to boost the potency of vaccine formulations. As most nanoparticles are taken up endosomally, there exist many strategies for facilitating endosomal escape. Due to the characteristic acidic environment of the endosomal compartment, redox-responsive nanovaccines can be used to achieve this goal. For example, some polymeric nanoparticles can act as proton sponges and induce lysosome swelling and rupture when encountering low pH environments [126]. Lysosomal rupture–triggered reactive oxygen species have also been shown to enhance proteasome activation, which can help to trigger MHC-I antigen presentation [55]. In one case, the common transfection agent, polyethylenimine,

was coated onto the surface of antigen-loaded polymeric nanoparticles, and this helped to facilitate cross-presentation of the loaded antigen after uptake [127]. Similar reducible polymeric systems like poly(γ-glutamic acid) nanoparticles [128] and cationic dextran nanogels [129] have also shown a similar ability for facilitating MHC-I restriction. Besides endosomal escape, there are other ways to enter the cytosol from the endosomal compartment. OVA-loaded α-alumina nanoparticles can engage noncanonical autophagy, where antigens are diverted into autophagosomes and the delayed antigen degradation allows for increased cross-presentation [130]. By taking advantage of this process, significant levels of OVA-specific T cells could be induced, enabling mice to completely reject established B16-OVA tumors *in vivo*. In another strategy, nanoparticles can be designed to directly cross cell membranes by incorporating cell penetrating peptides onto their surfaces [131-133]. Macropinocytosis of lipid-coated nanovaccines has also been reported [134].

Cytosolic localization gives delivered antigens access to MHC-I presentation, but it can also be leveraged to enhance immune stimulation. Recent work has shown that retinoic acid-inducible protein 1 ligands and STING ligands may be stronger activators of the immune system than traditional TLR-based adjuvants like CpG and MPLA [85, 135]. PC7A synthetic nanoparticles have been used to deliver antigen while simultaneously activating the STING pathway (Figure 1.3) [136, 137]. When loaded with OVA, the nanoformulation induced a threefold increase in antigen cross-presentation due to endosomal disruption by the redox-responsive

PC7A. Once in the cytosol, the PC7A also engaged the STING receptor, resulting in higher immune activation compared to poly(I:C) or other polymeric nanoparticle groups. The combination of potent STING activation and efficient antigen cross-presentation led to significant antitumor efficacy against loaded antigens in B16-OVA, B16-F10, MC38, and TC-1 mouse tumor models.

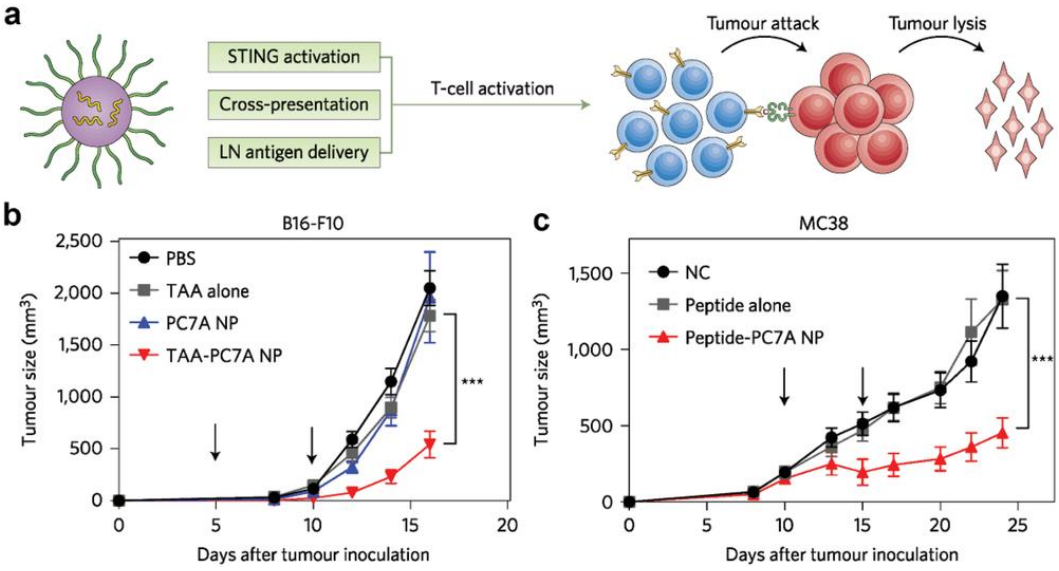

Figure 1.3: Synthetic nanoparticles activating the STING pathway for antitumor vaccination. a) Schematic depicting an antigen-loaded synthetic nanocarrier (PC7A) and its proposed mechanism of action. b,c) When used to treat tumor-bearing mice, antigen-loaded PC7A nanoparticles significantly enhanced survival in both a B16-F10 melanoma model (b) and an MC38 colon cancer model (c). Reproduced with permission. Copyright 2017, Springer Nature.

Instead of delivering antigens directly to the cytosol, some recent work has also focused on delivery of antigen-encoding RNA for *in situ* transcription and antigen production [120, 134, 138]. Acid-dissolvable calcium phosphate nanoparticles carrying messenger RNA (mRNA) encoding the tumor-associated

tyrosinase-related protein 2 (TRP2) could elicit stronger antigen-specific T cell responses and humoral responses against B16-F10 melanoma compared to peptide delivery [120]. In addition, PDL1 siRNA could be delivered to directly downregulate PDL1 in dendritic cells to reduce immunosuppression. Cytosolic delivery of both the mRNAs was shown to have a potent antitumor effect, significantly better than cytosolic delivery of either component alone. This strategy of RNA antigen sourcing has also been implemented using a highly modular RNA–lipoplex platform [134]. RNA-containing lipoplexes were optimized to target the spleen by modifying the charge ratios of the components, and the resulting formulation was shown to be taken up into the cytoplasm of dendritic cells and macrophages via macropinocytosis. The nanoparticles also induced TLR7-triggered IFNα production and IFN-α/β receptor–dependent activation of APCs. Introduction of antigen-encoding RNA induced generation of functional antigen-specific T cells and memory cells, which resulted in potent antitumor efficacy in several tumor models. Moving toward clinical translation, three human patients with advanced malignant melanoma received five doses of the nanovaccine encoding for four tumor antigens. All three patients showed systemic IFNα production, along with de novo priming and amplification of T cells against the vaccine antigens.

1.3.2.5 Artificial Antigen Presentation

Most cancer vaccines work by manipulating APCs, which can then further stimulate antigen-specific T cells and B cells. Recently, there has been significant interest in developing artificial APCs (aAPCs) that are capable of directly stimulating effector cells [139]. This strategy was originally developed in order to effectively expand T cells *ex vivo* for adoptive cell therapies such as CAR T cell therapy [140]. These aAPCs, which include both live cell–based and synthetic micro-/nanoparticle-based platforms, mimic professional APCs and can strongly activate T cells while avoiding the intensive labor, high cost, and difficulty in quality control when using autologous APCs. Similar to their natural counterparts, aAPCs require at least two signals to induce T cell activation. The first signal, a peptide–MHC complex, binds to its cognate T cell receptor (TCR) and establishes antigen specificity. To become fully activated, T cells require a second signal in the form of costimulatory molecules such as CD80 and CD86, which engage their corresponding receptor on the T cell surface [139]. With these two signals, aAPCs have the potential to act as a vaccine-like platform that can expand antigen-specific T cell populations, but without the use of immunological adjuvants. In addition to the minimum two signal requirement, at times a third signal, in the form of soluble cytokines, can further enhance the survivability of the activated T cells [141].

To generate nanoscale aAPCs capable of engaging and activating T cells, MHC–Ig along with a costimulatory signal, in the form of CD80 or anti-CD28, has been decorated onto the surface of nanoparticles (Figure 1.4) [142]. When

administered subcutaneously, nanoscale aAPCs exhibited greater lymphatic drainage compared with microscale aAPCs, which largely remained at the injection site. When administered into tumor-bearing mice that received adoptively transferred antigen-specific T cells, the nanoparticles were able to help significantly control tumor growth. It has also been demonstrated that aAPCs can be fashioned using magnetic nanomaterials [143]. After incubation with their cognate T cells, these magnetic aAPCs helped to induce significant proliferation and could also guide the T cells to tumors with the use of a magnetic field. In the future, such a platform may be directly used *in vivo* to promote antitumor activity. Interestingly, it has been found that the shape of nanoscale aAPCs can have a significant impact on their biological activity [144]. Ellipsoid nanoparticles were fabricated by stretching spherical PLGA nanoparticles, followed by conjugation with anti-CD28 and MHC–Ig loaded with a gp100 tumor antigen epitope. After intravenous injection, it was observed that the ellipsoid particles could induce more antigen-specific T cells in circulation compared with their spherical counterparts. Although there are currently limited examples of nanoparticulate aAPCs being used *in vivo*, this nanovaccine-like platform holds significant potential given its ability to help bypass the complicated processes of antigen processing and presentation.

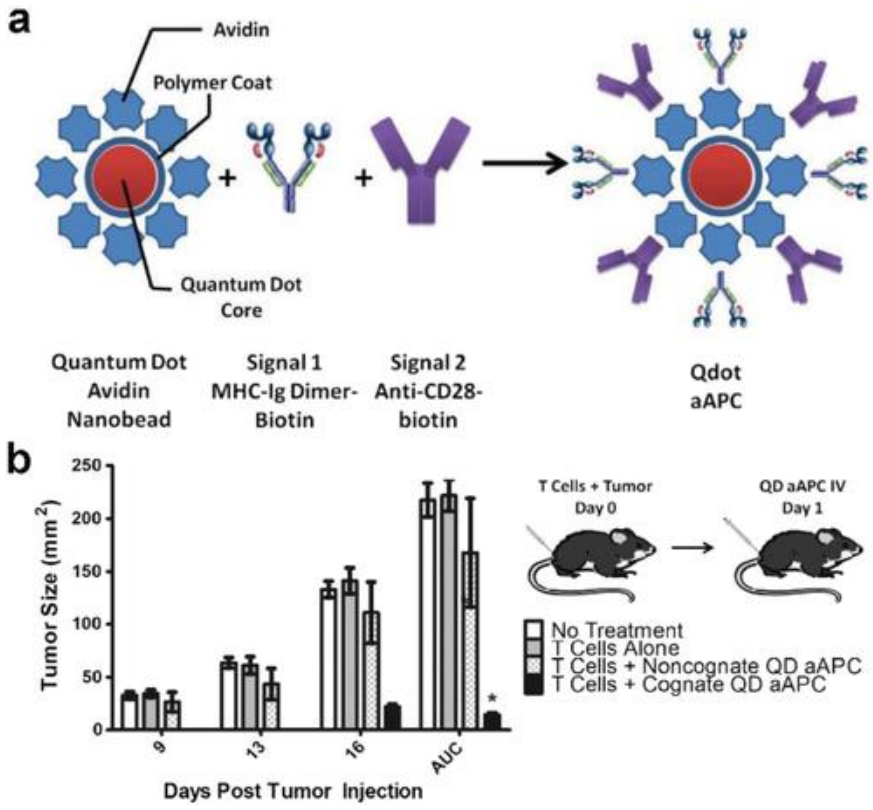

Figure 1.4: Quantum dot (QD) nanoparticles for artificial antigen presentation. a) Schematic depicting the artificial antigen presenting cell (aAPC) structure, where both the signals are attached to the nanoparticle surface using biotin–avidin interactions. b) When injected intravenously into B16 tumor–bearing mice that were also adoptively transferred with antigen-specific T cells, the aAPCs were able to significantly control tumor growth. Reproduced with permission. Copyright 2014, Elsevier Inc.

1.4 Cell Membrane-Coated Nanovaccines

1.4.1 Background

As discussed thus far, nanoparticle technology has the potential to significantly alter the landscape of anticancer vaccination, enabling the design of

new nanovaccines with improved efficacy compared with traditional formulations. More recently, there has been a noticeable paradigm shift within the field of nanomedicine in which a greater emphasis has been placed on biomimetic design principles [145-148]. Along these lines, a new cell membrane coating approach has emerged in which nanoparticles are cloaked with a layer of cell-derived membrane [149-151]. In contrast to traditional bottom-up synthetic strategies, top-down membrane coating directly leverages naturally occurring biological material for the fabrication of multifunctional nanoparticles. Using red blood cells (RBCs) as the source of membrane material, it was demonstrated that RBC membrane–coated nanoparticles gained the ability to avoid immune clearance and circulated for extended periods of time (Figure 1.5) [152]. The cell-mimicking properties of these biomimetic nanoparticles result from the transference of the originating cell's membrane proteins onto the surface of the nanoparticle substrate [153]. This approach for functionalization has proven to be highly generalizable, allowing for the delivery of a wide range of cargoes using different types of materials for the inner core [154, 155]. The outer membrane layer can also be modified with further functionality by facile means, affording additional flexibility to membrane-coated platforms [54, 156].

Since the first work on RBC membrane–coated nanoparticles was reported, research on cell membrane coatings has expanded in multiple directions. In addition to modulating the material composition of the inner core, the membrane can be sourced from a plethora of cell types, each resulting in unique formulations with

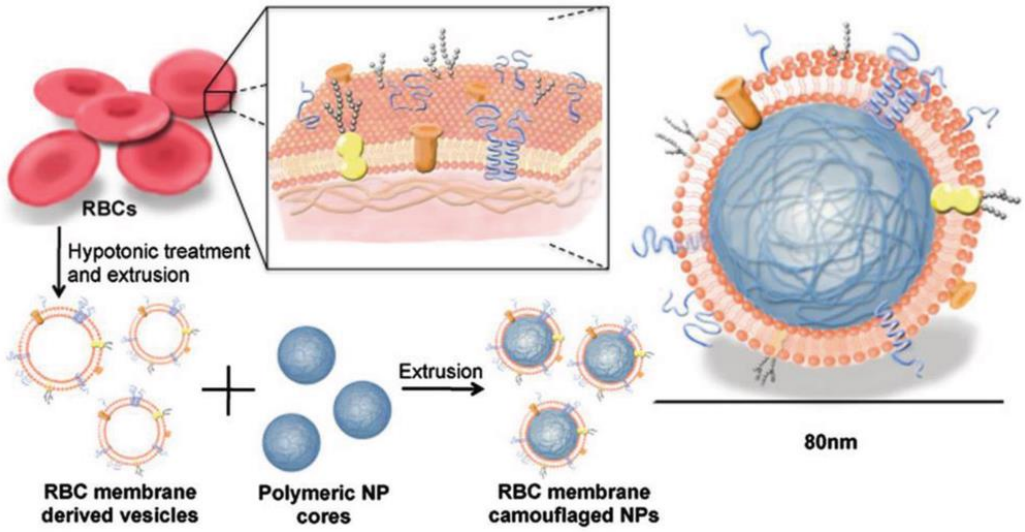

Figure 1.5: Functionalization of nanoparticles with a cell membrane coating. Schematic depicting the fabrication of red blood cell (RBC) membrane–coated nanoparticles. RBC vesicles are obtained by hypotonic treatment, followed by coating onto polymeric nanoparticle cores using extrusion. The resulting membrane-coated nanoparticle exhibits a characteristic core–shell structure. Reproduced with permission. Copyright 2011, National Academy of Sciences.

novel properties. For example, platelet membrane–coated nanoparticles exhibit the ability to target bacteria and damaged vasculature [157, 158], while cancer cell membrane–coated nanoparticles can homotypically target cancer cells [159]. White blood cell membrane, with its various toxin and cytokine receptors, has utility for treating sepsis [160]. Other membrane-coated formulations have also been reported using stem cell membrane [161], endothelial cell membrane [162], and even hybrid membranes generated from multiple cell types [163]. As a result of all the complex functionalities that can be incorporated, this approach has enabled the resulting biomimetic nanoparticles to excel in nontraditional areas of nanomedicine. A major example is detoxification, where membrane-coated particles can act as nanosponges to neutralize toxins by taking advantage of their

interactions with cell membranes [164-166]. By neutralizing these toxins and preventing them from attacking healthy cells, these nanoscale decoys have utility for the treatment of bacterial infections, animal envenoming, and even exposure to chemical warfare agents. The ability of cell membrane–coated nanoparticles to bind and present multiple antigens, combined with the flexibility of choosing various core materials, has also made them suitable for vaccine design [23, 24].

1.4.2 Cell Membrane-Coated Nanoparticles for Antibacterial Vaccination

Overall, vaccines represent one of the most efficient methods of reducing the global health burden posed by bacterial infections [167]. Toxoid vaccination represents an effective means of disarming bacteria of their virulent proteins, making it harder for the pathogens to colonize their host. This strategy is currently used in the clinic to vaccinate against tetanus and diphtheria [168]. In order to make bacterial toxins safe for administration, they are generally inactivated with harsh chemical or heat treatments that can damage antigenicity and reduce vaccination efficacy. By contrast, RBC nanosponges have demonstrated the ability to naturally detain and neutralize bacterial toxins when the two are mixed together, forming what are referred to as nanotoxoids [167, 169]. Using methicillin-resistant *Staphylococcus aureus* (MRSA) and its major virulence factor α-hemolysin as a model system, the corresponding nanotoxoid was able to generate

significant antitoxin titers, improving overall antibacterial immunity compared to a heat-denatured toxoid formulation [170]. While the control toxoid required 60 min of high heat exposure to achieve an acceptable safety profile, the nanotoxoid demonstrated excellent safety on a number of cell types at the outset. In animal models of both systemic and skin toxin burden, nanotoxoid vaccination on a prime with two boosts schedule resulted in almost complete protection. A later study also demonstrated the efficacy of this approach against live MRSA infection [171].

As the mechanism of toxin binding to membrane-coated nanoparticles relies on function rather than the specific structure of the toxin, the nanotoxoid platform can be easily generalized. To generate a multiantigenic nanotoxoid, RBC nanosponges were mixed with a crude hemolytic protein fraction isolated from MRSA culture (Figure 1.6) [172]. It was confirmed that the nanotoxoids contained several toxins on their surface, including α-hemolysin, γ-hemolysin, and Panton–Valentine leukocidin. Further, the nanotoxoids were found to be completely safe, whereas intense heat treatment of the hemolytic protein fraction could not completely abrogate its toxicity. When used as a vaccine, the multivalent nanotoxoids were capable of generating antibody titers against all of the aforementioned toxins, which helped to reduce bacterial burden upon live MRSA challenge. In addition to the nanotoxoid approach, another method of generating multiantigenic vaccines is to directly employ bacteria-derived membrane. Outer membrane vesicles (OMVs) are secreted from bacteria and are important in

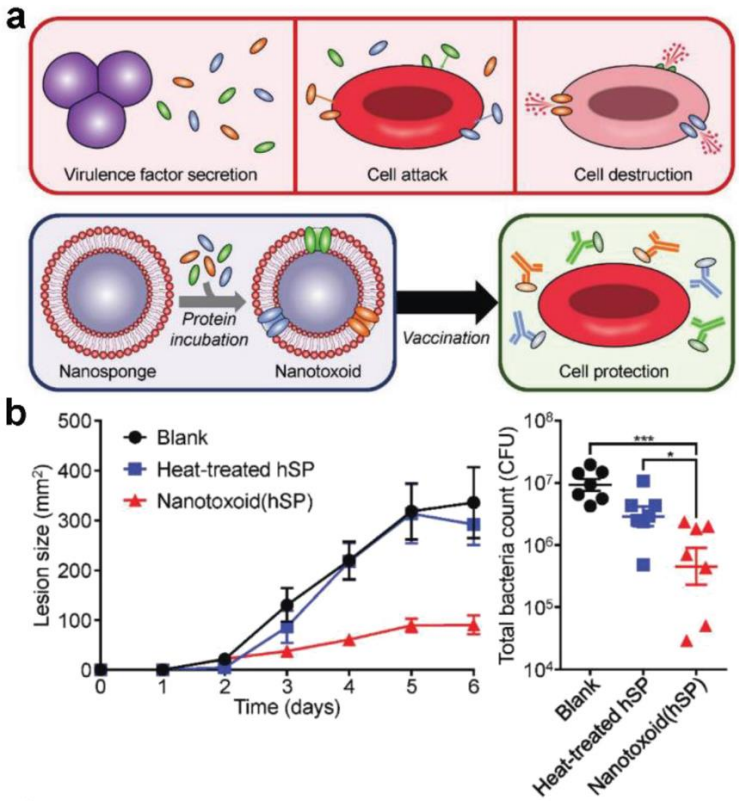

Figure 1.6: Membrane-coated nanoparticles for antibacterial vaccination. a) Schematic depicting the nanotoxoid concept, which can be used to develop vaccines against bacteria-secreted toxins. b) Vaccination using multiantigenic nanotoxoids fabricated with a hemolytic secreted protein (hSP) fraction from methicillin-resistant *Staphylococcus aureus* (MRSA) significantly inhibited lesion formation caused by subcutaneous MRSA challenge, leading to decreased bacteria counts. Reproduced with permission. Copyright 2017, Wiley-VCH.

pathogenesis as well as cell-to-cell signaling [173]. Some vaccines employing OMVs as the antigenic material have already been used in the clinic, as is the case with a formulation against meningococcal infection [174]. OMVs are attractive for use as antibacterial vaccines because they often share a similar biochemical membrane profile with their parent cell [175]. The utility of OMVs can be further improved by coating the material around a nanoparticulate core. In one instance, *Escherichia coli* OMVs were coated onto small gold nanoparticles, which

provided increased stability and size control compared with free OMVs [176]. Due to the ability to finely control their size, the membrane-coated particles efficiently localized to the lymph nodes, leading to strong and durable immune activation.

1.4.3 Cell Membrane-Coated Nanoparticles for Anticancer Vaccination

As a whole, antibacterial vaccines have been extremely successful in reducing mortality rates related to infection. Unfortunately, the same level of clinical success has not been achieved for formulations against cancer. Recently, the extension of cell membrane–coated nanoparticles to anticancer vaccination has become an active area of research. In one example, an RBC membrane–based nanocarrier was designed to deliver a hgp100 tumor antigen peptide and the adjuvant MPLA [177]. The platform was further modified with mannose on the surface to better target dendritic cells, and this led to enhanced localization to the draining lymph nodes. Both prophylactic and therapeutic efficacy were demonstrated in a B16-F10 subcutaneous tumor model, resulting in a slowing of tumor growth and a reduction in metastasis.

Since cancer cell membranes contain a plethora of autologous tumor antigens, utilizing the purified membrane of cancer cells as the antigenic material can be an effective approach in the design of nanoparticulate anticancer vaccines. This was initially demonstrated using B16-F10 melanoma membrane–coated

nanoparticles incorporated with MPLA [159]. The formulation significantly increased the maturation of bone marrow–derived dendritic cells and enhanced the stimulation of antigen-specific T cells. More recently, an in-depth set of studies was conducted using a platform in which cancer cell membrane was coated around CpG ODN–loaded polymer cores (Figure 1.7) [178]. CpG ODN 1826, a potent TLR9 agonist in mice, was encapsulated into PLGA cores through a double emulsion process, and B16-F10 membrane was coated onto the adjuvant-loaded cores by bath sonication. When the formulation was administered subcutaneously into mice, increased maturation of dendritic cells in the draining lymph nodes was observed, as indicated by the upregulation of protein markers such as CD40, CD80, CD86, and MHC-II, when compared to various controls. Notably, CpG encapsulated in nanoparticulate form was able to activate the immune system significantly better than free CpG, likely due to the preferential cellular uptake of the nanoparticles [179-182]. Additionally, it should be noted that TLR9 is located within the endosomal compartment, which highlights the power of leveraging the inherent properties of nanoparticles to purposefully manipulate immune responses. Mice vaccinated with the nanovaccine were able to generate antigen-specific $CD8^+$ T cells against gp100 and TRP2, both of which are melanoma-associated antigens [183]. When immunized mice were challenged with B16-F10 cancer cells, 86% of the mice exhibited no tumor growth, even after 150 days. In a therapeutic setting, it was demonstrated that the nanoformulation, along with a cocktail of anti-PD1

and anti-CTLA4 checkpoint inhibitors, was able to extend the survival of the tumor-bearing mice compared to either treatment alone.

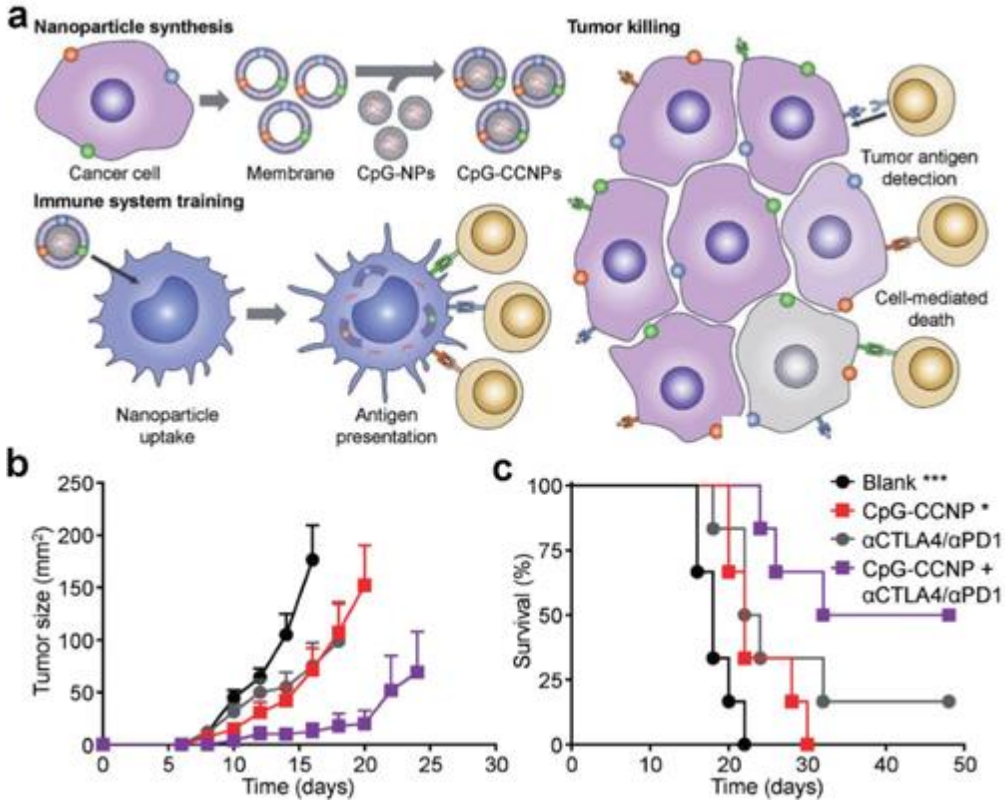

Figure 1.7: Membrane-coated nanoparticles for anticancer vaccination. a) Schematic depicting the fabrication of adjuvant-loaded cancer cell membrane–coated nanoparticles (CpG–CCNPs) and their proposed mechanism of action. b,c) When combined with a cocktail of checkpoint blockades (anti-CTLA4 and anti-PD1), treatment of established B16-F10 melanoma with the CpG–CCNP nanovaccine resulted in significantly slowed tumor growth (b) and improved survival (c). Reproduced with permission. Copyright 2017, Wiley-VCH.

Building upon the concept of using cancer cell membrane–coated nanoparticles for antitumor vaccination, various strategies have been employed to augment immune responses. For example, mannose was introduced to bestow

immune cell–targeting properties, helping to enhance uptake by dendritic cells and subsequently promoting their maturation [184]. As a result of this additional functionality, the targeted nanovaccine was able to offer better protection for vaccinated mice. It was claimed that this triple combination of an adjuvant, cancer cell membrane antigens, and a targeting ligand could work together to generate a robust anticancer immune response similar to levels generated against bacterial infections. In another example, immune stimulation was enhanced via the concurrent delivery of multiple adjuvants in an artificial cancer cell membrane–coated nanoparticle [185]. CpG-encapsulated calcium phosphate cores were fabricated by a water-in-oil microemulsion process and then coated with a membrane-mimicking liposome layer. Then, OVA-expressing B16-F10 cancer cell membrane proteins were purified by dialyzing the membrane against a detergent solution. The membrane proteins, along with the danger-associated molecular pattern Hsp70, were incorporated onto the nanoparticle surface to create the final formulation. This dual-adjuvant formulation was able to significantly upregulate maturation markers such as CD80, CD86, and MHC-II, and treated mice had fewer lung metastasis compared to formulations with just the CpG adjuvant. In all, the works described in this section demonstrate that cell membrane–coated nanoparticles have significant potential to be used as nanovaccines. Armed with the versatility to easily modulate both the adjuvant and the cancer membrane material, which can eventually be derived from a patient's own tumor, this platform may ultimately pave the way for potent, personalized anticancer vaccine therapies.

1.5 Conclusion

In this review, we have discussed the progress of using nanotechnology toward the design of cancer vaccines. In theory, vaccination represents an attractive option for cancer therapy, but in practice there are many challenges that need to be overcome in order for such platforms to achieve widespread clinical adoption. Generally, it is highly difficult for the immune system to generate a potent response against established tumors, which can employ various means to lower their immunogenicity over time. With the help of nanoscale delivery vehicles, researchers are exploring the design of novel vaccine formulations that can elicit immune responses capable of overcoming tumor immunosuppression. Nanocarriers offer many advantages, including the effective localization of payloads to the desired immune cell populations, loading of multiple cargoes into a single nanoparticle, and prolonged release characteristics.

More recently, a novel type of biomimetic platform, the cell membrane–coated nanoparticle, has emerged as a strong candidate to drive the further improvement of nanovaccine platforms. Membrane coating presents a facile means of introducing multiple functionalities onto the same nanoparticle without the need for complicated synthetic techniques. Regarding anticancer vaccination, the use of cancer cell membrane as the coating material offers an approach for creating vaccine formulations rich in tumor antigens. Combined with a nanoparticulate core carrying potent immune stimulators and the ability to easily target the resulting

nanoparticles to antigen presenting cells, cancer cell membrane–coated nanoparticles can achieve strong inhibition of tumor growth. These nanoformulations may be further improved through the continued optimization of adjuvant and membrane antigen combinations. Methods can also be developed for obtaining membrane material from the resected tumors of patients, enabling the facile fabrication of personalized vaccines.

Looking toward clinical translation, a main challenge will be scaling up nanoparticle production in an efficient and cost-effective manner. Nanoformulations will avoid many expenses required for live-cell vaccines, but there will likely need to be a substantial investment of time and resources to adapt current lab-scale manufacturing procedures to high-throughput workflows capable of production at the scale necessary for human patients. These workflows will also need to align with good manufacturing practices to meet quality requirements for regulatory approval. Finally, significant work will also need to be done on evaluating the synergy between vaccines and other types of cancer therapies. By simultaneously tackling the challenge of cancer treatment on multiple fronts, it may one day be possible to eliminate tumors altogether, regardless of their underlying characteristics.

Chapter 1, in full, is a reprint of the material as it appears in *Advanced Biosystems*, 2019, Ashley Kroll, Yao Jiang, Jiarong Zhou, Maya Holay, Ronnie Fang and Liangfang Zhang. The dissertation author was the primary author of this paper.

1.6 References

1. Rosenblum, M.D., K.A. Remedios, and A.K. Abbas, *Mechanisms of human autoimmunity.* J. Clin. Invest., 2015. **125**(6): p. 2228-33.

2. Wang, L., F.S. Wang, and M.E. Gershwin, *Human autoimmune diseases: a comprehensive update.* J. Intern. Med., 2015. **278**(4): p. 369-95.

3. Arias, C.A. and B.E. Murray, *Antibiotic-resistant bugs in the 21st century--a clinical super-challenge.* N. Engl. J. Med., 2009. **360**(5): p. 439-43.

4. Swann, J.B. and M.J. Smyth, *Immune surveillance of tumors.* J. Clin. Invest., 2007. **117**(5): p. 1137-46.

5. Kim, R., M. Emi, and K. Tanabe, *Cancer immunoediting from immune surveillance to immune escape.* Immunology, 2007. **121**(1): p. 1-14.

6. Mocellin, S., E. Wang, and F.M. Marincola, *Cytokines and immune response in the tumor microenvironment.* J. Immunother., 2001. **24**(5): p. 392-407.

7. Leight, J.L., A.P. Drain, and V.M. Weaver, *Extracellular Matrix Remodeling and Stiffening Modulate Tumor Phenotype and Treatment Response.* Annu. Rev. Cancer Biol., 2017. **1**(1): p. 313-334.

8. Chaudhary, B. and E. Elkord, *Regulatory T Cells in the Tumor Microenvironment and Cancer Progression: Role and Therapeutic Targeting.* Vaccines (Basel), 2016. **4**(3): p. 28.

9. Schaaf, M.B., A.D. Garg, and P. Agostinis, *Defining the role of the tumor vasculature in antitumor immunity and immunotherapy.* Cell Death Dis., 2018. **9**(2): p. 115.

10. Farkona, S., E.P. Diamandis, and I.M. Blasutig, *Cancer immunotherapy: the beginning of the end of cancer?* BMC Med., 2016. **14**: p. 73.

11. Pardoll, D.M., *The blockade of immune checkpoints in cancer immunotherapy.* Nat. Rev. Cancer, 2012. **12**(4): p. 252-64.

12. Rosenberg, S.A., J.C. Yang, and N.P. Restifo, *Cancer immunotherapy: moving beyond current vaccines.* Nat. Med., 2004. **10**(9): p. 909-15.

13. Topalian, S.L., F.S. Hodi, J.R. Brahmer, S.N. Gettinger, D.C. Smith, D.F. McDermott, J.D. Powderly, R.D. Carvajal, J.A. Sosman, M.B. Atkins, P.D. Leming, D.R. Spigel, S.J. Antonia, L. Horn, C.G. Drake, D.M. Pardoll, L. Chen, W.H. Sharfman, R.A. Anders, J.M. Taube, T.L. McMiller, H. Xu, A.J. Korman, M. Jure-Kunkel, S. Agrawal, D. McDonald, G.D. Kollia, A. Gupta, J.M. Wigginton, and M. Sznol, *Safety, activity, and immune correlates of anti-PD-1 antibody in cancer.* N. Engl. J. Med., 2012. **366**(26): p. 2443-54.

14. Hodi, F.S., S.J. O'Day, D.F. McDermott, R.W. Weber, J.A. Sosman, J.B. Haanen, R. Gonzalez, C. Robert, D. Schadendorf, J.C. Hassel, W. Akerley, A.J. van den Eertwegh, J. Lutzky, P. Lorigan, J.M. Vaubel, G.P. Linette, D. Hogg, C.H. Ottensmeier, C. Lebbe, C. Peschel, I. Quirt, J.I. Clark, J.D. Wolchok, J.S. Weber, J. Tian, M.J. Yellin, G.M. Nichol, A. Hoos, and W.J. Urba, *Improved survival with ipilimumab in patients with metastatic melanoma.* N. Engl. J. Med., 2010. **363**(8): p. 711-23.

15. Brahmer, J.R., S.S. Tykodi, L.Q. Chow, W.J. Hwu, S.L. Topalian, P. Hwu, C.G. Drake, L.H. Camacho, J. Kauh, K. Odunsi, H.C. Pitot, O. Hamid, S. Bhatia, R. Martins, K. Eaton, S. Chen, T.M. Salay, S. Alaparthy, J.F. Grosso, A.J. Korman, S.M. Parker, S. Agrawal, S.M. Goldberg, D.M. Pardoll, A. Gupta, and J.M. Wigginton, *Safety and activity of anti-PD-L1 antibody in patients with advanced cancer.* N. Engl. J. Med., 2012. **366**(26): p. 2455-65.

16. Guo, C., M.H. Manjili, J.R. Subjeck, D. Sarkar, P.B. Fisher, and X.Y. Wang, *Therapeutic cancer vaccines: past, present, and future.* Adv. Cancer Res., 2013. **119**: p. 421-75.

17. Plotkin, S., *History of vaccination.* Proc. Natl. Acad. Sci. U. S. A., 2014. **111**(34): p. 12283-7.

18. Whitney, C.G., F. Zhou, J. Singleton, A. Schuchat, C. Centers for Disease, and Prevention, *Benefits from immunization during the vaccines for children program era - United States, 1994-2013.* MMWR Morb. Mortal. Wkly. Rep., 2014. **63**(16): p. 352-5.

19. Finn, O.J., *Cancer vaccines: Between the idea and the reality.* Nat. Rev. Immunol., 2003. **3**(8): p. 630-641.

20. van der Burg, S.H., R. Arens, F. Ossendorp, T. van Hall, and C.J. Melief, *Vaccines for established cancer: overcoming the challenges posed by immune evasion.* Nat. Rev. Cancer, 2016. **16**(4): p. 219-33.

21. Banchereau, J. and A.K. Palucka, *Dendritic cells as therapeutic vaccines against cancer.* Nat. Rev. Immunol., 2005. **5**(4): p. 296-306.

22. Kantoff, P.W., C.S. Higano, N.D. Shore, E.R. Berger, E.J. Small, D.F. Penson, C.H. Redfern, A.C. Ferrari, R. Dreicer, R.B. Sims, Y. Xu, M.W. Frohlich, P.F. Schellhammer, and I.S. Investigators, *Sipuleucel-T immunotherapy for castration-resistant prostate cancer.* N. Engl. J. Med., 2010. **363**(5): p. 411-22.

23. Fang, R.H., A.V. Kroll, and L. Zhang, *Nanoparticle-Based Manipulation of Antigen-Presenting Cells for Cancer Immunotherapy.* Small, 2015. **11**(41): p. 5483-96.

24. Fang, R.H. and L. Zhang, *Nanoparticle-Based Modulation of the Immune System.* Annu. Rev. Chem. Biomol. Eng., 2016. **7**: p. 305-26.

25. Dagogo-Jack, I. and A.T. Shaw, *Tumour heterogeneity and resistance to cancer therapies.* Nat. Rev. Clin. Oncol., 2017. **15**(2): p. 81-94.

26. Law, S.K., *Antigen shedding and metastasis of tumour cells.* Clin. Exp. Immunol., 1991. **85**(1): p. 1-2.

27. Rabinovich, G.A., D. Gabrilovich, and E.M. Sotomayor, *Immunosuppressive Strategies that are Mediated by Tumor Cells.* Annu. Rev. Immunol., 2007. **25**(1): p. 267-296.

28. Mellman, I., G. Coukos, and G. Dranoff, *Cancer immunotherapy comes of age.* Nature, 2011. **480**(7378): p. 480-489.

29. Rosenberg, S.A., *IL-2: the first effective immunotherapy for human cancer.* J. Immunol., 2014. **192**(12): p. 5451-5458.

30. Chada, S., R. Ramesh, and A.M. Mhashilkar, *Cytokine- and chemokine-based gene therapy for cancer.* Curr. Opin. Mol. Ther., 2003. **5**(5): p. 463-474.

31. Fesnak, A.D., C.H. June, and B.L. Levine, *Engineered T cells: the promise and challenges of cancer immunotherapy.* Nat. Rev. Cancer, 2016. **16**(9): p. 566-581.

32. Brudno, J.N. and J.N. Kochenderfer, *Chimeric antigen receptor T-cell therapies for lymphoma.* Nat. Rev. Clin. Oncol., 2017. **15**(1): p. 31-46.

33. Rosenberg, S.A., N.P. Restifo, J.C. Yang, R.A. Morgan, and M.E. Dudley, *Adoptive cell transfer: a clinical path to effective cancer immunotherapy.* Nat. Rev. Cancer, 2008. **8**(4): p. 299-308.

34. Weiner, L.M., R. Surana, and S. Wang, *Monoclonal antibodies: versatile platforms for cancer immunotherapy.* Nat. Rev. Immunol., 2010. **10**(5): p. 317-327.

35. Gerber, H.P., P. Sapra, F. Loganzo, and C. May, *Combining antibody-drug conjugates and immune-mediated cancer therapy: What to expect?* Biochem. Pharmacol., 2016. **102**: p. 1-6.

36. Ribas, A. and J.D. Wolchok, *Cancer immunotherapy using checkpoint blockade.* Science, 2018. **359**(6382): p. 1350-1355.

37. Yarchoan, M., A. Hopkins, and E.M. Jaffee, *Tumor Mutational Burden and Response Rate to PD-1 Inhibition.* N. Engl. J. Med., 2017. **377**(25): p. 2500-2501.

38. Suen, H., R. Brown, S. Yang, P.J. Ho, J. Gibson, and D. Joshua, *The failure of immune checkpoint blockade in multiple myeloma with PD-1 inhibitors in a phase 1 study.* Leukemia, 2015. **29**(7): p. 1621-1622.

39. Morse, M.A. and H.K. Lyerly, *Checkpoint blockade in combination with cancer vaccines.* Vaccine, 2015. **33**(51): p. 7377-7385.

40. Overwijk, W.W., *Cancer vaccines in the era of checkpoint blockade: the magic is in the adjuvant.* Curr. Opin. Immunol., 2017. **47**: p. 103-109.

41. Dubensky, T.W., Jr. and S.G. Reed, *Adjuvants for cancer vaccines.* Semin. Immunol., 2010. **22**(3): p. 155-61.

42. Petersen, T.R., N. Dickgreber, and I.F. Hermans, *Tumor antigen presentation by dendritic cells.* Crit. Rev. Immunol., 2010. **30**(4): p. 345-86.

43. Slingluff, C.L., *The Present and Future of Peptide Vaccines for Cancer.* Cancer J. Sci. Am., 2011. **17**(5): p. 343-350.

44. Keenan, B.P. and E.M. Jaffee, *Whole Cell Vaccines—Past Progress and Future Strategies.* Semin. Oncol., 2012. **39**(3): p. 276-286.

45. Hammerich, L., A. Binder, and J.D. Brody, *In situ vaccination: Cancer immunotherapy both personalized and off-the-shelf.* Mol. Oncol., 2015. **9**(10): p. 1966-1981.

46. Parato, K.A., D. Senger, P.A.J. Forsyth, and J.C. Bell, *Recent progress in the battle between oncolytic viruses and tumours.* Nat. Rev. Cancer, 2005. **5**(12): p. 965-976.

47. Cheever, M.A. and C.S. Higano, *PROVENGE (Sipuleucel-T) in prostate cancer: the first FDA-approved therapeutic cancer vaccine.* Clin. Cancer Res., 2011. **17**(11): p. 3520-3526.

48. Graddis, T.J., C.J. McMahan, J. Tamman, K.J. Page, and J.B. Trager, *Prostatic acid phosphatase expression in human tissues.* Int. J. Clin. Exp. Pathol., 2011. **4**(3): p. 295-306.

49. Schumacher, T.N. and R.D. Schreiber, *Neoantigens in cancer immunotherapy.* Science, 2015. **348**(6230): p. 69-74.

50. Gros, A., M.R. Parkhurst, E. Tran, A. Pasetto, P.F. Robbins, S. Ilyas, T.D. Prickett, J.J. Gartner, J.S. Crystal, I.M. Roberts, K. Trebska-McGowan, J.R. Wunderlich, J.C. Yang, and S.A. Rosenberg, *Prospective identification of neoantigen-specific lymphocytes in the peripheral blood of melanoma patients.* Nat. Med., 2016. **22**(4): p. 433-438.

51. Fischer, N.O., A. Rasley, M. Corzett, M.H. Hwang, P.D. Hoeprich, and C.D. Blanchette, *Colocalized delivery of adjuvant and antigen using nanolipoprotein particles enhances the immune response to recombinant antigens.* J. Am. Chem. Soc., 2013. **135**(6): p. 2044-2047.

52. An, M., M. Li, J. Xi, and H. Liu, *Silica Nanoparticle as a Lymph Node Targeting Platform for Vaccine Delivery.* ACS Appl. Mater. Interfaces, 2017. **9**(28): p. 23466-23475.

53. Hanson, M.C., A. Bershteyn, M.P. Crespo, and D.J. Irvine, *Antigen delivery by lipid-enveloped PLGA microparticle vaccines mediated by in situ vesicle shedding.* Biomacromolecules, 2014. **15**(7): p. 2475-2481.

54. Fang, R.H., C.M. Hu, K.N. Chen, B.T. Luk, C.W. Carpenter, W. Gao, S. Li, D.E. Zhang, W. Lu, and L. Zhang, *Lipid-insertion enables targeting functionalization of erythrocyte membrane-cloaked nanoparticles.* Nanoscale, 2013. **5**(19): p. 8884-8.

55. Wang, C., P. Li, L. Liu, H. Pan, H. Li, L. Cai, and Y. Ma, *Self-adjuvanted nanovaccine for cancer immunotherapy: Role of lysosomal rupture-induced ROS in MHC class I antigen presentation.* Biomaterials, 2016. **79**: p. 88-100.

56. Radovic-Moreno, A.F., N. Chernyak, C.C. Mader, S. Nallagatla, R.S. Kang, L. Hao, D.A. Walker, T.L. Halo, T.J. Merkel, C.H. Rische, S. Anantatmula, M. Burkhart, C.A. Mirkin, and S.M. Gryaznov, *Immunomodulatory spherical nucleic acids.* Proc. Natl. Acad. Sci. U. S. A., 2015. **112**(13): p. 3892-3897.

57. He, Q., A.R. Mitchell, S.L. Johnson, C. Wagner-Bartak, T. Morcol, and S.J. Bell, *Calcium phosphate nanoparticle adjuvant.* Clin. Diagn. Lab. Immunol., 2000. **7**(6): p. 899-903.

58. Deng, L., T. Mohan, T.Z. Chang, G.X. Gonzalez, Y. Wang, Y.-M. Kwon, S.-M. Kang, R.W. Compans, J.A. Champion, and B.-Z. Wang, *Double-layered protein nanoparticles induce broad protection against divergent influenza A viruses.* Nat. Commun., 2018. **9**(1): p. 359.

59. Bishop, C.J., K.L. Kozielski, and J.J. Green, *Exploring the role of polymer structure on intracellular nucleic acid delivery via polymeric nanoparticles.* J. Control. Release, 2015. **219**: p. 488-499.

60. Petrovsky, N., *Comparative Safety of Vaccine Adjuvants: A Summary of Current Evidence and Future Needs.* Drug Saf., 2015. **38**(11): p. 1059-1074.

61. Tam, H.H., M.B. Melo, M. Kang, J.M. Pelet, V.M. Ruda, M.H. Foley, J.K. Hu, S. Kumari, J. Crampton, A.D. Baldeon, R.W. Sanders, J.P. Moore, S. Crotty, R. Langer, D.G. Anderson, A.K. Chakraborty, and D.J. Irvine, *Sustained antigen availability during germinal center initiation enhances antibody responses to vaccination.* Proc. Natl. Acad. Sci. U. S. A., 2016. **113**(43): p. E6639-E6648.

62. Bachmann, M.F. and G.T. Jennings, *Vaccine delivery: a matter of size, geometry, kinetics and molecular patterns.* Nat. Rev. Immunol., 2010. **10**(11): p. 787-796.

63. Reddy, S.T., A.J. van der Vlies, E. Simeoni, V. Angeli, G.J. Randolph, C.P. O'Neil, L.K. Lee, M.A. Swartz, and J.A. Hubbell, *Exploiting lymphatic transport and complement activation in nanoparticle vaccines.* Nat. Biotechnol., 2007. **25**(10): p. 1159-1164.

64. Shannahan, J.H., W. Bai, and J.M. Brown, *Implications of scavenger receptors in the safe development of nanotherapeutics.* Receptors Clin. Investig., 2015. **2**(3): p. e811.

65. Chen, P., X. Liu, Y. Sun, P. Zhou, Y. Wang, and Y. Zhang, *Dendritic cell targeted vaccines: Recent progresses and challenges.* Hum. Vaccin. Immunother., 2016. **12**(3): p. 612-622.

66. Bale, S.S., S.J. Kwon, D.A. Shah, A. Banerjee, J.S. Dordick, and R.S. Kane, *Nanoparticle-mediated cytoplasmic delivery of proteins to target cellular machinery.* ACS Nano, 2010. **4**(3): p. 1493-1500.

67. Behzadi, S., V. Serpooshan, W. Tao, M.A. Hamaly, M.Y. Alkawareek, E.C. Dreaden, D. Brown, A.M. Alkilany, O.C. Farokhzad, and M. Mahmoudi, *Cellular uptake of nanoparticles: journey inside the cell.* Chem. Soc. Rev., 2017. **46**(14): p. 4218-4244.

68. Dominguez, A.L. and J. Lustgarten, *Targeting the tumor microenvironment with anti-neu/anti-CD40 conjugated nanoparticles for the induction of antitumor immune responses.* Vaccine, 2010. **28**(5): p. 1383-1390.

69. Yuan, H., W. Jiang, C.A. von Roemeling, Y. Qie, X. Liu, Y. Chen, Y. Wang, R.E. Wharen, K. Yun, G. Bu, K.L. Knutson, and B.Y.S. Kim, *Multivalent bi-specific nanobioconjugate engager for targeted cancer immunotherapy.* Nat. Nanotechnol., 2017. **12**(8): p. 763-769.

70. Schütz, C., J.C. Varela, K. Perica, C. Haupt, M. Oelke, and J.P. Schneck, *Antigen-specific T cell Redirectors: a nanoparticle based approach for redirecting T cells.* Oncotarget, 2016. **7**(42): p. 68503-68512.

71. Xu, Z., S. Ramishetti, Y.-C. Tseng, S. Guo, Y. Wang, and L. Huang, *Multifunctional nanoparticles co-delivering Trp2 peptide and CpG adjuvant induce potent cytotoxic T-lymphocyte response against melanoma and its lung metastasis.* J. Control. Release, 2013. **172**(1): p. 259-265.

72. Xu, Z., Y. Wang, L. Zhang, and L. Huang, *Nanoparticle-delivered transforming growth factor-β siRNA enhances vaccination against advanced melanoma by modifying tumor microenvironment.* ACS Nano, 2014. **8**(4): p. 3636-3645.

73. Mullard, A., *New checkpoint inhibitors ride the immunotherapy tsunami.* Nat. Rev. Drug Discov., 2013. **12**(7): p. 489-492.

74. Wang, C., W. Sun, Y. Ye, Q. Hu, H.N. Bomba, and Z. Gu, *In situ activation of platelets with checkpoint inhibitors for post-surgical cancer immunotherapy.* Nat. Biomed. Eng., 2017. **1**: p. 0011.

75. Liu, Q., H. Zhu, K. Tiruthani, L. Shen, F. Chen, K. Gao, X. Zhang, L. Hou, D. Wang, R. Liu, and L. Huang, *Nanoparticle-Mediated Trapping of Wnt Family Member 5A in Tumor Microenvironments Enhances Immunotherapy for B-Raf Proto-Oncogene Mutant Melanoma.* ACS Nano, 2018. **12**(2): p. 1250-1261.

76. de Titta, A., M. Ballester, Z. Julier, C. Nembrini, L. Jeanbart, A.J. van der Vlies, M.A. Swartz, and J.A. Hubbell, *Nanoparticle conjugation of CpG enhances adjuvancy for cellular immunity and memory recall at low dose.* Proc. Natl. Acad. Sci. U. S. A., 2013. **110**(49): p. 19902-19907.

77. Chinnathambi, S., S. Chen, S. Ganesan, and N. Hanagata, *Binding mode of CpG oligodeoxynucleotides to nanoparticles regulates bifurcated cytokine induction via Toll-like receptor 9.* Sci. Rep., 2012. **2**: p. 534.

78. Thomas, S.N., E. Vokali, A.W. Lund, J.A. Hubbell, and M.A. Swartz, *Targeting the tumor-draining lymph node with adjuvanted nanoparticles reshapes the anti-tumor immune response.* Biomaterials, 2014. **35**(2): p. 814-824.

79. Fan, Y., R. Kuai, Y. Xu, L.J. Ochyl, D.J. Irvine, and J.J. Moon, *Immunogenic Cell Death Amplified by Co-localized Adjuvant Delivery for Cancer Immunotherapy.* Nano Lett., 2017. **17**(12): p. 7387-7393.

80. Molino, N.M., M. Neek, J.A. Tucker, E.L. Nelson, and S.-W. Wang, *Display of DNA on Nanoparticles for Targeting Antigen Presenting Cells.* ACS Biomater. Sci. Eng., 2017. **3**(4): p. 496-501.

81. Diwan, M., P. Elamanchili, H. Lane, A. Gainer, and J. Samuel, *Biodegradable nanoparticle mediated antigen delivery to human cord blood derived dendritic cells for induction of primary T cell responses.* J. Drug Target., 2003. **11**(8-10): p. 495-507.

82. Elamanchili, P., C.M.E. Lutsiak, S. Hamdy, M. Diwan, and J. Samuel, *"Pathogen-Mimicking" Nanoparticles for Vaccine Delivery to Dendritic Cells.* J. Immunother., 2007. **30**(4): p. 378-95.

83. Dowling, D.J., E.A. Scott, A. Scheid, I. Bergelson, S. Joshi, C. Pietrasanta, S. Brightman, G. Sanchez-Schmitz, S.D. Van Haren, J. Ninković, D. Kats, C. Guiducci, A. de Titta, D.K. Bonner, S. Hirosue, M.A. Swartz, J.A. Hubbell, and O. Levy, *Toll-like receptor 8 agonist nanoparticles mimic immunomodulating effects of the live BCG vaccine and enhance neonatal innate and adaptive immune responses.* J. Allergy Clin. Immunol., 2017. **140**(5): p. 1339-1350.

84. Fox, C.B., S.J. Sivananthan, M.S. Duthie, J. Vergara, J.A. Guderian, E. Moon, D. Coblentz, S.G. Reed, and D. Carter, *A nanoliposome delivery system to synergistically trigger TLR4 AND TLR7.* J. Nanobiotechnology, 2014. **12**: p. 17.

85. Hanson, M.C., M.P. Crespo, W. Abraham, K.D. Moynihan, G.L. Szeto, S.H. Chen, M.B. Melo, S. Mueller, and D.J. Irvine, *Nanoparticulate STING agonists are potent lymph node–targeted vaccine adjuvants.* J. Clin. Invest., 2015. **125**(6): p. 2532-2546.

86. Wilson, D.R., R. Sen, J.C. Sunshine, D.M. Pardoll, J.J. Green, and Y.J. Kim, *Biodegradable STING agonist nanoparticles for enhanced cancer immunotherapy.* Nanomedicine, 2018. **14**(2): p. 237-246.

87. Lizotte, P.H., A.M. Wen, M.R. Sheen, J. Fields, P. Rojanasopondist, N.F. Steinmetz, and S. Fiering, *In situ vaccination with cowpea mosaic virus nanoparticles suppresses metastatic cancer.* Nat. Nanotechnol., 2016. **11**(3): p. 295-303.

88. Peruzzi, P.P. and E.A. Chiocca, *Cancer immunotherapy: A vaccine from plant virus proteins.* Nat. Nanotechnol., 2016. **11**(3): p. 214-5.

89. Lebel, M.-È., K. Chartrand, E. Tarrab, P. Savard, D. Leclerc, and A. Lamarre, *Potentiating Cancer Immunotherapy Using Papaya Mosaic Virus-Derived Nanoparticles.* Nano Lett., 2016. **16**(3): p. 1826-1832.

90. Schumacher, R., M. Adamina, R. Zurbriggen, M. Bolli, E. Padovan, P. Zajac, M. Heberer, and G.C. Spagnoli, *Influenza virosomes enhance class I restricted CTL induction through CD4+ T cell activation.* Vaccine, 2004. **22**(5-6): p. 714-723.

91. Gilbert, S.C., *Virus-like particles as vaccine adjuvants.* Mol. Biotechnol., 2001. **19**(2): p. 169-177.

92. St John, A.L., C.Y. Chan, H.F. Staats, K.W. Leong, and S.N. Abraham, *Synthetic mast-cell granules as adjuvants to promote and polarize immunity in lymph nodes.* Nat. Mater., 2012. **11**(3): p. 250-257.

93. Sagiv-Barfi, I., D.K. Czerwinski, S. Levy, I.S. Alam, A.T. Mayer, S.S. Gambhir, and R. Levy, *Eradication of spontaneous malignancy by local immunotherapy.* Sci. Transl. Med., 2018. **10**(426): p. eaan4488.

94. Margaroni, M., M. Agallou, K. Kontonikola, K. Karidi, O. Kammona, C. Kiparissides, C. Gaitanaki, and E. Karagouni, *PLGA nanoparticles modified with a TNFα mimicking peptide, soluble Leishmania antigens and MPLA induce T cell priming in vitro via dendritic cell functional differentiation.* Eur. J. Pharm. Biopharm., 2016. **105**: p. 18-31.

95. Zhang, Y., N. Li, H. Suh, and D.J. Irvine, *Nanoparticle anchoring targets immune agonists to tumors enabling anti-cancer immunity without systemic toxicity.* Nat. Commun., 2018. **9**(1): p. 6.

96. Pradhan, P., H. Qin, J.A. Leleux, D. Gwak, I. Sakamaki, L.W. Kwak, and K. Roy, *The effect of combined IL10 siRNA and CpG ODN as pathogen-mimicking microparticles on Th1/Th2 cytokine balance in dendritic cells*

and protective immunity against B cell lymphoma. Biomaterials, 2014. **35**(21): p. 5491-5504.

97. Schmid, D., C.G. Park, C.A. Hartl, N. Subedi, A.N. Cartwright, R.B. Puerto, Y. Zheng, J. Maiarana, G.J. Freeman, K.W. Wucherpfennig, D.J. Irvine, and M.S. Goldberg, *T cell-targeting nanoparticles focus delivery of immunotherapy to improve antitumor immunity.* Nat. Commun., 2017. **8**(1): p. 1747.

98. Kosmides, A.K., J.-W. Sidhom, A. Fraser, C.A. Bessell, and J.P. Schneck, *Dual Targeting Nanoparticle Stimulates the Immune System To Inhibit Tumor Growth.* ACS Nano, 2017. **11**(6): p. 5417-5429.

99. Mi, Y., C.C. Smith, F. Yang, Y. Qi, K.C. Roche, J.S. Serody, B.G. Vincent, and A.Z. Wang, *A Dual Immunotherapy Nanoparticle Improves T-Cell Activation and Cancer Immunotherapy.* Adv. Mater., 2018. **30**(25): p. 1706098.

100. Lee, K.L., A.A. Murray, D.H.T. Le, M.R. Sheen, S. Shukla, U. Commandeur, S. Fiering, and N.F. Steinmetz, *Combination of Plant Virus Nanoparticle-Based in Situ Vaccination with Chemotherapy Potentiates Antitumor Response.* Nano Lett., 2017. **17**(7): p. 4019-4028.

101. An, M., C. Yu, J. Xi, J. Reyes, G. Mao, W.-Z. Wei, and H. Liu, *Induction of necrotic cell death and activation of STING in the tumor microenvironment via cationic silica nanoparticles leading to enhanced antitumor immunity.* Nanoscale, 2018. **10**(19): p. 9311-9319.

102. Min, Y., K.C. Roche, S. Tian, M.J. Eblan, K.P. McKinnon, J.M. Caster, S. Chai, L.E. Herring, L. Zhang, T. Zhang, J.M. DeSimone, J.E. Tepper, B.G. Vincent, J.S. Serody, and A.Z. Wang, *Antigen-capturing nanoparticles improve the abscopal effect and cancer immunotherapy.* Nat. Nanotechnol., 2017. **12**(9): p. 877-882.

103. Jobsri, J., A. Allen, D. Rajagopal, M. Shipton, K. Kanyuka, G.P. Lomonossoff, C. Ottensmeier, S.S. Diebold, F.K. Stevenson, and N. Savelyeva, *Plant virus particles carrying tumour antigen activate TLR7 and Induce high levels of protective antibody.* PLoS One, 2015. **10**(2): p. e0118096.

104. Purwada, A., Y.F. Tian, W. Huang, K.M. Rohrbach, S. Deol, A. August, and A. Singh, *Self-Assembly Protein Nanogels for Safer Cancer Immunotherapy.* Adv. Healthc. Mater., 2016. **5**(12): p. 1413-1419.

105. Rudra, J.S., S. Mishra, A.S. Chong, R.A. Mitchell, E.H. Nardin, V. Nussenzweig, and J.H. Collier, *Self-assembled peptide nanofibers raising durable antibody responses against a malaria epitope.* Biomaterials, 2012. **33**(27): p. 6476-6484.

106. Wang, H., Z. Luo, Y. Wang, T. He, C. Yang, and others, *Enzyme-Catalyzed Formation of Supramolecular Hydrogels as Promising Vaccine Adjuvants.* Adv. Funct. Mater., 2016. **26**(11): p. 1822-1829.

107. Umeki, Y., K. Mohri, Y. Kawasaki, and others, *Induction of Potent Antitumor Immunity by Sustained Release of Cationic Antigen from a DNA-Based Hydrogel with Adjuvant Activity.* Adv. Funct. Mater., 2015. **25**(36): p. 5758-5767.

108. Luo, Z., Q. Wu, C. Yang, H. Wang, T. He, Y. Wang, Z. Wang, H. Chen, X. Li, C. Gong, and Others, *A Powerful CD8+ T-Cell Stimulating D-Tetra-Peptide Hydrogel as a Very Promising Vaccine Adjuvant.* Adv. Mater., 2017. **29**(5): p. 1601776.

109. Singh, A., R. Agarwal, C.A. Diaz-Ruiz, N.J. Willett, P. Wang, L.A. Lee, Q. Wang, R.E. Guldberg, and A.J. García, *Nanoengineered particles for enhanced intra-articular retention and delivery of proteins.* Adv. Healthc. Mater., 2014. **3**(10): p. 1562-7, 1525.

110. Soni, K.S., S.S. Desale, and T.K. Bronich, *Nanogels: An overview of properties, biomedical applications and obstacles to clinical translation.* J. Control. Release, 2016. **240**: p. 109-126.

111. Sakr, O.S., O. Jordan, and G. Borchard, *Sustained protein release from hydrogel microparticles using layer-by-layer (LbL) technology.* Drug Deliv., 2016. **23**(8): p. 2747-2755.

112. Nakai, T., T. Hirakura, Y. Sakurai, T. Shimoboji, M. Ishigai, and K. Akiyoshi, *Injectable hydrogel for sustained protein release by salt-induced association of hyaluronic acid nanogel.* Macromol. Biosci., 2012. **12**(4): p. 475-83.

113. Nochi, T., Y. Yuki, H. Takahashi, S.-I. Sawada, M. Mejima, T. Kohda, N. Harada, I.G. Kong, A. Sato, N. Kataoka, D. Tokuhara, S. Kurokawa, Y. Takahashi, H. Tsukada, S. Kozaki, K. Akiyoshi, and H. Kiyono, *Nanogel antigenic protein-delivery system for adjuvant-free intranasal vaccines.* Nat. Mater., 2010. **9**(7): p. 572-578.

114. Solbrig, C.M., J.K. Saucier-Sawyer, V. Cody, W.M. Saltzman, and D.J. Hanlon, *Polymer nanoparticles for immunotherapy from encapsulated*

tumor-associated antigens and whole tumor cells. Mol. Pharm., 2007. **4**(1): p. 47-57.

115. Nembrini, C., A. Stano, K.Y. Dane, M. Ballester, A.J. van der Vlies, B.J. Marsland, M.A. Swartz, and J.A. Hubbell, *Nanoparticle conjugation of antigen enhances cytotoxic T-cell responses in pulmonary vaccination.* Proc. Natl. Acad. Sci. U. S. A., 2011. **108**(44): p. E989-97.

116. Ilyinskii, P.O., C.J. Roy, C.P. O'Neil, E.A. Browning, L.A. Pittet, D.H. Altreuter, F. Alexis, E. Tonti, J. Shi, P.A. Basto, M. Iannacone, A.F. Radovic-Moreno, R.S. Langer, O.C. Farokhzad, U.H. von Andrian, L.P.M. Johnston, and T.K. Kishimoto, *Adjuvant-carrying synthetic vaccine particles augment the immune response to encapsulated antigen and exhibit strong local immune activation without inducing systemic cytokine release.* Vaccine, 2014. **32**(24): p. 2882-2895.

117. Moon, J.J., H. Suh, A. Bershteyn, M.T. Stephan, H. Liu, B. Huang, M. Sohail, S. Luo, S.H. Um, H. Khant, J.T. Goodwin, J. Ramos, W. Chiu, and D.J. Irvine, *Interbilayer-crosslinked multilamellar vesicles as synthetic vaccines for potent humoral and cellular immune responses.* Nat. Mater., 2011. **10**(3): p. 243-251.

118. Kuai, R., L.J. Ochyl, K.S. Bahjat, A. Schwendeman, and J.J. Moon, *Designer vaccine nanodiscs for personalized cancer immunotherapy.* Nat. Mater., 2017. **16**(4): p. 489-496.

119. Silva, J.M., E. Zupancic, G. Vandermeulen, V.G. Oliveira, A. Salgado, M. Videira, M. Gaspar, L. Graca, V. Préat, and H.F. Florindo, *In vivo delivery of peptides and Toll-like receptor ligands by mannose-functionalized polymeric nanoparticles induces prophylactic and therapeutic anti-tumor immune responses in a melanoma model.* J. Control. Release, 2015. **198**: p. 91-103.

120. Wang, Y., L. Zhang, Z. Xu, L. Miao, and L. Huang, *mRNA Vaccine with Antigen-Specific Checkpoint Blockade Induces an Enhanced Immune Response against Established Melanoma.* Mol. Ther., 2018. **26**(2): p. 420-434.

121. Shi, G.-N., C.-N. Zhang, R. Xu, J.-F. Niu, H.-J. Song, X.-Y. Zhang, W.-W. Wang, Y.-M. Wang, C. Li, X.-Q. Wei, and D.-L. Kong, *Enhanced antitumor immunity by targeting dendritic cells with tumor cell lysate-loaded chitosan nanoparticles vaccine.* Biomaterials, 2017. **113**: p. 191-202.

122. Liang, R., J. Xie, J. Li, K. Wang, L. Liu, Y. Gao, M. Hussain, G. Shen, J. Zhu, and J. Tao, *Liposomes-coated gold nanocages with antigens and*

adjuvants targeted delivery to dendritic cells for enhancing antitumor immune response. Biomaterials, 2017. **149**: p. 41-50.

123. Qian, Y., H. Jin, S. Qiao, Y. Dai, C. Huang, L. Lu, Q. Luo, and Z. Zhang, *Targeting dendritic cells in lymph node with an antigen peptide-based nanovaccine for cancer immunotherapy.* Biomaterials, 2016. **98**: p. 171-183.

124. Bandyopadhyay, A., R.L. Fine, S. Demento, L.K. Bockenstedt, and T.M. Fahmy, *The impact of nanoparticle ligand density on dendritic-cell targeted vaccines.* Biomaterials, 2011. **32**(11): p. 3094-3105.

125. Saluja, S.S., D.J. Hanlon, F.A. Sharp, E. Hong, D. Khalil, E. Robinson, R. Tigelaar, T.M. Fahmy, and R.L. Edelson, *Targeting human dendritic cells via DEC-205 using PLGA nanoparticles leads to enhanced cross-presentation of a melanoma-associated antigen.* Int. J. Nanomedicine, 2014. **9**: p. 5231-5246.

126. Boussif, O., F. Lezoualc'h, M.A. Zanta, M.D. Mergny, D. Scherman, B. Demeneix, and J.P. Behr, *A versatile vector for gene and oligonucleotide transfer into cells in culture and in vivo: polyethylenimine.* Proc. Natl. Acad. Sci. U. S. A., 1995. **92**(16): p. 7297-7301.

127. Song, C., Y.-W. Noh, and Y.T. Lim, *Polymer nanoparticles for cross-presentation of exogenous antigens and enhanced cytotoxic T-lymphocyte immune response.* Int. J. Nanomedicine, 2016. **11**: p. 3753-3764.

128. Uto, T., M. Toyama, Y. Nishi, T. Akagi, F. Shima, M. Akashi, and M. Baba, *Uptake of biodegradable poly(γ-glutamic acid) nanoparticles and antigen presentation by dendritic cells in vivo.* Results Immunol., 2013. **3**: p. 1-9.

129. Li, D., F. Sun, M. Bourajjaj, Y. Chen, E.H. Pieters, J. Chen, J.B. van den Dikkenberg, B. Lou, M.G.M. Camps, F. Ossendorp, W.E. Hennink, T. Vermonden, and C.F. van Nostrum, *Strong in vivo antitumor responses induced by an antigen immobilized in nanogels via reducible bonds.* Nanoscale, 2016. **8**(47): p. 19592-19604.

130. Li, H., Y. Li, J. Jiao, and H.-M. Hu, *Alpha-alumina nanoparticles induce efficient autophagy-dependent cross-presentation and potent antitumour response.* Nat. Nanotechnol., 2011. **6**(10): p. 645-650.

131. Wang, K., Y. Yang, W. Xue, and Z. Liu, *Cell Penetrating Peptide-Based Redox-Sensitive Vaccine Delivery System for Subcutaneous Vaccination.* Mol. Pharm., 2018. **15**(3): p. 975-984.

132. Steinbach, J.M., Y.-E. Seo, and W.M. Saltzman, *Cell penetrating peptide-modified poly(lactic-co-glycolic acid) nanoparticles with enhanced cell internalization.* Acta Biomater., 2016. **30**: p. 49-61.

133. Wu, Z., K. Chen, I. Yildiz, A. Dirksen, R. Fischer, P.E. Dawson, and N.F. Steinmetz, *Development of viral nanoparticles for efficient intracellular delivery.* Nanoscale, 2012. **4**(11): p. 3567-3576.

134. Kranz, L.M., M. Diken, H. Haas, S. Kreiter, C. Loquai, K.C. Reuter, M. Meng, D. Fritz, F. Vascotto, H. Hefesha, C. Grunwitz, M. Vormehr, Y. Hüsemann, A. Selmi, A.N. Kuhn, J. Buck, E. Derhovanessian, R. Rae, S. Attig, J. Diekmann, R.A. Jabulowsky, S. Heesch, J. Hassel, P. Langguth, S. Grabbe, C. Huber, Ö. Türeci, and U. Sahin, *Systemic RNA delivery to dendritic cells exploits antiviral defence for cancer immunotherapy.* Nature, 2016. **534**(7607): p. 396-401.

135. Goodwin, T.J. and L. Huang, *Investigation of phosphorylated adjuvants co-encapsulated with a model cancer peptide antigen for the treatment of colorectal cancer and liver metastasis.* Vaccine, 2017. **35**(19): p. 2550-2557.

136. Luo, M., H. Wang, Z. Wang, H. Cai, Z. Lu, Y. Li, M. Du, G. Huang, C. Wang, X. Chen, M.R. Porembka, J. Lea, A.E. Frankel, Y.-X. Fu, Z.J. Chen, and J. Gao, *A STING-activating nanovaccine for cancer immunotherapy.* Nat. Nanotechnol., 2017. **12**(7): p. 648-654.

137. Fiering, S., *Cancer immunotherapy: Making allies of phagocytes.* Nat. Nanotechnol., 2017. **12**(7): p. 615-616.

138. Oberli, M.A., A.M. Reichmuth, J.R. Dorkin, M.J. Mitchell, O.S. Fenton, A. Jaklenec, D.G. Anderson, R. Langer, and D. Blankschtein, *Lipid Nanoparticle Assisted mRNA Delivery for Potent Cancer Immunotherapy.* Nano Lett., 2017. **17**(3): p. 1326-1335.

139. Eggermont, L.J., L.E. Paulis, J. Tel, and C.G. Figdor, *Towards efficient cancer immunotherapy: advances in developing artificial antigen-presenting cells.* Trends Biotechnol., 2014. **32**(9): p. 456-465.

140. Turtle, C.J. and S.R. Riddell, *Artificial Antigen-Presenting Cells for Use in Adoptive Immunotherapy.* Cancer J., 2010. **16**(4): p. 374-381.

141. Steenblock, E.R. and T.M. Fahmy, *A comprehensive platform for ex vivo T-cell expansion based on biodegradable polymeric artificial antigen-presenting cells.* Mol. Ther., 2008. **16**(4): p. 765-772.

142. Perica, K., A. De León Medero, M. Durai, Y.L. Chiu, J.G. Bieler, L. Sibener, M. Niemöller, M. Assenmacher, A. Richter, M. Edidin, M. Oelke, and J. Schneck, *Nanoscale artificial antigen presenting cells for T cell immunotherapy.* Nanomedicine, 2014. **10**(1): p. 119-129.

143. Zhang, Q., W. Wei, P. Wang, L. Zuo, F. Li, J. Xu, X. Xi, X. Gao, G. Ma, and H.-Y. Xie, *Biomimetic Magnetosomes as Versatile Artificial Antigen-Presenting Cells to Potentiate T-Cell-Based Anticancer Therapy.* ACS Nano, 2017. **11**(11): p. 10724-10732.

144. Meyer, R.A., J.C. Sunshine, K. Perica, A.K. Kosmides, K. Aje, J.P. Schneck, and J.J. Green, *Biodegradable nanoellipsoidal artificial antigen presenting cells for antigen specific T-cell activation.* Small, 2015. **11**(13): p. 1519-1525.

145. Hu, C.M.J., R.H. Fang, and L.F. Zhang, *Erythrocyte-Inspired Delivery Systems.* Adv. Healthc. Mater., 2012. **1**(5): p. 537-547.

146. Fang, R.H., C.M.J. Hu, and L.F. Zhang, *Nanoparticles disguised as red blood cells to evade the immune system.* Expert Opin. Biol. Th., 2012. **12**(4): p. 385-389.

147. Dehaini, D., R.H. Fang, and L. Zhang, *Biomimetic strategies for targeted nanoparticle delivery.* Bioeng. Transl. Med., 2016. **1**(1): p. 30-46.

148. Yoo, J.W., D.J. Irvine, D.E. Discher, and S. Mitragotri, *Bio-inspired, bioengineered and biomimetic drug delivery carriers.* Nat. Rev. Drug Discov., 2011. **10**(7): p. 521-35.

149. Fang, R.H., A.V. Kroll, W.W. Gao, and L.F. Zhang, *Cell Membrane Coating Nanotechnology.* Adv. Mater., 2018. **30**(23): p. 1706759.

150. Kroll, A.V., R.H. Fang, and L.F. Zhang, *Biointerfacing and Applications of Cell Membrane-Coated Nanoparticles.* Bioconjug. Chem., 2017. **28**(1): p. 23-32.

151. Fang, R.H., Y. Jiang, J.C. Fang, and L.F. Zhang, *Cell membrane-derived nanomaterials for biomedical applications.* Biomaterials, 2017. **128**: p. 69-83.

152. Hu, C.-M.J., L. Zhang, S. Aryal, C. Cheung, R.H. Fang, and L. Zhang, *Erythrocyte membrane-camouflaged polymeric nanoparticles as a biomimetic delivery platform.* Proc. Natl. Acad. Sci. U. S. A., 2011. **108**(27): p. 10980-10985.

153. Hu, C.M., R.H. Fang, B.T. Luk, K.N. Chen, C. Carpenter, W. Gao, K. Zhang, and L. Zhang, *'Marker-of-self' functionalization of nanoscale particles through a top-down cellular membrane coating approach.* Nanoscale, 2013. **5**(7): p. 2664-8.

154. Aryal, S., C.M. Hu, R.H. Fang, D. Dehaini, C. Carpenter, D.E. Zhang, and L. Zhang, *Erythrocyte membrane-cloaked polymeric nanoparticles for controlled drug loading and release.* Nanomedicine (Lond.), 2013. **8**(8): p. 1271-80.

155. Gao, W., C.M. Hu, R.H. Fang, B.T. Luk, J. Su, and L. Zhang, *Surface functionalization of gold nanoparticles with red blood cell membranes.* Adv. Mater., 2013. **25**(26): p. 3549-53.

156. Chai, Z., X. Hu, X. Wei, C. Zhan, L. Lu, K. Jiang, B. Su, H. Ruan, D. Ran, R.H. Fang, L. Zhang, and W. Lu, *A facile approach to functionalizing cell membrane-coated nanoparticles with neurotoxin-derived peptide for brain-targeted drug delivery.* J. Control. Release, 2017. **264**: p. 102-111.

157. Wei, X.L., M. Ying, D. Dehaini, Y.Y. Su, A.V. Kroll, J.R. Zhou, W.W. Gao, R.H. Fang, S. Chien, and L.F. Zhang, *Nanoparticle Functionalization with Platelet Membrane Enables Multifactored Biological Targeting and Detection of Atherosclerosis.* ACS Nano, 2018. **12**(1): p. 109-116.

158. Hu, C.-M.J., R.H. Fang, K.-C. Wang, B.T. Luk, S. Thamphiwatana, D. Dehaini, P. Nguyen, P. Angsantikul, C.H. Wen, A.V. Kroll, C. Carpenter, M. Ramesh, V. Qu, S.H. Patel, J. Zhu, W. Shi, F.M. Hofman, T.C. Chen, W. Gao, K. Zhang, S. Chien, and L. Zhang, *Nanoparticle biointerfacing by platelet membrane cloaking.* Nature, 2015. **526**(7571): p. 118-121.

159. Fang, R.H., C.-M.J. Hu, B.T. Luk, W. Gao, J.A. Copp, Y. Tai, D.E. O'Connor, and L. Zhang, *Cancer cell membrane-coated nanoparticles for anticancer vaccination and drug delivery.* Nano Lett., 2014. **14**(4): p. 2181-2188.

160. Thamphiwatana, S., P. Angsantikul, T. Escajadillo, Q. Zhang, J. Olson, B.T. Luk, S. Zhang, R.H. Fang, W. Gao, V. Nizet, and L. Zhang, *Macrophage-like nanoparticles concurrently absorbing endotoxins and proinflammatory cytokines for sepsis management.* Proc. Natl. Acad. Sci. U. S. A., 2017. **114**(43): p. 11488-11493.

161. Lai, P.Y., R.Y. Huang, S.Y. Lin, Y.H. Lin, and C.W. Chang, *Biomimetic stem cell membrane-camouflaged iron oxide nanoparticles for theranostic applications.* RSC Adv., 2015. **5**(119): p. 98222-98230.

162. Silva, A.K.A., R. Di Corato, T. Pellegrino, S. Chat, G. Pugliese, N. Luciani, F. Gazeau, and C. Wilhelm, *Cell-derived vesicles as a bioplatform for the encapsulation of theranostic nanomaterials.* Nanoscale, 2013. **5**(23): p. 11374-11384.

163. Dehaini, D., X. Wei, R.H. Fang, S. Masson, P. Angsantikul, B.T. Luk, Y. Zhang, M. Ying, Y. Jiang, A.V. Kroll, W. Gao, and L. Zhang, *Erythrocyte-Platelet Hybrid Membrane Coating for Enhanced Nanoparticle Functionalization.* Adv. Mater., 2017. **29**(16): p. 1606209.

164. Chen, Y., M. Chen, Y. Zhang, J.H. Lee, T. Escajadillo, H. Gong, R.H. Fang, W. Gao, V. Nizet, and L. Zhang, *Broad-Spectrum Neutralization of Pore-Forming Toxins with Human Erythrocyte Membrane-Coated Nanosponges.* Adv. Healthc. Mater., 2018: p. 1701366.

165. Hu, C.M.J., R.H. Fang, J. Copp, B.T. Luk, and L.F. Zhang, *A biomimetic nanosponge that absorbs pore-forming toxins.* Nat. Nanotechnol., 2013. **8**(5): p. 336-340.

166. Fang, R.H., B.T. Luk, C.M. Hu, and L. Zhang, *Engineered nanoparticles mimicking cell membranes for toxin neutralization.* Adv. Drug Deliv. Rev., 2015. **90**: p. 69-80.

167. Angsantikul, P., S. Thamphiwatana, W. Gao, and L. Zhang, *Cell Membrane-Coated Nanoparticles As an Emerging Antibacterial Vaccine Platform.* Vaccines, 2015. **3**(4): p. 814-828.

168. Mendoza, N., P. Ravanfar, A. Satyaprakah, S. Pillai, and R. Creed, *Existing antibacterial vaccines.* Dermatol. Ther., 2009. **22**(2): p. 129-142.

169. Angsantikul, P., R.H. Fang, and L.F. Zhang, *Toxoid Vaccination against Bacterial Infection Using Cell Membrane-Coated Nanoparticles.* Bioconjug. Chem., 2018. **29**(3): p. 604-612.

170. Hu, C.-M.J., R.H. Fang, B.T. Luk, and L. Zhang, *Nanoparticle-detained toxins for safe and effective vaccination.* Nat. Nanotechnol., 2013. **8**(12): p. 933-938.

171. Wang, F., R.H. Fang, B.T. Luk, C.-M.J. Hu, S. Thamphiwatana, D. Dehaini, P. Angsantikul, A.V. Kroll, Z. Pang, W. Gao, W. Lu, and L. Zhang, *Nanoparticle-Based Antivirulence Vaccine for the Management of Methicillin-Resistant Skin Infection.* Adv. Funct. Mater., 2016. **26**(10): p. 1628-1635.

172. Wei, X., J. Gao, F. Wang, M. Ying, P. Angsantikul, A.V. Kroll, J. Zhou, W. Gao, W. Lu, R.H. Fang, and L. Zhang, *In Situ Capture of Bacterial Toxins for Antivirulence Vaccination.* Adv. Mater., 2017. **29**(33): p. 1701644.

173. Wang, S., J. Gao, and Z. Wang, *Outer membrane vesicles for vaccination and targeted drug delivery.* Wiley Interdiscip. Rev. Nanomed. Nanobiotechnol., 2018: p. e1523.

174. Petousis-Harris, H., J. Paynter, J. Morgan, P. Saxton, B. McArdle, F. Goodyear-Smith, and S. Black, *Effectiveness of a group B outer membrane vesicle meningococcal vaccine against gonorrhoea in New Zealand: a retrospective case-control study.* Lancet, 2017. **390**(10102): p. 1603-1610.

175. Rosenthal, J.A., L. Chen, J.L. Baker, D. Putnam, and M.P. DeLisa, *Pathogen-like particles: biomimetic vaccine carriers engineered at the nanoscale.* Curr. Opin. Biotechnol., 2014. **28**: p. 51-58.

176. Gao, W., R.H. Fang, S. Thamphiwatana, B.T. Luk, J. Li, P. Angsantikul, Q. Zhang, C.-M.J. Hu, and L. Zhang, *Modulating antibacterial immunity via bacterial membrane-coated nanoparticles.* Nano Lett., 2015. **15**(2): p. 1403-1409.

177. Guo, Y., D. Wang, Q. Song, T. Wu, X. Zhuang, Y. Bao, M. Kong, Y. Qi, S. Tan, and Z. Zhang, *Erythrocyte Membrane-Enveloped Polymeric Nanoparticles as Nanovaccine for Induction of Antitumor Immunity against Melanoma.* ACS Nano, 2015. **9**(7): p. 6918-6933.

178. Kroll, A.V., R.H. Fang, Y. Jiang, J. Zhou, X. Wei, C.L. Yu, J. Gao, B.T. Luk, D. Dehaini, W. Gao, and L. Zhang, *Nanoparticulate Delivery of Cancer Cell Membrane Elicits Multiantigenic Antitumor Immunity.* Adv. Mater., 2017. **29**(47): p. 1703969.

179. Oyewumi, M.O., A. Kumar, and Z. Cui, *Nano-microparticles as immune adjuvants: correlating particle sizes and the resultant immune responses.* Expert Rev. Vaccines, 2010. **9**(9): p. 1095-1107.

180. Joshi, V.B., S.M. Geary, and A.K. Salem, *Biodegradable Particles as Vaccine Delivery Systems: Size Matters.* AAPS J., 2013. **15**(1): p. 85-94.

181. Manolova, V., A. Flace, M. Bauer, K. Schwarz, P. Saudan, and M.F. Bachmann, *Nanoparticles target distinct dendritic cell populations according to their size.* Eur. J. Immunol., 2008. **38**(5): p. 1404-1413.

182. Foged, C., B. Brodin, S. Frokjaer, and A. Sundblad, *Particle size and surface charge affect particle uptake by human dendritic cells in an in vitro model.* Int. J. Pharm., 2005. **298**(2): p. 315-322.

183. Castelli, C., L. Rivoltini, G. Andreola, M. Carrabba, N. Renkvist, and G. Parmiani, *T-cell recognition of melanoma-associated antigens.* J. Cell. Physiol., 2000. **182**(3): p. 323-331.

184. Yang, R., J. Xu, L. Xu, X. Sun, Q. Chen, Y. Zhao, R. Peng, and Z. Liu, *Cancer Cell Membrane-Coated Adjuvant Nanoparticles with Mannose Modification for Effective Anticancer Vaccination.* ACS Nano, 2018. **12**(6): p. 5121-5129.

185. Kang, T., Y. Huang, Q. Zhu, H. Cheng, Y. Pei, J. Feng, M. Xu, G. Jiang, Q. Song, T. Jiang, H. Chen, X. Gao, and J. Chen, *Necroptotic cancer cells-mimicry nanovaccine boosts anti-tumor immunity with tailored immune-stimulatory modality.* Biomaterials, 2018. **164**: p. 80-97.

Chapter 2

Cancer Cell Membrane-Coated Nanoparticles for Anticancer Vaccination

2.1 Introduction

Recent successes in the field of immunotherapy have provided convincing evidence that, if properly stimulated, the immune system is capable of successfully battling a variety of cancer types [1-3]. Despite this fact, an effective anticancer vaccine that is widely applicable and facile to administer, while highly sought after, has continued to remain elusive [4, 5]. Fundamentally, the challenge lies in the need to generate potent and specific immune responses that enable the body to successfully distinguish between healthy and diseased tissue [6]. By the time a neoplastic growth reaches the malignant stage, the most immunogenic tumor-specific antigens have generally been eliminated via negative selection [7, 8]. Some promising strategies under clinical investigation have focused on common tumor-associated antigens, which are dysregulated wild-type proteins [9, 10]. However, the applicability of such single-antigen approaches is dependent on tumor phenotype, and they may also be subject to some of the same limitations facing targeted monotherapies as tumors evolve mechanisms of escape [11, 12]. On the other end of the spectrum, whole cell vaccine preparations are capable of delivering a wide range of autologous antigens [13, 14], but they have traditionally been ineffective. This may be a result of significant interference from a surplus of nontumor-related antigenic material [15] or difficulties in direct administration, which have necessitated more complex cell-based strategies [14, 16, 17]. Additionally, the immunosuppressive microenvironment of established tumors is

often hard to break [18, 19], leading to suboptimal efficacy despite effective training of the immune system.

Advances in genomics have enabled the elucidation of individual cancer mutanomes, which can be leveraged to identify multiple vaccine epitopes on a personalized level [20, 21]. Other studies have demonstrated that high mutational burden can lead to neoantigen targets that are recognized by the immune system, and this correlates with clinical response to checkpoint blockade therapies [22, 23]. While personalized epitope identification and vaccine manufacture may currently not be practical at large-scale, these findings confirm that, despite the challenges facing whole cell formulations, there is a wealth of relevant antigens to be found in autologous tumor material. Applying the principles of biomimetic nanotechnology [24-26], we explored the presentation of cancer-derived membrane material in a context that could enable potent, multiantigenic immune responses for anticancer vaccine design (Figure 2.1). It was demonstrated that nanoparticulate delivery of the membrane, along with an immunostimulatory adjuvant, could facilitate enhanced antigen presentation, leading to the activation of tumor-specific cellular responses. Further, when used in conjunction with checkpoint blockade therapy to help break tumor immunosuppression [27-29], the nanovaccine formulation was able to achieve significant control of tumor growth in a therapeutic setting.

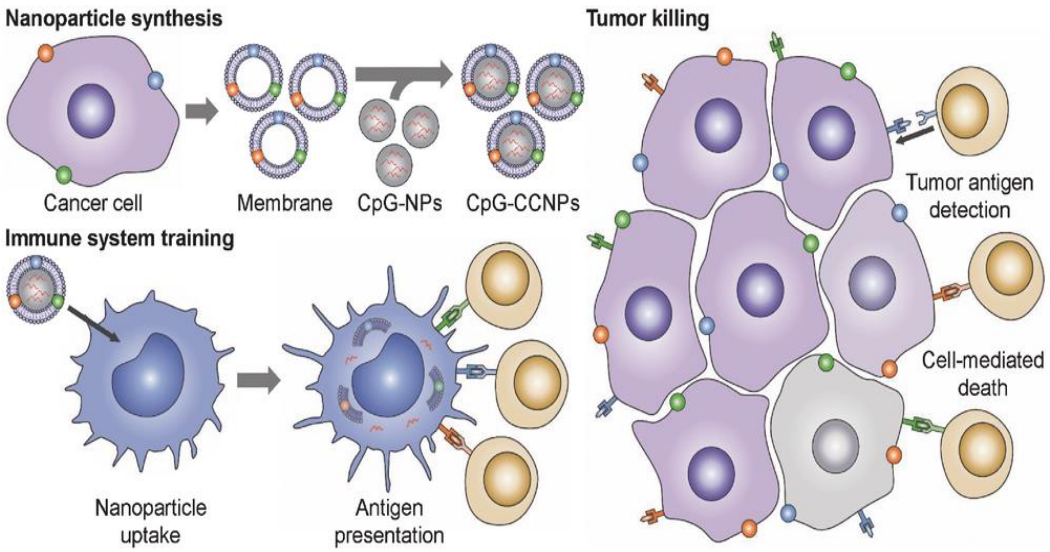

Figure 2.1: Schematic of CpG-CCNPs for anticancer vaccination. Membrane derived from cancer cells (purple), along with the associated tumor antigens (small colored spheres), is coated onto adjuvant-loaded nanoparticle cores (CpG-NPs) to yield a nanoparticulate anticancer vaccine (CpG-CCNPs). Upon delivery to antigen presenting cells (blue), the vaccine formulation enables activation of T cells (tan) with multiple specificities. After detecting the antigens present on the tumor, the T cells are capable of initiating cancer cell death (gray).

2.2 Experimental Methods

2.2.1 B16-F10 Murine Melanoma Cell Culture and Membrane Derivation

B16-F10 mouse melanoma cells (CRL-6475; American Type Culture Collection) were cultured at 37 °C with 5% CO_2 in T175 tissue culture flasks

(Becton Dickinson) with Dulbecco's Modified Eagle Medium (DMEM; Mediatech) supplemented with 10% bovine growth serum (Hyclone) and 1% penicillin-streptomycin (Gibco). At 80–90% confluency, ≈16–18 million cells per flask were collected in phosphate buffered saline (PBS; Mediatech) by scraping, pelleted at 700 × *g* for 7 min in a Sorvall Legend Micro21R centrifuge, then resuspended in a 50:50 solution of cryopreservation medium (Hyclone) and complete DMEM. Cell aliquots were stored at −20 °C before use. To derive membrane, cells were first washed in a starting buffer containing 30 × 10^{-3} m Tris-HCl pH 7.0 (Quality Biological) with 0.0759 m sucrose (Sigma-Aldrich) and 0.225 m D-mannitol (Sigma-Aldrich), then mechanically disrupted in the presence of phosphatase inhibitor and protease inhibitor cocktails (Sigma-Aldrich) using a Kinematica Polytron PT 10/35 probe homogenizer at 70% power for 15 passes. Membrane was separated from the resulting homogenate by differential centrifugation using a Beckman Coulter Optima L-90K Ultracentrifuge. Homogenate was pelleted at 10 000 × *g* for 25 min, and the supernatant was then pelleted at 150 000 × *g* for 35 min. The resulting pellet of cell membrane was washed in 0.2 × 10^{-3} m ethylenediaminetetraacetic acid (EDTA; USB Corporation) in DNase free/RNase free water (Invitrogen) and stored in the same solution at −20 °C until use. Total membrane protein content was quantified by a BCA protein assay kit (Pierce).

2.2.2 Cancer Cell Membrane-Coated Nanoparticle Preparation and Characterization

Polymeric cores were prepared using 0.18 dL g^{-1} carboxyl-terminated 50:50 poly(lactic-*co*-glycolic) acid (PLGA; LACTEL Absorbable Polymers) using a double emulsion process. PLGA was dissolved in dichloromethane at a concentration of 50 mg mL^{-1}. 500 µL of polymer was added to 100 µL of 200 × 10^{-3} m Tris-HCl pH 8 and sonicated using a Fisher Scientific 150E Sonic Dismembrator at 70% power pulsed (2 s on/1 s off) for 1 min. An outer aqueous phase consisting of 5 mL of 10 × 10^{-3} m Tris-HCl pH 8 was added to the polymer solution and sonicated at the same setting for 2 min. The emulsion was then added to 10 mL of 10 × 10^{-3} m Tris-HCl pH 8 and magnetically stirred at 700 × *g* for 2.5 h. After stirring, the particles were pelleted at 21 100 × *g* for 8 min, and washed twice in 10 × 10^{-3} m Tris-HCl pH 8. Adjuvant-loaded polymeric cores (CpG-NPs) were made by including CpG oligodeoxynucleotide 1826 (CpG), synthesized using the sequence 5′-TCCATGACGTTCCTGACGTT-3 with all phosphorothioate bonds (Integrated DNA Technologies), at 500 × 10^{-6} m to the inner phase of the double emulsion during nanoparticle synthesis. To optimize the loading, CpG-NPs were made with CpG inputs of 250, 500, 1000, and 2000 pmol per 1 mg of PLGA. Each formulation was lyophilized overnight, then resuspended in 1 mL of acetone. PLGA was precipitated and pelleted with the addition of 1 mL water followed by centrifugation at 21 100 × *g* for 20 min. CpG concentration of the supernatants were

measured using a Quant-iT Oligreen ssDNA quantification kit (Invitrogen) according to manufacturer's instructions. Further studies employed an initial input of 1000 pmol CpG per 1 mg of PLGA.

B16-F10 cancer cell membrane-coated CpG-NPs (CpG-CCNPs) were made by pelleting the CpG-NP cores and resuspending them in solution containing B16-F10 cell membrane. The mixture was sonicated in a 1.5 mL disposable sizing cuvette (Brandtech) using a Fisher Scientific FS30D bath sonicator at a frequency of 42 kHz and a power of 100 W for 2 min. The nanoparticles were washed twice in 10×10^{-3} m Tris-HCl pH 8, and resuspended to a concentration of 25 mg polymer per 1 mL of solution in 5×10^{-3} m Tris-HCl pH 7.5 and 0.2×10^{-3} m EDTA in DNase free/RNase free water for *in vitro* studies or in 10% sucrose with the same buffer concentrations for *in vivo* studies. If not used immediately, particles were stored at −20 °C. In the study, CpG-CCNPs were fabricated with 100 µg of membrane protein per 1 mg of PLGA. Size and surface zeta potential of CCNPs were determined through DLS measurements using a Malvern ZEN 3600 Zetasizer. To test the stability of CCNPs in 10% sucrose solution, particles were stored at 4 °C for 2 weeks with size measured by DLS every other day. The morphology of CCNPs was examined by transmission electron microscopy using a Zeiss Libra 120 PLUS EF-TEM. Samples were resuspended in 10×10^{-3} m Tris-HCl pH 8, deposited onto a glow discharged carbon-coated 400 square mesh copper grid (Electron Microscopy Sciences), and negatively stained with 1 wt% uranyl acetate (Electron Microscopy Sciences).

2.2.3 Membrane Antigen Retention

Identification of characteristic B16-F10 tumor antigens was completed via western blotting. B16-F10 whole cells were collected from culture by scraping, lysed using 0.2% Triton X-100 (Sigma-Aldrich) in water, and sonicated. B16-F10 lysed cells, B16-F10 membrane, and CpG-CCNPs were analyzed for protein content using a BCA assay, then each diluted to 0.2 mg mL^{-1} in water. Each sample was then mixed with NuPAGE 4 × lithium dodecyl sulfate sample loading buffer (Novex) and heated for 10 min at 70 °C. 25 μL of each sample was loaded into 12-well Bolt 4–12% Bis-Tris gels (Invitrogen) and run at 165 V for 45 min in 3-(*N*-morpholino)propanesulfonic acid running buffer (Novex). Proteins were transferred to 0.45 μm nitrocellulose membrane (Pierce) in Bolt transfer buffer (Novex) at 10 V for 60 min. After blocking with 5% milk (Genesee Scientific) in PBS with 0.05% Tween 20 (National Scientific), blots were immunostained with mouse antimouse gp100 (EP4863(2); Abcam), rabbit antimouse TRP2 (E-10; Santa Cruz Biotechnology), or mouse antimouse MART1 (A103; Santa Cruz Biotechnology). The appropriate horseradish peroxidase-conjugated secondary (Biolegend) was used for secondary staining. Membranes were developed with ECL western blotting substrate (Pierce) in an ImageWorks Mini-Medical/90 Developer.

2.2.4 *In Vitro* Uptake and Activity

All animal studies were designed and proceeded in compliance to the University of California, San Diego Institutional Animal Care and Use Committee. Female C57BL/6NHsd mice were obtained at 6–10 weeks old from Envigo Harlan. BMDC culture was adapted from a previously published protocol [25]. Healthy mice were euthanized using carbon dioxide asphyxiation followed by cervical dislocation. Both femurs were dissected, cleaned in 70% ethanol, and cut on both ends. Bone marrow was then flushed out of the bone with a 1 mL sterile syringe using warm BMDC basal media consisting of 500 mL Isocove's Modification of DMEM with 2×10^{-3} m L-Glutamine and 25×10^{-3} m 4-(2-hydroxyethyl)-1-piperazineethanesulfonic acid (HEPES) (Mediatech) supplemented with 50 mL USDA certified fetal bovine serum (Omega Scientific), 500 µL 55×10^{-3} m β-mercaptoethanol (Gibco), 5 mL 200×10^{-3} m L-Glutamine (Gibco), and 5 mL penicillin-streptomycin. Cells were then pelleted at $700 \times g$ for 5 min, resuspended in BMDC growth media, consisting of the basal media further supplemented with 10 ng mL^{-1} granulocyte/macrophage-colony stimulating factor (GM-CSF; Biolegend), to a concentration of 1×10^6 cells mL^{-1}, and plated into petri plates at 2×10^6 cells per plate. On the third day of culture, 10 mL of BMDC growth media was added to each plate.

To make CpG-CCNPs with fluorescently labeled polymeric cores, 1,1′-dioctadecyl-3,3,3′,3′-tetramethylindodicarbocyanine, 4-chlorobenzenesulfonate

salt (DiD, ex/em = 644/663 nm; Biotium) was added to the PLGA solution at 0.1 wt% of the polymer during nanoparticle synthesis. For the nanoparticle uptake study, BMDCs were collected on day 5 using 1×10^{-3} mEDTA in PBS. Cells were washed once in PBS, resuspended in BMDC basal media, and plated into 24-well suspension plates. DiD-labeled CpG-CCNPs were added at a final concentration of 1.4 mg mL^{-1}. At each timepoint (0, 15, 30 min, 1, 2, 6, 12, 24 h), media was removed, and the cells were detached with trypsin-EDTA (Gibco). Cells were collected, washed once in trypsin-EDTA, washed twice in PBS, and resuspended in 200 µL of 10% phosphate buffered formalin (Fisher). The adjuvant uptake study was conducted similarly, instead employing CpG-CCNPs synthesized with CpG containing a 5′ 6-FAM modification (Integrated DNA Technologies). Free dye-labeled CpG was used at an equivalent concentration for comparison. For all experiments, after each time point was collected and processed, 1 drop of NucBlue Live ReadyProbe Reagent UV stain (Molecular Probes) was added and data were collected using a Becton Dickinson FacsCanto-II flow cytometer. All data were analyzed using FlowJo software.

The activity of delivered CpG was examined using a BMDC cytokine release assay. BMDCs were plated on day 6 into 96-well plates at a concentration of 8×10^4 cells mL^{-1} in BMDC growth media. Dilutions of CpG-CCNP or free CpG were added to the cells. After 2 h of incubation, the cells were washed three times with fresh BMDC growth media and cultured for another 2 d. Supernatant was then collected and measured for the presence of proinflammatory cytokines

using mouse IL-6 and IL-12p40 ELISA kits (Biolegend) according to manufacturer's instructions.

Antigen and adjuvant colocalization was visualized by imaging BMDCs incubated with dual-labeled CpG-CCNPs. B16-F10 membrane was labeled using CF647 succinimidyl ester dye (Biotium) and used to coat CpG-CCNPs fabricated with FAM-modified CpG. BMDCs were seeded into 8-well chamber slides at 7.5 × 10^4 cells mL^{-1} and incubated with the nanoparticles for 15 min at 0.7 mg mL^{-1}. Cells were then washed three times with PBS, fixed with 10% formalin for 30 min, then washed again three times with PBS and mounted onto coverslips using VECTASHIELD mounting media with DAPI (Vector Laboratories). Samples were imaged on a Deltavision RT Deconvolution Microscope at 60 × magnification.

2.2.5 *In Vivo* Cellular Localization and Dendritic Cell Activation

To assess *in vivo* localization, DiD-labeled CpG-CCNPs were injected subcutaneously into each hock of female C57BL/6NHsd mice. After 24 h, the popliteal lymph nodes were collected into 500 µL of dissociation buffer consisting of 1 mg mL^{-1} collagenase D from *Clostridium histolyticum* (Roche) and 1 mg mL^{-1}DNase I grade II, from bovine pancreas (Roche) in Dulbecco's PBS with calcium and magnesium (Gibco). Lymph nodes were dissociated manually by pipetting and then were stained with fluorescein isothiocyanate (FITC)-labeled antibodies for dendritic cells (antimouse CD11c, N418; Biolegend), macrophages

(antimouse F4/80, BM8; Biolegend), T cells (antimouse CD3, 17A2; Biolegend), B cells (antimouse CD19, 6D5; Biolegend), and granulocytes (antimouse Ly-6G/Ly-6C, RB6-8C5; Biolegend) for 30 min. Appropriate dye-labeled antibody isotypes (Biolegend) were used for gating purposes with cells from an untreated lymph node. After washing, dead cells were labeled with propidium iodide (Biolegend). Data were collected using a Becton Dickinson FACSCanto-II flow cytometer and analyzed using FlowJo software.

Dendritic cell activation following immunization with CpG-CCNPs, CpG-NPs, CCNPs, or additional controls was determined by testing dendritic cell maturation and lymph node cytokine secretion. To test vaccines with antigens and adjuvants delivered as separate components, additional controls of CCNP with free CpG and B16-F10 whole lysate with free CpG were also administered. The CCNPs with free CpG formulation was made by mixing the two components such that the final ratio was 25 mg of PLGA per 3.5 nmol of CpG. Whole cell lysate was prepared by three freeze-thaw cycles at −80 °C for 10 min followed by 10 min at 37 °C. The amount of protein used for the formulation was normalized by the amount of Na^+K^+-ATPase, a characteristic membrane protein, compared with CCNPs as determined by immunoblotting. To examine dendritic cell maturation *in vivo*, 50 μL of each formulation at 25 mg mL^{-1} of nanoparticle, or equivalent, was injected into the hock. After 24 h, the popliteal lymph nodes of all treated mice were collected into 500 μL dissociation buffer and manually dissociated. Cells were stained using FITC antimouse CD11c with either Alexa647-conjugated antimouse

CD40 (HM40-3; Biolegend), CD80 (12-10A1; Biolegend), CD86 (GL-1; Biolegend), or MHC-II (M5/114.15.2; Biolegend). Appropriate dye-labeled antibody isotypes (Biolegend) were used for gating purposes with cells from an untreated lymph node. After 30 min of incubation at 4 °C, the cells were washed and stained with CellTrace Calcein Violet, AM (Molecular Probes) in PBS according to manufacturer's instructions. Data were collected using a Becton Dickinson FACSCanto-II flow cytometer and analyzed using FlowJo software. To analyze cytokine production, lymph node-derived single cell suspensions were plated with 500 μL of BMDC growth media in 24-well tissue culture plates. After 48 h, supernatant was collected and analyzed for cytokine content using IL-6 and IL-12p40 ELISA kits according to the manufacturer's instructions.

2.2.6 Adoptive T Cell Proliferation and Native T Cell Generation

B6.Cg-Thy1^{a}/Cy Tg(TcraTcrb)8Rest/J (pmel-1) transgenic mice were obtained from the Jackson Laboratory at 4–6 weeks old. The spleen, popliteal lymph node, and inguinal lymph nodes of one pmel-1 mouse were collected for dissociation into single cell suspensions. The red blood cells in the spleen were removed using lysis buffer (Biolegend), and all remaining cells were pooled together. CD8+ T cells were separated out using CD8a (Ly-2) microbeads (Miltenyi Biotec) on Miltenyi Biotec MACS LS separation columns per manufacturer's instructions. After separation, cells were washed in PBS and stained with

carboxyfluorescein succinimidyl ester (CFSE; eBiosciences). Cells were then diluted to 2.5×10^6 cells mL^{-1} and 200 µL was transferred to naïve C57BL/6NHsd recipients. 2 h postinjection, each mouse was injected with 50 µL of various vaccine formulations in both hocks. 4 d after treatment, the spleens were collected and dissociated into single cell suspensions. Adoptively transferred T cells were stained for using allophycocyanin (APC)-conjugated antimouse CD8a (53-6.7; Biolegend) and Pacific Blue-conjugated antimouse CD90.1 (OX-7; Biolegend). Data were collected using a Becton Dickinson FACSCanto-II flow cytometer and analyzed using FlowJo software. CFSE dilution was used to assess the degree of T cell proliferation.

To assess the native generation of antigen-specific T cells, C57BL/6NHsd mice were vaccinated subcutaneously with 50 µL of the different formulations in each hock on days 0, 2, and 4. On day 10, spleens were collected and processed into single cell suspensions using mechanical dissociation. After lysing the red blood cells, 5×10^6 splenocytes were plated into 6-well suspension plates and pulsed with either 1 µg mL^{-1} of mouse gp100 peptide with sequence EGSRNQDWL (Anaspec) or 1 µg mL^{-1} of TRP2 peptide with sequence SVYDFFVWL (Anaspec) in BMDC growth media. After 7 d, cells were collected, washed in PBS, and stained with APC-conjugated antimouse CD8a and either phycoerythrin (PE)-labeled H-2Db gp100 tetramer (MBL International) or H-2Kb TRP2 tetramer (MBL International). Data were collected using a Becton Dickinson FACSCanto-II flow cytometer and analyzed using FlowJo software.

2.2.7 *In Vivo* Immunity and Therapeutic Efficacy

To study the protection conferred by vaccination, C57BL/6NHsd mice were vaccinated with 50 µL of the different formulations at 25 mg mL^{-1} of PLGA, or equivalent, on days 0, 7, and 14. On day 20, the right flank of each mouse was shaved and, on day 21, mice were challenged with 2×10^5 B16-F10 cells subcutaneously on the right flank. Tumors were measured every other day and the experimental endpoint was defined as either death or tumor size greater than 200 mm^2.

To study the antitumor therapeutic effect, C57BL/6NHsd mice were first challenged on the right flank with 5×10^4 B16-F10 cells on day 0. On days 1, 2, 4, and 7, mice were vaccinated subcutaneously in the same flank with 200 µL of the nanoparticulate formulations. The subcutaneous route was chosen in this case to accommodate the larger dosage that was employed. The checkpoint blockade cocktail, consisting of 100 µg anti-CTLA4 (9H10; BioXCell) and 200 µg anti-PD1 (RMP1-14; BioXCell) was administered intraperitoneally on the same days. Tumors were measured every other day and the experimental endpoint was defined as either death or tumor size greater than 200 mm^2.

2.3 Results and Discussion

CpG oligodeoxynucleotide 1826 (CpG), a nucleic acid-based immunological adjuvant known to trigger the maturation of antigen presenting cells, was encapsulated into biodegradable poly(lactic-*co*-glycolic acid) (PLGA) nanoparticle cores via a double emulsion process (Figure 2.2a). The amount of CpG that could be loaded started saturating at an initial input of 1 nmol per 1 mg of PLGA, and ≈100 pmol of the adjuvant could be loaded at this ratio. To introduce tumor antigen material, the membrane derived from B16-F10 mouse melanoma cells was coated onto CpG-loaded PLGA cores (CpG-NPs). The process used for coating did not significantly alter the amount of adjuvant within the polymeric cores. Dynamic light scattering (DLS) measurements showed an increase in nanoparticle size after coating, and the zeta potential of the adjuvant-loaded, cancer cell membrane-coated nanoparticles (CpG-CCNPs) increased to approximately that of pure membrane (Figure 2.2b,c). Successful coating was confirmed by transmission electron microscopy (TEM), which revealed a characteristic core–shell structure (Figure 2.2d). Over time, the CpG-CCNPs stayed stable in solution (Figure 2.2e). Importantly, the presence of known membrane-bound tumor-associated antigens [30], including MART1, TRP2, and gp100, was confirmed by western blotting (Figure 2.2f). When normalized by total protein amount, significant antigen enrichment was observed on the derived membrane and CpG-CCNPs when compared with whole cell lysate.

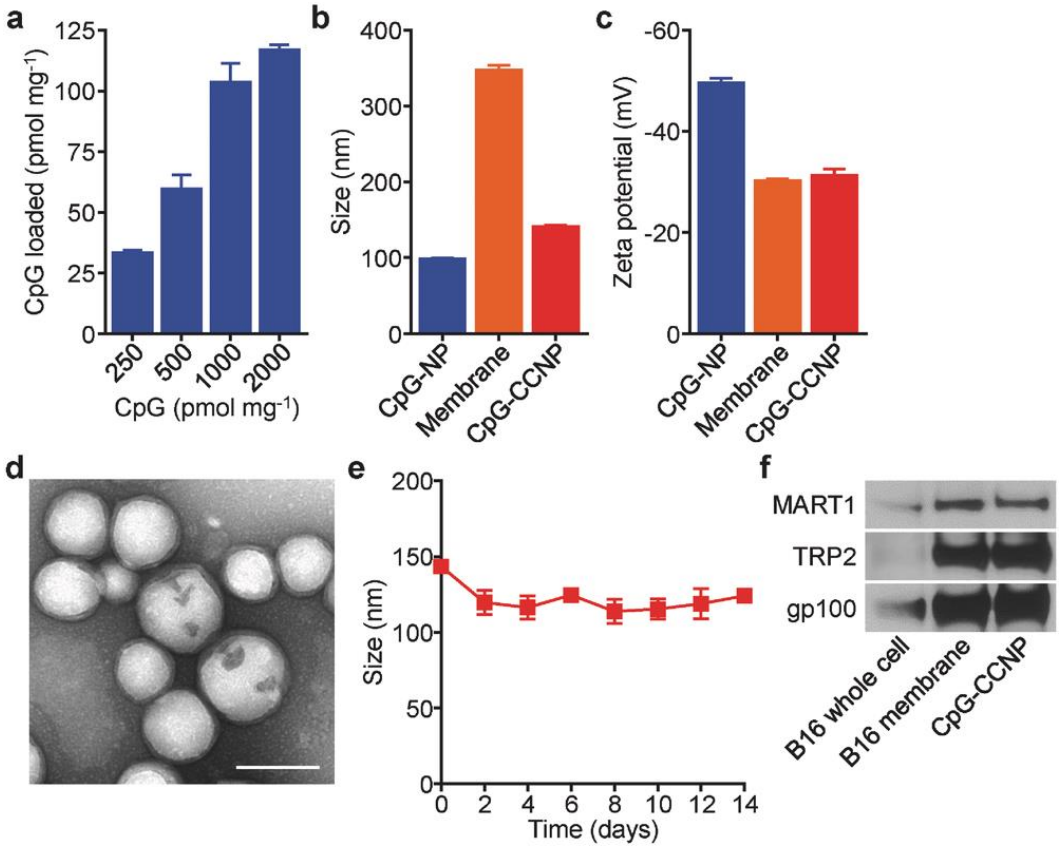

Figure 2.2: Preparation and characterization of CpG-CCNPs. a) CpG encapsulation into PLGA cores with increasing inputs, normalized by polymer weight (n = 3, mean ± SD). b) Size of CpG-NPs, B16-F10 membrane vesicles, and CpG-CCNPs (n = 3; mean ± SD). c) Surface zeta potential of CpG-NPs, B16-F10 membrane vesicles, and CpG-CCNPs (n = 3; mean ± SD). d) TEM image of CpG-CCNPs negatively stained with uranyl acetate. Scale bar = 100 nm. e) Size stability over time of CpG-CCNPs stored in 10% sucrose (n = 3; mean ± SD). f) Western blots for known melanoma-associated antigens MART1, TRP2, and gp100 on B16-F10 cells, B16-F10 membrane, and CpG-CCNPs.

To study the interaction of the nanoformulation with antigen presenting cells, bone marrow-derived dendritic cells (BMDCs) were employed. When incubated with dye-labeled CpG-CCNPs, quick uptake was observed until saturation was achieved at ≈6 h (Figure 2.3a). CpG is known to activate proinflammatory responses in antigen presenting cells [31], which is necessary for generating potent antitumor immunity. Using a fluorescently tagged CpG, the

adjuvant was shown to much more readily be internalized by BMDCs when encapsulated within the membrane-coated nanoparticles, which are in the ideal size range for endocytosis [32, 33] (Figure 2.3b). To test the implications of this enhanced internalization and confirm the integrity of CpG after encapsulation, the biological activity of CpG in free form versus nanoparticulate form was assessed (Figure 2.3c,d). Secretion of two representative proinflammatory cytokines, interleukin-6 (IL-6) and IL-12, was significantly enhanced for the CpG-CCNP formulation, which was approximately an order of magnitude more immunostimulatory than free CpG. This effect is likely due to the fact that nanoparticulate CpG more readily localizes to the endosomal compartment during uptake, where it can engage its endosomal recognition site on toll-like receptor 9 (TLR-9) [34]. It should be noted that CCNPs without adjuvant induced significantly less cytokine secretion when incubated with BMDCs at equivalent nanoparticle concentrations. While the CpG employed in the studies here was murine-specific, other variants could easily be substituted to promote immunity in humans [35]. Further, the integrity of the nanoparticle structure was assessed by fluorescent imaging using dye-labeled CpG and membrane protein, and significant colocalization of the two signals confirmed the ability of the CpG-CCNPs to co-deliver both adjuvant and antigen to the same BMDC (Figure 2.3e). Upon *in vivo* administration subcutaneously via the hock, the nanoformulation could easily be detected at the draining lymph node after 1 h, with some appearing at an adjacent node after 24 h. Little signal was observed at the spleen given its considerable

distance from the injection site. Within the draining lymph node, antigen presenting cells such as dendritic cells and macrophages exhibited the highest percentage of nanoparticle uptake; B cells and granulocytes also displayed some uptake, while the limited amount of signal observed for T cells was likely the result of nonspecific interactions with the nanoformulation (Figure 2.3f).

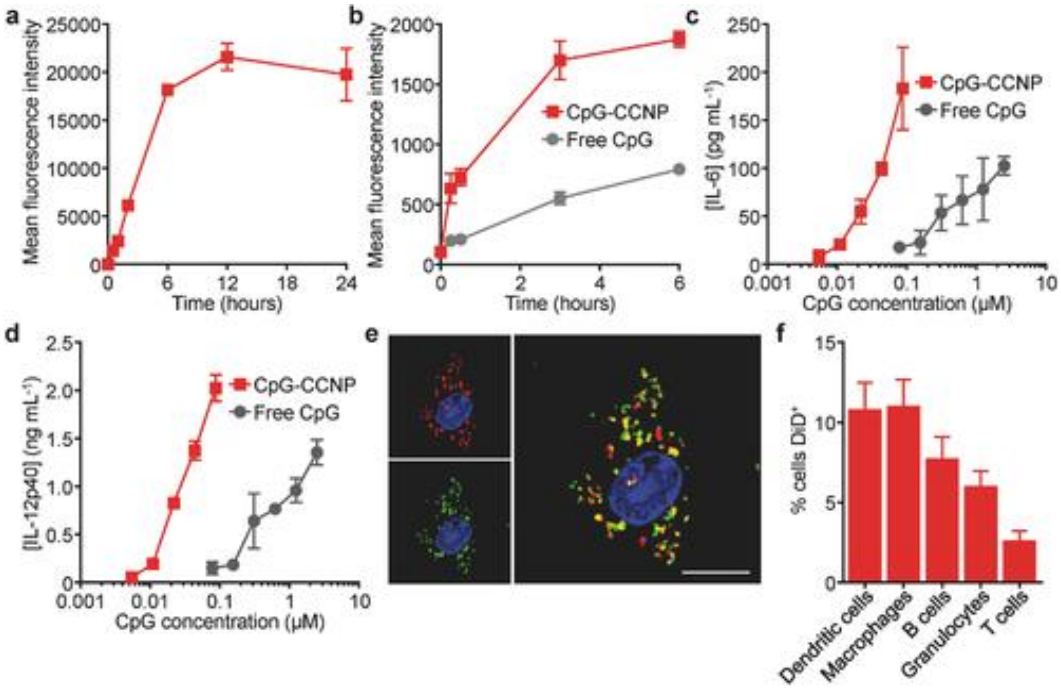

Figure 2.3: Delivery of antigen and adjuvant to immune cells. a) Uptake kinetics of dye-labeled CpG-CCNPs by BMDCs (n = 3; mean ± SD). b) Uptake kinetics of dye-conjugated CpG in free form or within CpG-CCNPs by BMDCs (n = 3; mean ± SD). c,d) Secretion of the proinflammatory cytokines IL-6 (c) and IL-12p40 (d) by BMDCs when incubated with either free CpG or CpG-CCNPs (n = 3; mean ± SD). e) Confocal microscopy colocalization of CpG and membrane proteins upon uptake of dual-labeled CpG-CCNPs by a BMDC. Green = CpG, red = membrane, blue = cell nucleus; scale bar = 10 μm. f) Uptake of dye-labeled CpG-CCNPs by different immune cell subsets in the draining lymph node after *in vivo* administration (n = 6; mean ± SD).

The effect of the nanoformulation on BMDC maturation *in vitro* was studied by looking at the upregulated expression of costimulatory markers CD40, CD80, and CD86, as well as MHC-II. Consistent with the fact that the dendritic cell maturation process is largely driven by the detection of pathogen-associated molecular patterns such as CpG, it was observed that both CpG-CCNPs and CpG-NPs without any antigen were equally potent. Without CpG, the antigen-only CCNP formulation exhibited significantly decreased activity. A similar pattern was seen when assessing the secretion of IL-6 and IL-12 by the BMDCs. When administered *in vivo*, the CpG-CCNP and CpG-NP formulations were likewise able to induce significant dendritic cell maturation at the draining lymph node after 24 h (Figure 2.4a–d). They also outperformed additional controls, including CCNPs with free CpG and whole cell lysate with free CpG, highlighting the advantage of nanoparticulate formulations. The level of cytokine secretion at the draining lymph node was shown to be mostly dependent on the presence of CpG, with all adjuvanted formulations performing similarly (Figure 2.4e,f). This effect was localized, as analysis of cytokine levels in the serum did not yield anything significantly above baseline.

To confirm the utility of the CpG-CCNP formulation for antitumor vaccination, its ability to elicit antigen-specific immune responses was verified using T cell-based assays. First, pmel-1 CD8+ T cells, which specifically recognize a gp100 epitope, were adoptively transferred to recipient mice, which were subsequently vaccinated with the various formulations (Figure 2.5a). Treatment

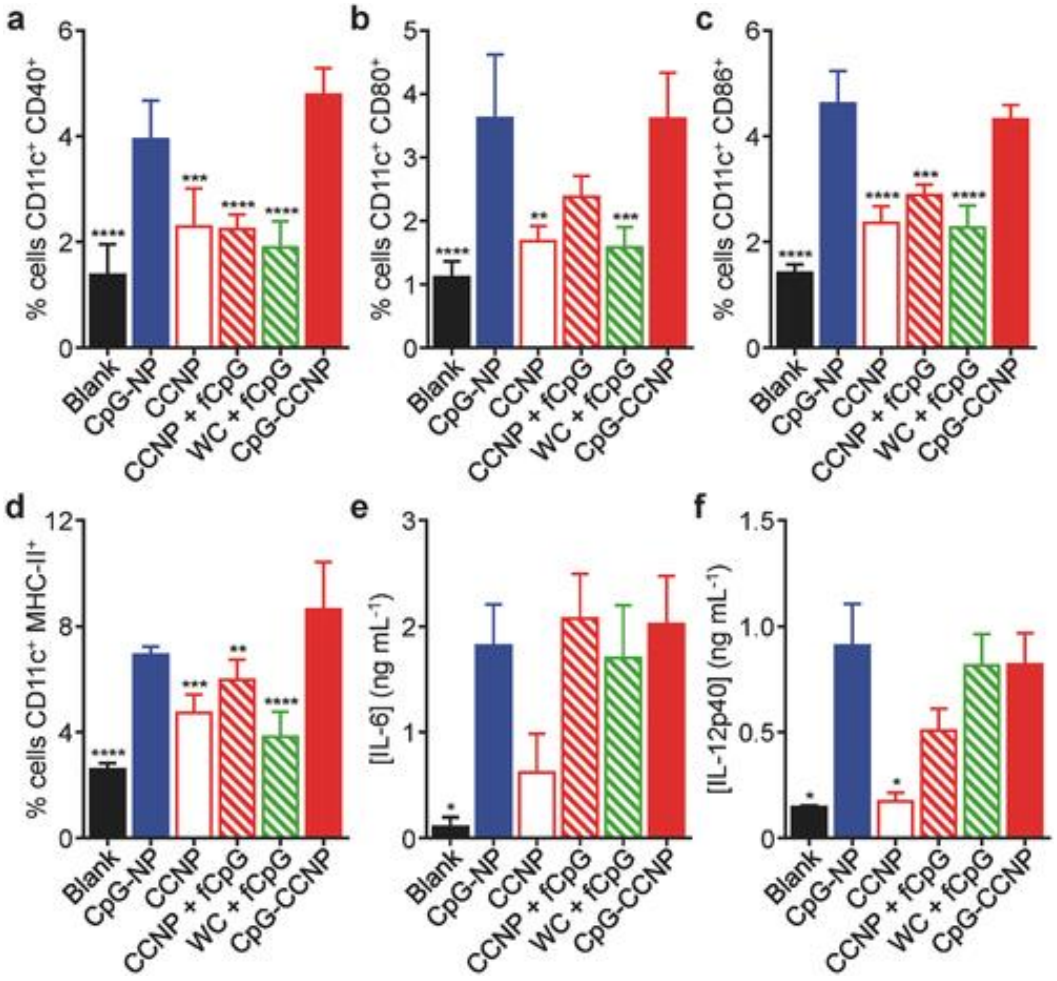

Figure 2.4: Characterization of *in vivo* dendritic cell maturation. Analysis of dendritic cell maturation markers a) CD40, b) CD80, c) CD86, and d) MHC-II in the draining lymph nodes after administration with CpG-CCNPs and various control formulations, including whole cell lysate with free CpG (WC + fCpG), CCNPs with free CpG (CCNP + fCpG), CCNPs, CpG-NPs, and blank solution (n = 4; mean ± SD). e,f) Concentration of proinflammatory cytokines e) IL-6 and f) IL-12p40 secreted by immune cells isolated from the draining lymph nodes after vaccination with CpG-CCNPs or various control formulations (n = 4; mean ± SEM). *p < 0.05, **p < 0.01, ***p < 0.001, ****p < 0.0001 (compared to CpG-CCNP); one-way ANOVA.

with CpG-CCNPs resulted in the highest degree of pmel-1 T cell proliferation, indicating that the formulation was able to effectively deliver the gp100 antigen for presentation under an immunostimulatory context. Additionally, after a set of vaccinations in naïve mice, the CpG-CCNPs were able to promote the native

generation of T cells with multiple tumor antigen specificities (Figure 2.5b,c). T cells specific for both gp100 and TRP2 could be isolated and expanded from mice vaccinated with the CpG-CCNPs. Further, when cultured *ex vivo*, immune cell preparations from mice vaccinated with the formulation showed significantly enhanced production of IFNγ and IL-2 when stimulated with a gp100 peptide, a TRP2 peptide, or whole cell lysate, suggesting robust effector-level response against those targets. While these studies were generally limited to probing for immunity against well characterized epitopes, it could be reasonably inferred that the CpG-CCNP formulation was concurrently generating additional responses against other tumor-relevant antigens.

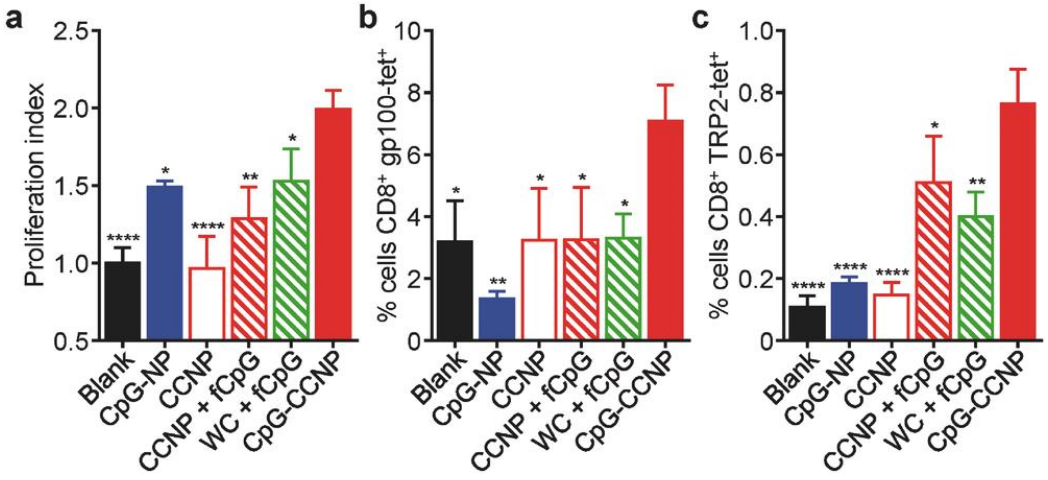

Figure 2.5: Characterization of *in vivo* T cell responses. a) Proliferation index of adoptively transferred pmel-1 CD8+ T cells after *in vivo* stimulation by CpG-CCNPs or various control formulations, including whole cell lysate with free CpG (WC + fCpG), CCNPs with free CpG (CCNP + fCpG), CCNPs, CpG-NPs, and blank solution (n = 3; mean ± SD). b,c) Tetramer staining analysis of T cells specific for gp100 (b) and TRP2 (c) after *ex vivo* restimulation of splenocytes from mice vaccinated with CpG-CCNPs or various control formulations (n = 3; mean ± SD). *p < 0.05, **p < 0.01, ****p < 0.0001 (compared to CpG-CCNP); one-way ANOVA.

To assess if the enhanced cellular immunity afforded by the CpG-CCNP formulation could translate into functional rejection of tumor cells, a prophylactic study using the wild-type B16-F10 model, which is poorly immunogenic [21, 36, 37], was carried out (Figure 2.6a–c). In mice vaccinated with CpG-CCNPs, there was significant activity, and tumor occurrence was prevented in 86% of mice 150 d after challenge with the tumor cells. Formulations consisting of either whole cell lysate with free CpG or CCNPs with free CpG both showed modest control of tumor growth, extending median survival from 20 d for the untreated group to 34 and 40 d, respectively. All but one of the mice in these groups reached the experimental endpoint by day 48 after challenge. CCNPs without adjuvant had minimal protective benefit, with the mice in these groups achieving a median survival of 28 days. Finally, mice vaccinated with CpG-NPs that had no antigenic material exhibited tumor growth kinetics identical to the blank control and displayed a median survival of 22 d. The results suggest that codelivery of both tumor antigen material and the CpG adjuvant together in the same vehicle is necessary for eliciting maximal antitumor immunity. The fact that CpG-NPs alone had no effect is encouraging and demonstrates that the inclusion of cancer membrane material helped to provide appropriate cues for the specific detection and elimination of malignant cells by the immune system.

The utility of the nanoparticulate vaccine formulation was further tested in a more clinically relevant therapeutic setting (Figure 2.7a–c). In this study, mice

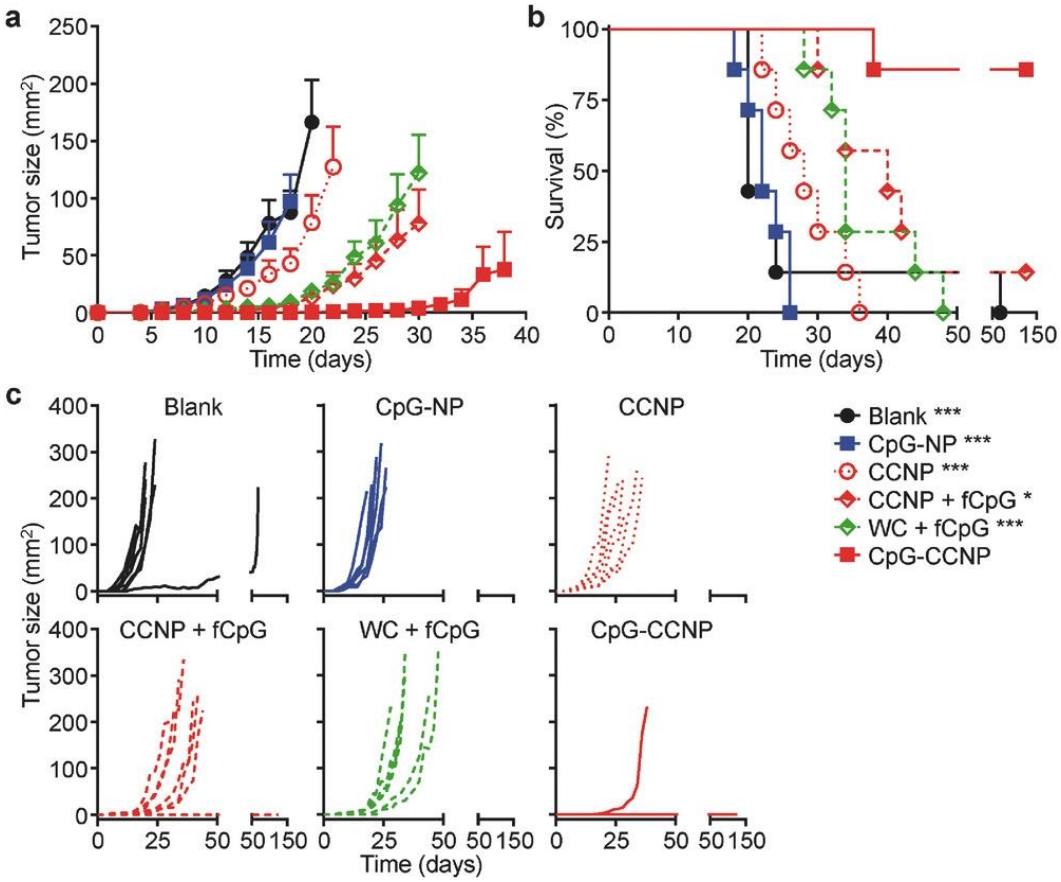

Figure 2.6: Prophylactic efficacy. a–c) Mice immunized with CpG-CCNPs and various control formulations, including whole cell lysate with free CpG (WC + fCpG), CCNPs with free CpG (CCNP + fCpG), CCNPs, CpG-NPs, and blank solution, on days 0, 7, and 14 were challenged with B16-F10 cells on day 21. Average tumor sizes (a), survival (b), and individual tumor growth kinetics (c) were plotted over time (n = 7; mean ± SEM). Reporting of average tumor sizes was halted after the first mouse died in each respective group. *$p < 0.05$, ***$p < 0.001$ (compared to CpG-CCNP in survival plot); log-rank test.

were challenged with B16-F10 cells and subsequently treated with the nanoformulation. Using this design, CpG-CCNPs alone displayed a modest ability to control tumor growth and extend survival. Given the aggressive nature of the B16-F10 tumor model, the results were not unexpected, especially given that vaccination largely focuses on the training phase of adaptive immunity. Despite

adequately enabling the immune system to recognize the appropriate targets, vaccine formulations for boosting cellular immunity may not be particularly well-suited for potentiating effector functionality in the presence of strong immunosuppression [38]. As such, the CpG-CCNPs were combined with a checkpoint blockade cocktail consisting of anti-CTLA4 and anti-PD1, and treatment with the combination enabled significantly enhanced control of tumor growth. Median survival was extended from 18 d for the blank control to 32 d for the treated group, and 50% of tumors were still below the experimental endpoint

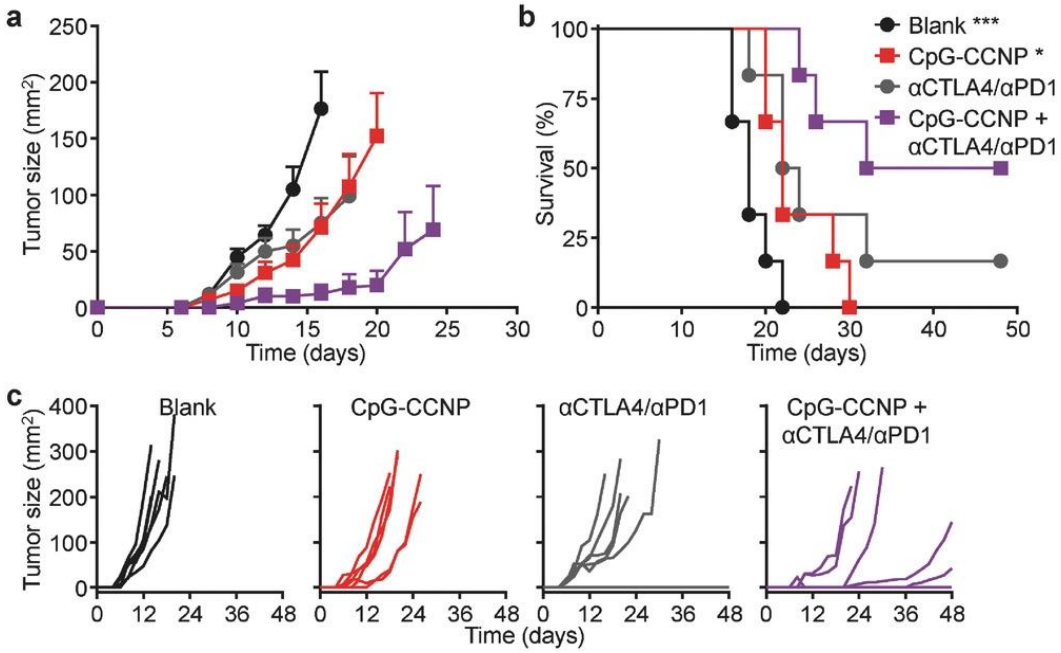

Figure 2.7: Therapeutic efficacy. a–c) After challenge with B16-F10 cells on day 0, mice were treated using CpG-CCNPs combined with a checkpoint blockade cocktail of anti-CTLA4 plus anti-PD1 (αCTLA4/αPD1), CpG-CCNPs alone, or the checkpoint blockade cocktail alone on days 1, 2, 4, and 7. Average tumor sizes (a), survival (b), and individual tumor growth kinetics (c) were plotted over time (n = 6; mean ± SEM). Reporting of average tumor sizes was halted after the first mouse died in each respective group. *$p < 0.05$, ***$p < 0.001$ (compared to CpG-CCNP + αCTLA4/αPD1 in survival plot); log-rank test.

threshold on day 48 postchallenge. In contrast, the checkpoint blockades, which have not shown significant efficacy in a related B16 model [39], was about as effective as CpG-CCNPs. The results confirm that the nanoparticulate vaccine formulation can act synergistically with other immunotherapies, modulating different aspects of immunity to promote the strongest antitumor responses.

2.4 Conclusion

In conclusion, we have reported on a biomimetic nanoparticulate anticancer vaccine formulation capable of activating multiantigenic immunity. The design leverages the unique advantages of recent nanoparticle technology, delivering both syngeneic cancer material along with a potent immunological adjuvant in a format that promotes effective antigen presentation. The final formulation is capable of generating strong antitumor responses *in vivo* and can work together with other immunotherapies such as checkpoint blockades to help control tumor growth. It is increasingly understood that presentation of tumor antigens alone, even in highly immunogenic contexts, may not be able to overcome the immunosuppressive tumor microenvironment [38, 40]. As such, efforts have shifted toward the rational design of combinatorial approaches that leverage multiple modes of action [41-43], including employing such strategies as adjuvant therapies to surgical resection [44]. In doing such, the potential adverse effects of immunomodulatory cocktails will also need to be considered [45]. The present nanoparticle-based cancer cell

membrane coating strategy represents a generalizable and effective means of boosting endogenous immunity against autologous material, which may, in the future, be derived from a patient's own resected primary tumor as a means to prevent relapse. All of this is accomplished in a manner that is unique when compared to current strategies and can possibly pave the way for enhanced personalized anticancer vaccines.

Chapter 2, in full, is a reprint of the material as it appears in *Advanced Materials*, 2017, Ashley Kroll, Ronnie Fang, Yao Jiang, Jiarong Zhou, Xiaoli Wei, Chun Lai Yu, Jie Gao, Brian Luk, Diana Dehaini, Weiwei Gao and Liangfang Zhang. The dissertation author was a primary investigator and author of this material.

2.5 References

1. Khalil, D.N., E.L. Smith, R.J. Brentjens, and J.D. Wolchok, *The future of cancer treatment: immunomodulation, CARs and combination immunotherapy.* Nat Rev Clin Oncol, 2016. **13**(5): p. 273-90.

2. Yang, Y., *Cancer immunotherapy: harnessing the immune system to battle cancer.* J Clin Invest, 2015. **125**(9): p. 3335-7.

3. Mellman, I., G. Coukos, and G. Dranoff, *Cancer immunotherapy comes of age.* Nature, 2011. **480**(7378): p. 480-9.

4. Tabi, Z. and S. Man, *Challenges for cancer vaccine development.* Adv Drug Deliv Rev, 2006. **58**(8): p. 902-15.

5. Finn, O.J., *Cancer vaccines: between the idea and the reality.* Nat Rev Immunol, 2003. **3**(8): p. 630-41.

6. Buonaguro, L., A. Petrizzo, M.L. Tornesello, and F.M. Buonaguro, *Translating tumor antigens into cancer vaccines.* Clin Vaccine Immunol, 2011. **18**(1): p. 23-34.

7. Kim, R., M. Emi, and K. Tanabe, *Cancer immunoediting from immune surveillance to immune escape.* Immunology, 2007. **121**(1): p. 1-14.

8. Mittal, D., M.M. Gubin, R.D. Schreiber, and M.J. Smyth, *New insights into cancer immunoediting and its three component phases--elimination, equilibrium and escape.* Curr Opin Immunol, 2014. **27**: p. 16-25.

9. Parmiani, G., C. Castelli, P. Dalerba, R. Mortarini, L. Rivoltini, F.M. Marincola, and A. Anichini, *Cancer immunotherapy with peptide-based vaccines: what have we achieved? Where are we going?* J Natl Cancer Inst, 2002. **94**(11): p. 805-18.

10. Slingluff, C.L., Jr., *The present and future of peptide vaccines for cancer: single or multiple, long or short, alone or in combination?* Cancer J, 2011. **17**(5): p. 343-50.

11. Gottesman, M.M., *Mechanisms of cancer drug resistance.* Annu Rev Med, 2002. **53**: p. 615-27.

12. Nathanson, D.A., B. Gini, J. Mottahedeh, K. Visnyei, T. Koga, G. Gomez, A. Eskin, K. Hwang, J. Wang, K. Masui, A. Paucar, H. Yang, M. Ohashi,

S. Zhu, J. Wykosky, R. Reed, S.F. Nelson, T.F. Cloughesy, C.D. James, P.N. Rao, H.I. Kornblum, J.R. Heath, W.K. Cavenee, F.B. Furnari, and P.S. Mischel, *Targeted therapy resistance mediated by dynamic regulation of extrachromosomal mutant EGFR DNA.* Science, 2014. **343**(6166): p. 72-6.

13. Keenan, B.P. and E.M. Jaffee, *Whole cell vaccines--past progress and future strategies.* Semin Oncol, 2012. **39**(3): p. 276-86.

14. de Gruijl, T.D., A.J. van den Eertwegh, H.M. Pinedo, and R.J. Scheper, *Whole-cell cancer vaccination: from autologous to allogeneic tumor- and dendritic cell-based vaccines.* Cancer Immunol Immunother, 2008. **57**(10): p. 1569-77.

15. Lokhov, P.G. and E.E. Balashova, *Cellular cancer vaccines: an update on the development of vaccines generated from cell surface antigens.* J Cancer, 2010. **1**: p. 230-41.

16. Palucka, K. and J. Banchereau, *Cancer immunotherapy via dendritic cells.* Nat Rev Cancer, 2012. **12**(4): p. 265-77.

17. Vandenberk, L., J. Belmans, M. Van Woensel, M. Riva, and S.W. Van Gool, *Exploiting the Immunogenic Potential of Cancer Cells for Improved Dendritic Cell Vaccines.* Front Immunol, 2015. **6**: p. 663.

18. Rabinovich, G.A., D. Gabrilovich, and E.M. Sotomayor, *Immunosuppressive strategies that are mediated by tumor cells.* Annu Rev Immunol, 2007. **25**: p. 267-96.

19. Zou, W., *Immunosuppressive networks in the tumour environment and their therapeutic relevance.* Nat Rev Cancer, 2005. **5**(4): p. 263-74.

20. Carreno, B.M., V. Magrini, M. Becker-Hapak, S. Kaabinejadian, J. Hundal, A.A. Petti, A. Ly, W.R. Lie, W.H. Hildebrand, E.R. Mardis, and G.P. Linette, *Cancer immunotherapy. A dendritic cell vaccine increases the breadth and diversity of melanoma neoantigen-specific T cells.* Science, 2015. **348**(6236): p. 803-8.

21. Castle, J.C., S. Kreiter, J. Diekmann, M. Lower, N. van de Roemer, J. de Graaf, A. Selmi, M. Diken, S. Boegel, C. Paret, M. Koslowski, A.N. Kuhn, C.M. Britten, C. Huber, O. Tureci, and U. Sahin, *Exploiting the mutanome for tumor vaccination.* Cancer Res, 2012. **72**(5): p. 1081-91.

22. Snyder, A., V. Makarov, T. Merghoub, J. Yuan, J.M. Zaretsky, A. Desrichard, L.A. Walsh, M.A. Postow, P. Wong, T.S. Ho, T.J. Hollmann, C. Bruggeman, K. Kannan, Y. Li, C. Elipenahli, C. Liu, C.T. Harbison, L.

Wang, A. Ribas, J.D. Wolchok, and T.A. Chan, *Genetic basis for clinical response to CTLA-4 blockade in melanoma.* N Engl J Med, 2014. **371**(23): p. 2189-2199.

23. Rizvi, N.A., M.D. Hellmann, A. Snyder, P. Kvistborg, V. Makarov, J.J. Havel, W. Lee, J. Yuan, P. Wong, T.S. Ho, M.L. Miller, N. Rekhtman, A.L. Moreira, F. Ibrahim, C. Bruggeman, B. Gasmi, R. Zappasodi, Y. Maeda, C. Sander, E.B. Garon, T. Merghoub, J.D. Wolchok, T.N. Schumacher, and T.A. Chan, *Cancer immunology. Mutational landscape determines sensitivity to PD-1 blockade in non-small cell lung cancer.* Science, 2015. **348**(6230): p. 124-8.

24. Hu, C.M., R.H. Fang, K.C. Wang, B.T. Luk, S. Thamphiwatana, D. Dehaini, P. Nguyen, P. Angsantikul, C.H. Wen, A.V. Kroll, C. Carpenter, M. Ramesh, V. Qu, S.H. Patel, J. Zhu, W. Shi, F.M. Hofman, T.C. Chen, W. Gao, K. Zhang, S. Chien, and L. Zhang, *Nanoparticle biointerfacing by platelet membrane cloaking.* Nature, 2015. **526**(7571): p. 118-21.

25. Fang, R.H., C.M. Hu, B.T. Luk, W. Gao, J.A. Copp, Y. Tai, D.E. O'Connor, and L. Zhang, *Cancer cell membrane-coated nanoparticles for anticancer vaccination and drug delivery.* Nano Lett, 2014. **14**(4): p. 2181-8.

26. Hu, C.M., L. Zhang, S. Aryal, C. Cheung, R.H. Fang, and L. Zhang, *Erythrocyte membrane-camouflaged polymeric nanoparticles as a biomimetic delivery platform.* Proc Natl Acad Sci U S A, 2011. **108**(27): p. 10980-5.

27. Schlosser, H.A., S. Theurich, A. Shimabukuro-Vornhagen, U. Holtick, D.L. Stippel, and M. von Bergwelt-Baildon, *Overcoming tumor-mediated immunosuppression.* Immunotherapy, 2014. **6**(9): p. 973-88.

28. Ghirelli, C. and T. Hagemann, *Targeting immunosuppression for cancer therapy.* J Clin Invest, 2013. **123**(6): p. 2355-7.

29. Vinay, D.S., E.P. Ryan, G. Pawelec, W.H. Talib, J. Stagg, E. Elkord, T. Lichtor, W.K. Decker, R.L. Whelan, H. Kumara, E. Signori, K. Honoki, A.G. Georgakilas, A. Amin, W.G. Helferich, C.S. Boosani, G. Guha, M.R. Ciriolo, S. Chen, S.I. Mohammed, A.S. Azmi, W.N. Keith, A. Bilsland, D. Bhakta, D. Halicka, H. Fujii, K. Aquilano, S.S. Ashraf, S. Nowsheen, X. Yang, B.K. Choi, and B.S. Kwon, *Immune evasion in cancer: Mechanistic basis and therapeutic strategies.* Semin Cancer Biol, 2015. **35 Suppl**: p. S185-S198.

30. Novellino, L., C. Castelli, and G. Parmiani, *A listing of human tumor antigens recognized by T cells: March 2004 update.* Cancer Immunol Immunother, 2005. **54**(3): p. 187-207.

31. Bode, C., G. Zhao, F. Steinhagen, T. Kinjo, and D.M. Klinman, *CpG DNA as a vaccine adjuvant.* Expert Rev Vaccines, 2011. **10**(4): p. 499-511.

32. Shang, L., K. Nienhaus, and G.U. Nienhaus, *Engineered nanoparticles interacting with cells: size matters.* J Nanobiotechnology, 2014. **12**: p. 5.

33. Oh, N. and J.H. Park, *Endocytosis and exocytosis of nanoparticles in mammalian cells.* Int J Nanomedicine, 2014. **9 Suppl 1**: p. 51-63.

34. Chaturvedi, A. and S.K. Pierce, *How location governs toll-like receptor signaling.* Traffic, 2009. **10**(6): p. 621-8.

35. Vollmer, J., R. Weeratna, P. Payette, M. Jurk, C. Schetter, M. Laucht, T. Wader, S. Tluk, M. Liu, H.L. Davis, and A.M. Krieg, *Characterization of three CpG oligodeoxynucleotide classes with distinct immunostimulatory activities.* Eur J Immunol, 2004. **34**(1): p. 251-62.

36. Seliger, B., U. Wollscheid, F. Momburg, T. Blankenstein, and C. Huber, *Characterization of the major histocompatibility complex class I deficiencies in B16 melanoma cells.* Cancer Res, 2001. **61**(3): p. 1095-9.

37. Xu, D., P. Gu, P.Y. Pan, Q. Li, A.I. Sato, and S.H. Chen, *NK and CD8+ T cell-mediated eradication of poorly immunogenic B16-F10 melanoma by the combined action of IL-12 gene therapy and 4-1BB costimulation.* Int J Cancer, 2004. **109**(4): p. 499-506.

38. van der Burg, S.H., R. Arens, F. Ossendorp, T. van Hall, and C.J. Melief, *Vaccines for established cancer: overcoming the challenges posed by immune evasion.* Nat Rev Cancer, 2016. **16**(4): p. 219-33.

39. Curran, M.A., W. Montalvo, H. Yagita, and J.P. Allison, *PD-1 and CTLA-4 combination blockade expands infiltrating T cells and reduces regulatory T and myeloid cells within B16 melanoma tumors.* Proc Natl Acad Sci U S A, 2010. **107**(9): p. 4275-80.

40. Melief, C.J., T. van Hall, R. Arens, F. Ossendorp, and S.H. van der Burg, *Therapeutic cancer vaccines.* J Clin Invest, 2015. **125**(9): p. 3401-12.

41. Twyman-Saint Victor, C., A.J. Rech, A. Maity, R. Rengan, K.E. Pauken, E. Stelekati, J.L. Benci, B. Xu, H. Dada, P.M. Odorizzi, R.S. Herati, K.D. Mansfield, D. Patsch, R.K. Amaravadi, L.M. Schuchter, H. Ishwaran, R. Mick, D.A. Pryma, X. Xu, M.D. Feldman, T.C. Gangadhar, S.M. Hahn, E.J.

Wherry, R.H. Vonderheide, and A.J. Minn, *Radiation and dual checkpoint blockade activate non-redundant immune mechanisms in cancer.* Nature, 2015. **520**(7547): p. 373-7.

42. Morse, M.A. and H.K. Lyerly, *Checkpoint blockade in combination with cancer vaccines.* Vaccine, 2015. **33**(51): p. 7377-7385.

43. Kleponis, J., R. Skelton, and L. Zheng, *Fueling the engine and releasing the break: combinational therapy of cancer vaccines and immune checkpoint inhibitors.* Cancer Biol Med, 2015. **12**(3): p. 201-8.

44. Gibney, G.T., R.R. Kudchadkar, R.C. DeConti, M.S. Thebeau, M.P. Czupryn, L. Tetteh, C. Eysmans, A. Richards, M.J. Schell, K.J. Fisher, C.E. Horak, H.D. Inzunza, B. Yu, A.J. Martinez, I. Younos, and J.S. Weber, *Safety, correlative markers, and clinical results of adjuvant nivolumab in combination with vaccine in resected high-risk metastatic melanoma.* Clin Cancer Res, 2015. **21**(4): p. 712-20.

45. Larkin, J., V. Chiarion-Sileni, R. Gonzalez, J.J. Grob, C.L. Cowey, C.D. Lao, D. Schadendorf, R. Dummer, M. Smylie, P. Rutkowski, P.F. Ferrucci, A. Hill, J. Wagstaff, M.S. Carlino, J.B. Haanen, M. Maio, I. Marquez-Rodas, G.A. McArthur, P.A. Ascierto, G.V. Long, M.K. Callahan, M.A. Postow, K. Grossmann, M. Sznol, B. Dreno, L. Bastholt, A. Yang, L.M. Rollin, C. Horak, F.S. Hodi, and J.D. Wolchok, *Combined Nivolumab and Ipilimumab or Monotherapy in Untreated Melanoma.* N Engl J Med, 2015. **373**(1): p. 23-34.

Chapter 3

Development of Red Blood Cell Membrane-Coated Nanoparticles as “Nanotoxoid” Antivirulence Vaccines

3.1 Nanotoxoid for Antivirulence Vaccination

3.1.1 Introduction

The continued rise of antibiotic-resistant bacteria has become a significant burden on global health and is responsible for an increased rate of life-threatening infections observed in the clinic [1]. The issue continues to rise to the forefront as the development of new antibiotics has slowed to a near halt [2], prompting physicians and scientists to explore alternative strategies to control bacterial infections [3]. Among the different approaches, antivirulence vaccination is a compelling strategy as it promotes host immunity by training the body to detect and disarm specific mechanisms employed by pathogens during host invasion [4]. This approach has been shown to inhibit the ability of pathogens to colonize within a host and is less susceptible to the development of resistance as it does not exert direct selective pressure on individual bacterium [5]. Antivirulence vaccination is most commonly accomplished through the use of toxoids, or inactivated forms of live bacterial toxins, which include the commonly used tetanus toxoid [6] and diphtheria toxoid [7]. Conventionally, these toxoids are prepared by denaturation via either chemical or heat treatment in order to eliminate the dangerous effects of the original toxin [8]. However, such inactivation methods are often disruptive and can lead to altered antigen presentation as well as compromised immunogenicity [9]. To overcome the tradeoff between safety and efficacy, emerging techniques

are being developed to produce vaccine candidates that faithfully present antigenic epitopes for immune processing [10].

Methicillin-resistant *Staphylococcus aureus* (MRSA) is an antibiotic-resistant pathogen that represents a significant threat to public health, especially in hospital environments where many patients have weakened immune systems that are incapable of naturally fending off infection [11]. It can cause severe skin lesions and can ultimately be life-threatening upon systemic invasion [12]. The pace of resistance exhibited by MRSA has severely limited treatment options, with many strains of the bacteria being unresponsive to all of the most commonly used antibiotics [13, 14]. This has led researchers to explore other forms of treatment, including the aforementioned antivirulence therapy. Known to secrete many different types of exotoxins, MRSA represents a good target for such therapies. One of its major virulence factors is α-hemolysin (Hla) [15], a toxin that forms heptameric pores on cell surfaces, which contributes greatly to the pathogenesis of MRSA during the process of infection [16]. In fact, it has been shown that the virulence of the pathogen correlates strongly with the level of Hla production [17, 18]. Further, immunization with a mutant form of Hla has been shown to confer protection against *Staphylococcus aureus* (*S. aureus)* pneumonia in mice [19]. Passive immunization with anti-Hla antibodies also protected against skin lesions caused by subsequent *S. aureus* infection, further attesting to the utility of such a strategy for combating the pathogen.

The application of novel nanomaterials toward vaccine design has the potential to bring about significant improvements via efficient and finely controlled immune manipulation [20-25]. We have previously demonstrated a nanoparticle-mediated toxin detainment strategy for the preparation of a safe and potent toxoid formulation. Biomimetic nanoparticles are fabricated with a cell membrane-derived coating that presents a natural substrate for pore-forming toxins [26, 27], leading to their stable entrapment onto the nanoparticles and enabling safe delivery *in vivo* for immune processing [28]. Owing to the nondisruptive approach of this detainment strategy, the platform was demonstrated to be superior to a traditionally formed toxoid by generating higher anti-Hla titers with increased avidity. Further, vaccination with the detained toxin conferred a significant survival benefit in a murine model of lethal toxin challenge. In the present work, we investigated the protective capabilities of nanoparticle-detained staphylococcal Hla, denoted nanotoxoid(Hla), against live bacterial challenge using a mouse model of MRSA skin infection (Figure 3.1.1). The immune potentiating effect of the nanoparticle formulation was studied more in-depth by looking at the formation of germinal centers in the draining lymph nodes (dLNs) of vaccinated mice, which was then correlated to anti-Hla titer production. The ability of the nanotoxoid(Hla) vaccine to protect against MRSA infection and lessen bacterial colonization was evaluated in a mouse model of skin lesion formation. Beyond local infection, the effect of the nanoparticle vaccination on bacterial invasiveness was further studied by enumerating the bacterial load in major organs.

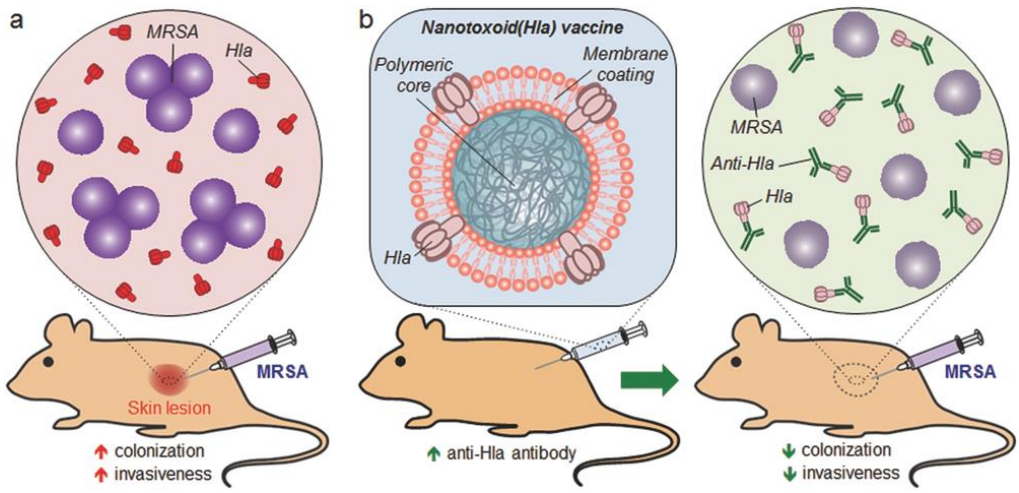

Figure 3.1.1: Schematic of nanotoxoid(Hla) protection against MRSA infection. a) Under normal conditions, MRSA bacteria employ Hla to help them colonize the site of challenge, resulting in significant skin lesion formation and systemic invasiveness. b) After vaccination with the nanotoxoid(Hla) formulation, anti-Hla titers are induced. These antibodies neutralize the toxin produced by the MRSA bacteria at the site of challenge, reducing the ability of the pathogen to colonize and enter into systemic circulation.

3.1.2 Experimental Methods

3.1.2.1 Preparation and Characterization of Nanotoxoid(Hla)

RBC membrane-coated nanoparticles were prepared as previously described[26]. Polymeric cores were made using 0.67 dL g^{-1} carboxy-terminated 50:50 PLGA (LACTEL Absorbable Polymers) with a modified nanoprecipitation method. The polymer was dissolved in acetone at a concentration of 10 mg mL^{-1} and added rapidly to 2 mL of deionized water. The mixture was placed under vacuum for 3 h to evaporate the organic solvent. To obtain the membrane material,

RBCs collected from 6 week old male CD-1 mice (Harlan Laboratories) were treated with hypotonic medium and washed multiple times by centrifugation. The final RBC membrane-coated nanoparticles, denoted nanotoxoid(-), were synthesized by sonicating a mixture of the PLGA cores and RBC membrane using a Fisher Scientific FS30D bath sonicator at a frequency of 42 kHz and a power of 100 W for 2 min. The membrane material from 1 mL of mouse blood was used to coat 5 mg of 100 nm PLGA cores. The nanotoxoid(Hla) was generated by incubating 0.2 mg of nanotoxoid(-) with 3 μg of Hla at 37 °C for 15 min. Nanoparticle concentrations for both the nanotoxoid(Hla) and nanotoxoid(-) formulations were expressed as milligrams of PLGA per 1 mL of solution (mg mL^{-1}). The mixture was then filtered through a Sepharose CL-4B (Sigma-Aldrich) column to obtain purified nanotoxoid(Hla) free of unbound toxin. The size and the zeta potential of the different nanoformulations were measured by dynamic light scattering using a Malvern ZEN 3600 Zetasizer. The structure of the nanotoxoid(Hla) was examined using a Zeiss Libra 120 PLUS EF-TEM Transmission Electron Microscope. Samples were negatively stained with 0.1 wt% uranyl acetate prior to visualization.

3.1.2.2 Nanotoxoid(Hla) Loading Analysis

An immunogold staining assay was carried out to confirm insertion of Hla onto the RBC membrane-coated nanoparticles. One drop of nanotoxoid(Hla) or nanotoxoid(-) solution was added onto a glow-discharged carbon-coated 400-mesh

copper grid (Electron Microscopy Sciences). The grids were then washed before subjecting to blocking with 1 wt% bovine serum albumin (BSA), primary immunostaining with polyclonal rabbit anti-Hla antibody (Sigma-Aldrich), and secondary staining with gold-labeled anti-rabbit IgG antibody (Sigma-Aldrich). Images were obtained using a Zeiss Libra 120 PLUS EF-TEM Transmission Electron Microscope without negative staining. To analyze Hla retention by dot blot analysis, 1 μL of nanotoxoid(Hla) solution at 2 mg mL^{-1} was dropped onto a nitrocellulose membrane and allowed to fully dry under vacuum. Afterward, the membrane was blocked with 1 wt% BSA solution and then probed with a polyclonal rabbit anti-Hla primary antibody (Sigma-Aldrich) followed by a donkey antirabbit IgG-horseradish peroxidase (HRP) conjugate secondary antibody (Biolegend). The blot was developed with ECL western blotting substrate (Pierce) using a Mini-Medical/90 Developer (ImageWorks). Nanotoxoid(-) solution at 2 mg mL^{-1} was used as negative control and Hla solution corresponding to 100% loading (30 μg mL^{-1}) was used as positive control. Blot intensity was measured by analyzing the mean gray values of dots via Image J software.

3.1.2.3 Germinal Center Analysis

All animal experiments followed protocols that were reviewed, approved, and performed under the regulatory supervision of the University of California, San Diego's institutional biosafety program and the Institutional Animal Care and Use Committee. Six-week old male CD-1 mice (Harlan Laboratories) were immunized

subcutaneously in the lateral tarsal region just above the ankle with 0.1 mg of nanotoxoid(Hla). Nanotoxoid(-) and PBS were used as negative controls. On day 21 postimmunization, the mice were euthanized and the draining popliteal lymph nodes were collected for analysis. For immunohistochemical analysis, the lymph nodes were cryosectioned and stained with antimouse/antihuman B220-Pacific Blue, antimouse IgD-Alexa Fluor 488, and antimouse/antihuman GL-7-Alexa Fluor 647 antibodies (Biolegend). For flow cytometry analysis, Lymph nodes were digested in 1 mg mL^{-1}collagenase D (Roche) solution and stained with the above antibodies. Data were collected using a BD FACSCanto-II flow cytometer and analyzed using FlowJo software.

3.1.2.4 Anti-Hla Titer Analysis

Mice were subcutaneously administered with 0.1 mg of nanotoxoid(Hla), 0.1 mg of nanotoxoid(-) or PBS, followed by a boost 14 days later (n = 6). On days 0, 14, and 35, the serum of each mouse was collected to assay for Hla-specific antibody titers by an enzyme-linked immunosorbent assay (ELISA). A 96-well plate was coated overnight with 2 μg ml^{-1} Hla using commercial coating buffer (Biolegend). The wells were then blocked with 5 wt% milk before adding serially diluted serum samples as the primary antibody. Goat antimouse IgG-HRP (Biolegend) was then employed as the secondary antibody. The plate was developed with 1-Step Slow TMB-ELISA substrate (Pierce) and measured at 450 nm with a Tecan Infinite M200 Multiplate Reader.

3.1.2.5 MRSA Infection and Vaccine Efficacy

The MRSA strain USA300 TCH1516 (American Type Culture Collection) was used in this study. The bacteria were cultured at 37 °C in tryptic soy broth, harvested by centrifugation, washed, suspended with PBS, and adjusted to the appropriate concentration by optical density measurements before use. Mice immunized with 0.1 mg of nanotoxoid(Hla), 0.1 mg of nanotoxoid(-), or PBS on days 0 and 14 were challenged with 1×10^9 CFU of the bacteria on day 35. The bacteria were inoculated subcutaneously in the back region in an area that was carefully shaved using hair clippers before the challenge. The dermonecrotic area was monitored daily and reported as the width multiplied by the length of the visible lesion. On day 6 postchallenge the mice were euthanized; perfused with PBS via the heart; and the skin, heart, liver, spleen, lung, and kidney of each mouse were excised and processed for enumeration. Briefly, organs were homogenized in sterile PBS using a Biospec Mini BeadBeater, diluted tenfold serially with PBS, plated onto tryptic soy agar, and finally the colonies were counted after 24 h of incubation at 37 °C.

3.1.3 Results and Discussion

Nanoparticles coated with red blood cell (RBC) membrane were prepared using a previously described protocol [29]. Briefly, mouse RBCs were subjected to

hypotonic treatment to obtain purified RBC membrane ghosts, which were then fused onto the surface of preformed nanoparticle cores made using poly(lactic-*co*-glycolic acid) (PLGA) through a sonication method. As the RBC membrane coating serves as a natural substrate for the pore-forming Hla, nanotoxoid(Hla) complexes were formed by incubating free Hla with unloaded nanoparticles, herein denoted nanotoxoid(-). Free Hla was subsequently removed from the nanotoxoid(Hla) complexes by size exclusion chromatography to obtain a purified formulation. Physicochemical characterization showed that the resulting nanotoxoid(Hla) was about 115 nm in diameter and had a surface zeta potential of −32 mV (Figure 3.1.2a,b), both of which were similar to those of the unloaded nanotoxoid(-), suggesting that toxin insertion did not have a major impact on overall nanoparticle properties. This was further confirmed via transmission electron microscopy (TEM) of negatively stained nanotoxoid(Hla), which revealed that the characteristic core–shell structure of the RBC membrane-coated nanoparticle was preserved even after toxin loading, consistent with what has been previously observed [26, 28] (Figure 3.1.2c).

To confirm successful detainment of Hla by the RBC membrane-coated nanoparticles, different immunoassays were performed. On the TEM image, Hla-specific antibody labeling of nanotoxoid(Hla) followed by secondary labeling using an immunogold conjugate showed significant colocalization of the electron-dense gold signal with regions of intermediate density occupied by the nanoparticles, indicating a significant presence of Hla-specific epitopes on the nanotoxoid(Hla)

(Figure 3.1.2d). Conversely, no gold signal could be detected in the nanotoxoid(-) sample subjected to the exact same staining procedure, confirming that the positive signal seen in the nanotoxoid(Hla) was not due to nonspecific antibody staining. Note that in the absence of negative staining, the morphological appearance of the nanotoxoid differs from what is observed in Figure 3.1.3c. The uranyl acetate stain can act as a fixative, serving to stabilize the nanoparticles and to enhance the core–shell structure of the nanoparticles. Dot blot analysis was used to further confirm the presence of Hla on nanotoxoid(Hla) samples (Figure 3.1.2e). Using anti-Hla as the primary immunostain, nanotoxoid(Hla) gave a positive signal whereas nanotoxoid(-) did not give any discernable signal. As a positive control, free Hla at the initial input concentration used to prepare nanotoxoid(Hla) was tested in parallel, and image analysis of the blot intensities revealed that ≈95% of the Hla was retained on the nanoparticles after purification, suggesting high affinity of the toxin for the membrane-coated nanoparticles. It has been shown previously that the strong sequestration of toxin by the nanoparticle detainment strategy resulted in little release over time, which effectively neutralized the activity of the toxin and enables safe delivery both *in vitro* and *in vivo* [28].

Next, the ability of the nanotoxoid(Hla) formulation to promote anti-Hla immune responses was studied. Of particular interest was the formation of germinal centers (GCs), which is a critical step in the potentiation of the humoral immune response against foreign antigens [30, 31]. It is in these regions that B cells mature, and it has been shown that improved retention of antigens via nanoparticle-

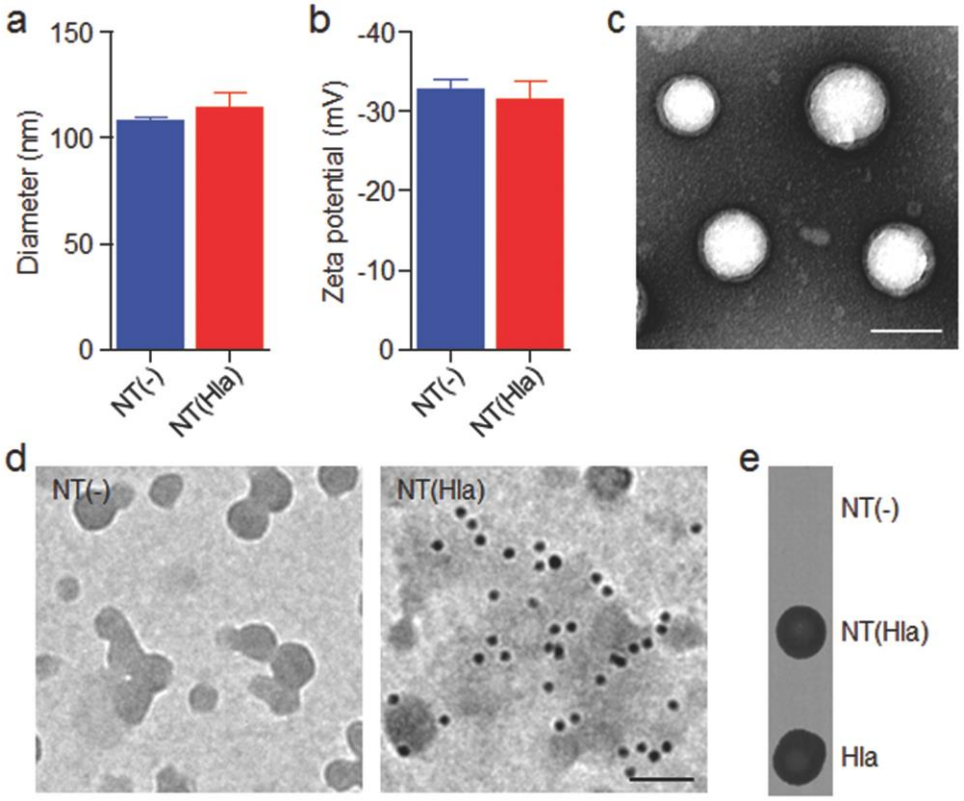

Figure 3.1.2: Nanotoxoid(Hla) characterization. a) Size and b) zeta potential of nanotoxoid(-) [denoted "NT(-)"] and nanotoxoid(Hla) [denoted "NT(Hla)"] (n = 3). Error bars represent standard deviation. c) TEM image of nanotoxoid(Hla) after negative staining with uranyl acetate. Scale bar = 100 nm. d) TEM images of immunogold-stained NT(-) (left) and NT(Hla) (right) with anti-Hla as the primary immunostain and gold-labeled anti-IgG as the secondary stain. The gold (≈10 nm) appears as dark punctates on the images. Scale bar = 100 nm. e) Dot blotting results using anti-Hla as the primary immunostain. Quantification by image analysis revealed that 95.2% of the Hla input was retained on the final NT(Hla) formulation.

mediated delivery can better facilitate GC formation [32]. We therefore sought to evaluate lymphatic B cell activation in mice immunized with the nanotoxoid(Hla) formulation. Immunostaining was employed to detect the presence of GCs in the dLNs of mice immunized subcutaneously with the nanoformulation. PBS and unloaded nanotoxoid(-) were administered as controls. Histological analysis of the dLNs from mice immunized with nanotoxoid(Hla) revealed GL-7$^+$ regions

characteristic of GC nucleation (Figure 3.1.3a). In contrast, there was no visual evidence of GC formation in the PBS or nanotoxoid(-) immunization groups, confirming the nonimmunogenicity of the naturally derived nanoparticle vector itself [33]. Flow cytometry results (Figure 3.1.3b) showed that 45.6% of $B220^{+}IgD^{low}$ B cells in the dLNs of the nanotoxoid(Hla) group exhibited a GL-7^{+} germinal center phenotype. In contrast, only 15.7% and 13.6% of cells in mice administered with PBS and nanotoxoid(-), respectively, exhibited the same phenotype.

The ability of nanotoxoid(Hla) to elicit a humoral immune response against Hla was further investigated. Mice were subcutaneously injected with nanotoxoid(Hla), nanotoxoid(-), or PBS on day 0 and were subsequently administered a booster on day 14. The serum of the mice in each group was sampled on days 0, 14, and 35 to assess Hla-specific IgG titers (Figure 3.1.3c–e). Nanotoxoid(Hla) vaccination elicited significant anti-Hla titers on day 14, and there was a further increase when assayed on day 35. In contrast, the nanotoxoid(-) and PBS vaccinations resulted in no detectable anti-Hla titers over the course of the study. The nanotoxoid(Hla)-induced antibody responses have previously been shown to be durable, with little to no drop in titers over the course of a five-month period [28]. Taken together, the data demonstrates that the nanotoxoid(Hla) formulation can effectively elicit potent anti-Hla immune responses, despite complete deactivation of the toxin [26]. This is notable finding given that the formulation is absent of immunological adjuvants, which are commonly required

for conventional toxoid formulations and help to boost germinal center antibody activity [34].

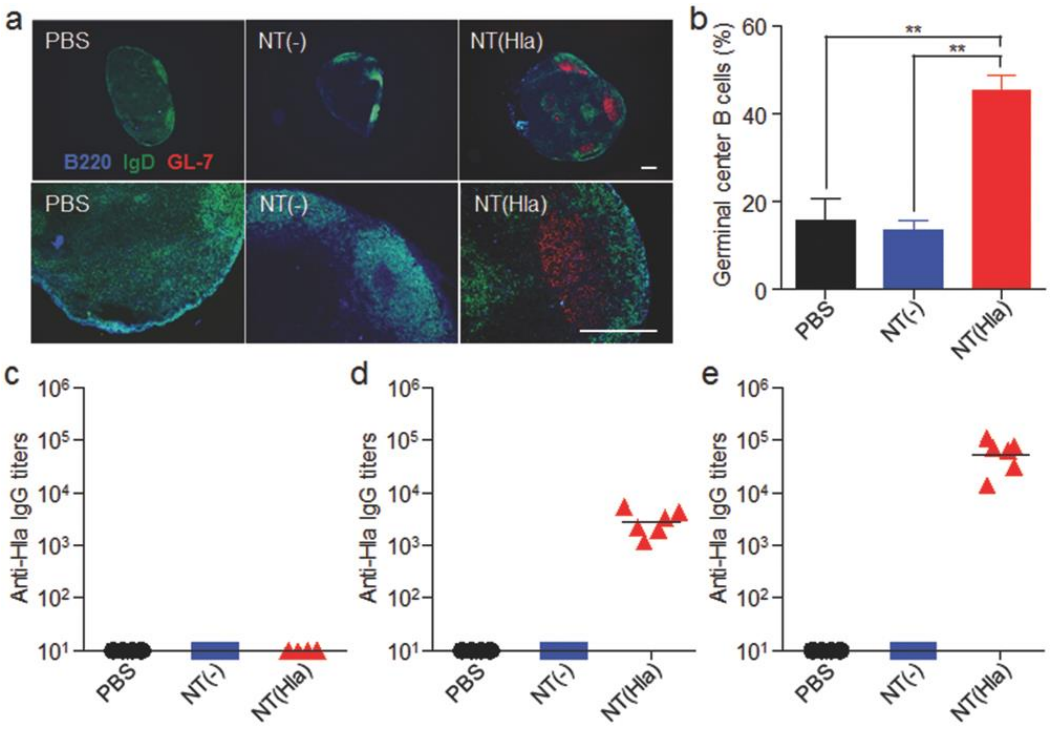

Figure 3.1.3: Germinal center formation and antibody production induced by nanotoxoid(Hla) vaccination. a,b) Mice were vaccinated with PBS, nanotoxoid(-) [NT(-)], or nanotoxoid(Hla) [NT(Hla)] (n = 3). The draining lymph nodes were collected 21 d later for the analysis of B220 (blue), IgD (green), and GL-7 (red) expression by either immunohistochemistry (a) or flow cytometry (b). Scale bars = 250 μm. For flow cytometric analysis, cells were first gated on $B220^{+}IgD^{low}$ and the numbers reported are the percentage $GL\text{-}7^{+}$ cells within that population. Error bars represent the standard error. Statistical significance was determined by one-way ANOVA (**P < 0.01). c–e) Mice were vaccinated with PBS, NT(-), or NT(Hla) on day 0 with a boost on day 14 (n = 6). On days 0 (c), 14 (d), and 35 (e), serum was collected and the anti-Hla IgG titers were quantified by ELISA. Lines represent geometric means.

To evaluate the protective capability of the nanotoxoid(Hla) vaccine against MRSA infection, we employed a mouse skin infection model. MRSA represents one of the most common causes of skin infections, both in the community and in hospitals [12]. Because the pathogen is hard to treat with

common antibiotics, the infection can quickly progress and lead to serious complications, from physical disfigurement to permanent organ damage, and in many cases even death. For this experiment, mice were immunized with nanotoxoid(Hla) on day 0 and given a booster dose on day 14. Mice injected with nanotoxoid(-) or PBS were used as control groups. On day 35, the mice were subcutaneously challenged with live MRSA bacteria, and the efficacy in the different experimental groups was assessed over time by monitoring the dermonecrotic area resulting from bacterial burden. The progression of skin lesion development in mice immunized with nanotoxoid(Hla) was significantly attenuated compared with mice in the nanotoxoid(-) and PBS groups, which both experienced rapid lesion formation (Figure 3.1.4a,b). On day 6 postinfection, there was an approximately fivefold reduction in dermonecrotic area on mice treated with the nanotoxoid(Hla) formulation compared to the control groups.

At the conclusion of the observation period, the bacterial burden was quantified in the infected skin region of each mouse (Figure 3.1.4c). For the nanotoxoid(-) and PBS groups, the bacterial burdens of the infected skin tissue were 1.7×10^7 and 2.2×10^7 CFU, respectively. Mice immunized with nanotoxoid(Hla) showed an average burden of 1.5×10^6 CFU, representing 11.3- and 14.7-fold reductions compared with the nanotoxoid(-) and PBS groups, respectively. It has previously been shown that nanotoxoid(Hla) is capable of significantly inhibiting Hla-mediated skin damage in the subcutaneous space, suggesting that the titers generated by the formulation are sufficiently high to enable extravascular

neutralizing activity [28]. This prevents the necrotic effect of high Hla concentrations [35], thus preserving integrity of the local tissue. In this study, the nanoparticle vaccine formulation was likewise able to reduce skin lesion formation, demonstrating its ability to facilitate neutralization of Hla produced by the bacteria *in situ* upon subcutaneous challenge. Given the importance of Hla in MRSA pathogenesis, neutralization of the toxin also resulted in decreased bacterial burden, likely due to increased clearance by immune cells protected from the cytotoxic activity of Hla [36]. Despite the significant reduction in both lesion formation and bacterial load at the site of infection, the inability of the nanotoxoid(Hla) to completely mitigate disease suggests a sizable role played by other virulence factors, which can serve as targets for future nanotoxoid vaccine formulations.

MRSA infections can quickly progress and enter systemic circulation, leading to a markedly worse prognosis in the clinic [11]. Patients with invasive MRSA can precipitously develop life-threatening infections in different organs such as the blood, heart, bone, and kidney. As an MRSA skin infection runs the significant risk of further dissemination, the effect of nanotoxoid(Hla) vaccination on MRSA invasiveness after subcutaneous challenge was studied. Mice were vaccinated with nanotoxoid(Hla), nanotoxoid(-), or PBS on day 0 with a booster dose on day 14 and subcutaneously inoculated with MRSA on day 35. On day 6 postinfection, the bacterial counts in the heart, kidney, spleen, lung, and liver were

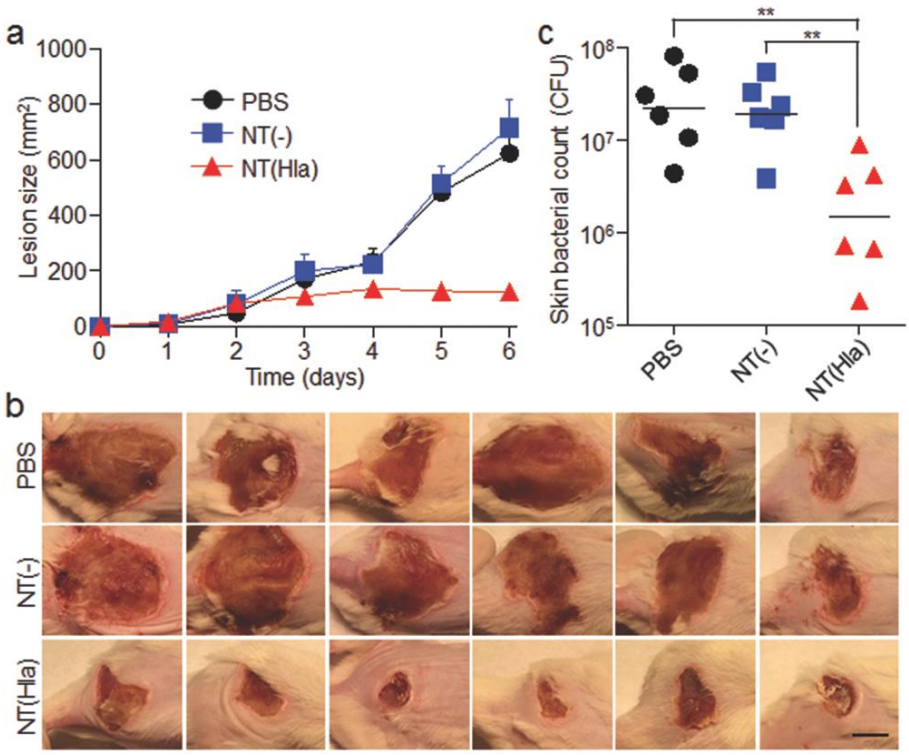

Figure 3.1.4: Effect of nanotoxoid(Hla) vaccination on MRSA skin colonization. Mice vaccinated with PBS, nanotoxoid(-) [NT(-)], or nanotoxoid(Hla) [NT(Hla)] on days 0 and 14 were challenged subcutaneously with 1×10^9 CFU of MRSA bacteria on day 35. a) The skin lesions were monitored over the course of 6 d ($n = 6$). Error bars represent the standard error. b) Images of skin lesions on day 6 postinfection. Scale bar = 1 cm. c) On day 6 postinfection, the affected skin and underlying tissue were collected and the bacterial burden enumerated ($n = 6$). Lines represent the geometric mean. Statistical significance determined by one-way ANOVA (**$P < 0.01$).

analyzed (Figure 3.1.5). In most of the organs that were analyzed, the nanotoxoid(Hla) group showed a significant drop in bacterial burden compared to the nanotoxoid(-) and PBS control groups. Of note, the kidney and spleen, two organs that traditionally experience heavy bacterial burden per unit weight [37], both had reductions of approximately two orders of magnitude. The sharp decrease in organ penetration can likely be attributed primarily to better immune management at the site of infection, which results in improved integrity of the skin

protective barrier and fewer bacteria entering the circulation system. Additionally, the presence of high amounts of neutralizing titers within the body can further hamper the capacity of invading MRSA bacteria to colonize individual organs, as shown by previous studies on the effect of anti-Hla vaccination in animal models of sepsis [38]. Overall, the results demonstrate that nanotoxoid(Hla) not only prevents superficial damage, but also decreases MRSA invasiveness, which can ultimately help to prevent many of the harsh complications associated with MRSA infections.

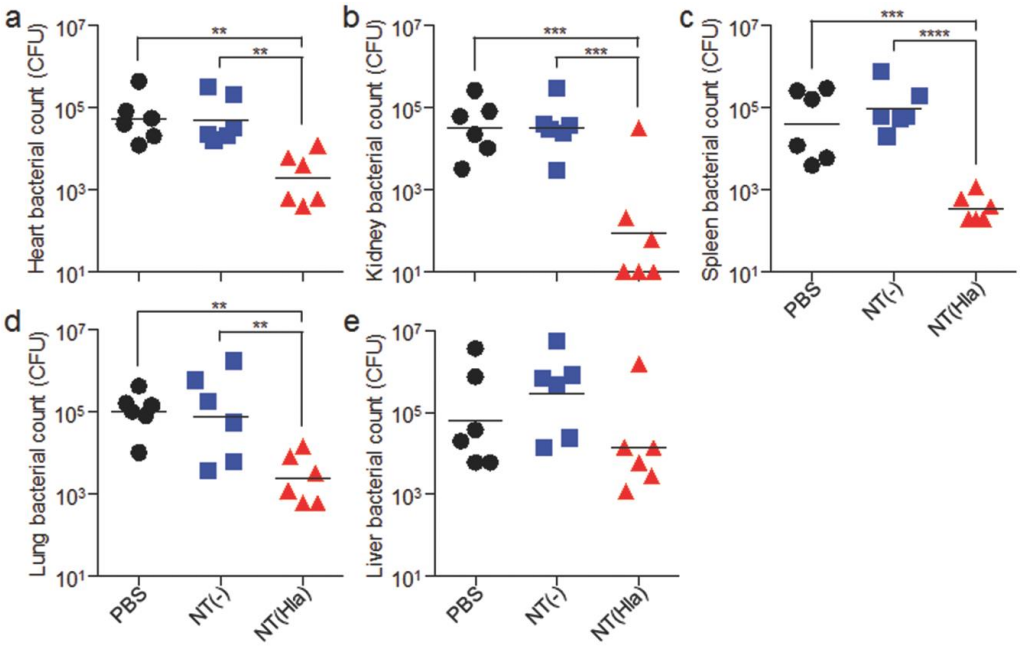

Figure 3.1.5: Effect of nanotoxoid(Hla) vaccination on MRSA invasiveness. Mice vaccinated with PBS, nanotoxoid(-) [NT(-)], or nanotoxoid(Hla) [NT(Hla)] on days 0 and 14 were challenged subcutaneously with 1×10^9 CFU of MRSA bacteria on day 35. On day 6 postinfection, the major organs, including the a) heart, b) kidney, c) spleen, d) lung, and e) liver were collected and the bacterial burden of each was enumerated (n = 6). Lines represent geometric means. Statistical significance was determined by one-way ANOVA (**P < 0.01, ***P < 0.001, and ****P < 0.0001).

3.1.4 Conclusion

This study investigated the use of nanoparticle-detained toxins for antivirulence vaccination as a prophylactic strategy against live MRSA skin infection. Such strategies address an important need in the clinical management of bacterial infections as the rise of antibiotic resistance has been difficult to overcome. An increasing emphasis has been placed on novel strategies that transcend traditional treatment paradigms. The nanotoxoid(Hla) has been shown capable of safely delivering the Hla toxin in its native form without the need for subunit engineering or denaturation. Additionally, the anti-Hla titers elicited by the nanoformulation are of high avidity and long-lived. In this study, we demonstrated that nanotoxoid(Hla) was capable of promoting strong humoral immunity in an adjuvant-free setting via efficient germinal center formation. Using a mouse skin infection model, it was demonstrated that immunity could substantially attenuate the ability of live bacteria to colonize and systemically invade their hosts, which could ultimately abrogate the negative consequences of severe MRSA infections.

Successful validation of nanotoxoid(Hla) vaccination for protection against live MRSA challenge opens the door for further development of similar platforms against many other common yet deadly bacterial pathogens. Pore-forming toxins are one of the most common protein toxins found in nature and represent a large class of virulence factors that have natural affinity for cell membrane substrates [39], and the reported detainment strategy has been shown effective in neutralizing

such toxins secreted by several different organisms, including *S. aureus, Escherichia coli, and Helicobacter pylori* [26]. By targeting the common mechanism by which many virulence factors function, the nanotoxoid formulation can be applied to an entire class of toxins without specific knowledge of each toxin's precise molecular structure. This strategy opens the door for the nanotoxoid to be used as a diverse vaccine carrier for multitoxin vaccination, as many pathogens secrete multiple membrane-attacking virulence factors [40]. By presenting multiple virulent antigens, nanotoxoid can further increase vaccine efficacy and limit bacterial colonization. In addition, changing the membrane coating material [41-43] could further broaden applicability to toxins that do not specifically target RBCs. Overall, the nanoparticle-based antivirulence vaccine platform is primed to help usher in a new generation of treatments that can address some of the most critical needs in the current management of bacterial infections.

3.1.5 References

1. Howard, D.H., R.D. Scott, 2nd, R. Packard, and D. Jones, *The global impact of drug resistance.* Clin Infect Dis, 2003. **36**(Suppl 1): p. S4-10.

2. Bush, K., P. Courvalin, G. Dantas, J. Davies, B. Eisenstein, P. Huovinen, G.A. Jacoby, R. Kishony, B.N. Kreiswirth, E. Kutter, S.A. Lerner, S. Levy, K. Lewis, O. Lomovskaya, J.H. Miller, S. Mobashery, L.J. Piddock, S. Projan, C.M. Thomas, A. Tomasz, P.M. Tulkens, T.R. Walsh, J.D. Watson, J. Witkowski, W. Witte, G. Wright, P. Yeh, and H.I. Zgurskaya, *Tackling antibiotic resistance.* Nat Rev Microbiol, 2011. **9**(12): p. 894-6.

3. Clatworthy, A.E., E. Pierson, and D.T. Hung, *Targeting virulence: a new paradigm for antimicrobial therapy.* Nat Chem Biol, 2007. **3**(9): p. 541-8.

4. Ramachandran, G., *Gram-positive and gram-negative bacterial toxins in sepsis: a brief review.* Virulence, 2014. **5**(1): p. 213-8.

5. Rasko, D.A. and V. Sperandio, *Anti-virulence strategies to combat bacteria-mediated disease.* Nat Rev Drug Discov, 2010. **9**(2): p. 117-28.

6. Blencowe, H., J. Lawn, J. Vandelaer, M. Roper, and S. Cousens, *Tetanus toxoid immunization to reduce mortality from neonatal tetanus.* Int J Epidemiol, 2010. **39 Suppl 1**: p. i102-9.

7. Kurosky, S., K.L. Davis, and S.J. Karve, *Tetanus Toxoid, Diphtheria Toxoid, and Acellular Puertussis (Tdap) Vaccine Compliance among Adolescents in the United States.* Value in Health, 2014. **17**(3): p. A278-A278.

8. Cryz, S.J., Jr., E. Furer, and R. Germanier, *Effect of chemical and heat inactivation on the antigenicity and immunogenicity of Vibrio cholerae.* Infect Immun, 1982. **38**(1): p. 21-6.

9. Kernodle, D.S., *Expectations regarding vaccines and immune therapies directed against Staphylococcus aureus alpha-hemolysin.* J Infect Dis, 2011. **203**(11): p. 1692-3; author reply 1693-4.

10. Karauzum, H., R.P. Adhikari, J. Sarwar, V.S. Devi, L. Abaandou, C. Haudenschild, M. Mahmoudieh, A.R. Boroun, H. Vu, T. Nguyen, K.L. Warfield, S. Shulenin, and M.J. Aman, *Structurally designed attenuated subunit vaccines for S. aureus LukS-PV and LukF-PV confer protection in a mouse bacteremia model.* PLoS One, 2013. **8**(6): p. e65384.

11. Klevens, R.M., M.A. Morrison, J. Nadle, S. Petit, K. Gershman, S. Ray, L.H. Harrison, R. Lynfield, G. Dumyati, J.M. Townes, A.S. Craig, E.R. Zell,

G.E. Fosheim, L.K. McDougal, R.B. Carey, S.K. Fridkin, and M.I. Active Bacterial Core surveillance, *Invasive methicillin-resistant Staphylococcus aureus infections in the United States.* JAMA, 2007. **298**(15): p. 1763-71.

12. Lowy, F.D., *Staphylococcus aureus infections.* N Engl J Med, 1998. **339**(8): p. 520-32.

13. Rivera, A.M. and H.W. Boucher, *Current concepts in antimicrobial therapy against select gram-positive organisms: methicillin-resistant Staphylococcus aureus, penicillin-resistant pneumococci, and vancomycin-resistant enterococci.* Mayo Clin Proc, 2011. **86**(12): p. 1230-43.

14. Boucher, H., L.G. Miller, and R.R. Razonable, *Serious infections caused by methicillin-resistant Staphylococcus aureus.* Clin Infect Dis, 2010. **51 Suppl 2**: p. S183-97.

15. Otto, M., *Basis of virulence in community-associated methicillin-resistant Staphylococcus aureus.* Annu Rev Microbiol, 2010. **64**: p. 143-62.

16. Li, M., B.A. Diep, A.E. Villaruz, K.R. Braughton, X. Jiang, F.R. DeLeo, H.F. Chambers, Y. Lu, and M. Otto, *Evolution of virulence in epidemic community-associated methicillin-resistant Staphylococcus aureus.* Proc Natl Acad Sci U S A, 2009. **106**(14): p. 5883-8.

17. Bubeck Wardenburg, J. and O. Schneewind, *Vaccine protection against Staphylococcus aureus pneumonia.* J Exp Med, 2008. **205**(2): p. 287-94.

18. O'Reilly, M., J.C. de Azavedo, S. Kennedy, and T.J. Foster, *Inactivation of the alpha-haemolysin gene of Staphylococcus aureus 8325-4 by site-directed mutagenesis and studies on the expression of its haemolysins.* Microb Pathog, 1986. **1**(2): p. 125-38.

19. Kennedy, A.D., J. Bubeck Wardenburg, D.J. Gardner, D. Long, A.R. Whitney, K.R. Braughton, O. Schneewind, and F.R. DeLeo, *Targeting of alpha-hemolysin by active or passive immunization decreases severity of USA300 skin infection in a mouse model.* J Infect Dis, 2010. **202**(7): p. 1050-8.

20. Moon, J.J., B. Huang, and D.J. Irvine, *Engineering nano- and microparticles to tune immunity.* Adv Mater, 2012. **24**(28): p. 3724-46.

21. Fang, R.H., A.V. Kroll, and L. Zhang, *Nanoparticle-Based Manipulation of Antigen-Presenting Cells for Cancer Immunotherapy.* Small, 2015. **11**(41): p. 5483-96.

22. Tao, Y., E.G. Ju, Z.H. Li, J.S. Ren, and X.G. Qu, *Engineered CpG- Antigen Conjugates Protected Gold Nanoclusters as Smart Self- Vaccines for Enhanced Immune Response and Cell Imaging.* Advanced Functional Materials, 2014. **24**(7): p. 1004-1010.

23. Balmert, S.C. and S.R. Little, *Biomimetic delivery with micro- and nanoparticles.* Adv Mater, 2012. **24**(28): p. 3757-78.

24. Li, Z., K. Dong, Y. Zhang, E. Ju, Z. Chen, J. Ren, and X. Qu, *Biomimetic nanoassembly for targeted antigen delivery and enhanced Th1-type immune response.* Chem Commun (Camb), 2015. **51**(88): p. 15975-8.

25. Li, Z., Z. Liu, M. Yin, X. Yang, J. Ren, and X. Qu, *Combination delivery of antigens and CpG by lanthanides-based core-shell nanoparticles for enhanced immune response and dual-mode imaging.* Adv Healthc Mater, 2013. **2**(10): p. 1309-13.

26. Hu, C.M., R.H. Fang, J. Copp, B.T. Luk, and L. Zhang, *A biomimetic nanosponge that absorbs pore-forming toxins.* Nat Nanotechnol, 2013. **8**(5): p. 336-40.

27. Wang, F., W. Gao, S. Thamphiwatana, B.T. Luk, P. Angsantikul, Q. Zhang, C.M. Hu, R.H. Fang, J.A. Copp, D. Pornpattananangkul, W. Lu, and L. Zhang, *Hydrogel Retaining Toxin-Absorbing Nanosponges for Local Treatment of Methicillin-Resistant Staphylococcus aureus Infection.* Adv Mater, 2015. **27**(22): p. 3437-43.

28. Hu, C.M., R.H. Fang, B.T. Luk, and L. Zhang, *Nanoparticle-detained toxins for safe and effective vaccination.* Nat Nanotechnol, 2013. **8**(12): p. 933-8.

29. Copp, J.A., R.H. Fang, B.T. Luk, C.M. Hu, W. Gao, K. Zhang, and L. Zhang, *Clearance of pathological antibodies using biomimetic nanoparticles.* Proc Natl Acad Sci U S A, 2014. **111**(37): p. 13481-6.

30. Moon, J.J., H. Suh, M.E. Polhemus, C.F. Ockenhouse, A. Yadava, and D.J. Irvine, *Antigen-displaying lipid-enveloped PLGA nanoparticles as delivery agents for a Plasmodium vivax malaria vaccine.* PLoS One, 2012. **7**(2): p. e31472.

31. McHeyzer-Williams, L.J. and M.G. McHeyzer-Williams, *Antigen-specific memory B cell development.* Annu Rev Immunol, 2005. **23**: p. 487-513.

32. Moon, J.J., H. Suh, A.V. Li, C.F. Ockenhouse, A. Yadava, and D.J. Irvine, *Enhancing humoral responses to a malaria antigen with nanoparticle*

vaccines that expand Tfh cells and promote germinal center induction. Proc Natl Acad Sci U S A, 2012. **109**(4): p. 1080-5.

33. Rao, L., L.L. Bu, J.H. Xu, B. Cai, G.T. Yu, X. Yu, Z. He, Q. Huang, A. Li, S.S. Guo, W.F. Zhang, W. Liu, Z.J. Sun, H. Wang, T.H. Wang, and X.Z. Zhao, *Red Blood Cell Membrane as a Biomimetic Nanocoating for Prolonged Circulation Time and Reduced Accelerated Blood Clearance.* Small, 2015. **11**(46): p. 6225-36.

34. DeFranco, A.L., D.C. Rookhuizen, and B. Hou, *Contribution of Toll-like receptor signaling to germinal center antibody responses.* Immunol Rev, 2012. **247**(1): p. 64-72.

35. Berube, B.J. and J. Bubeck Wardenburg, *Staphylococcus aureus alpha-toxin: nearly a century of intrigue.* Toxins (Basel), 2013. **5**(6): p. 1140-66.

36. Miller, L.S. and J.S. Cho, *Immunity against Staphylococcus aureus cutaneous infections.* Nat Rev Immunol, 2011. **11**(8): p. 505-18.

37. Kokai-Kun, J.F., T. Chanturiya, and J.J. Mond, *Lysostaphin as a treatment for systemic Staphylococcus aureus infection in a mouse model.* J Antimicrob Chemother, 2007. **60**(5): p. 1051-9.

38. Adhikari, R.P., H. Karauzum, J. Sarwar, L. Abaandou, M. Mahmoudieh, A.R. Boroun, H. Vu, T. Nguyen, V.S. Devi, S. Shulenin, K.L. Warfield, and M.J. Aman, *Novel structurally designed vaccine for S. aureus alpha-hemolysin: protection against bacteremia and pneumonia.* PLoS One, 2012. **7**(6): p. e38567.

39. Fang, R.H., B.T. Luk, C.M. Hu, and L. Zhang, *Engineered nanoparticles mimicking cell membranes for toxin neutralization.* Adv Drug Deliv Rev, 2015. **90**: p. 69-80.

40. Aman, M.J. and R.P. Adhikari, *Staphylococcal bicomponent pore-forming toxins: targets for prophylaxis and immunotherapy.* Toxins (Basel), 2014. **6**(3): p. 950-72.

41. Fang, R.H., C.M. Hu, B.T. Luk, W. Gao, J.A. Copp, Y. Tai, D.E. O'Connor, and L. Zhang, *Cancer cell membrane-coated nanoparticles for anticancer vaccination and drug delivery.* Nano Lett, 2014. **14**(4): p. 2181-8.

42. Hu, C.M., R.H. Fang, K.C. Wang, B.T. Luk, S. Thamphiwatana, D. Dehaini, P. Nguyen, P. Angsantikul, C.H. Wen, A.V. Kroll, C. Carpenter, M. Ramesh, V. Qu, S.H. Patel, J. Zhu, W. Shi, F.M. Hofman, T.C. Chen, W.

Gao, K. Zhang, S. Chien, and L. Zhang, *Nanoparticle biointerfacing by platelet membrane cloaking.* Nature, 2015. **526**(7571): p. 118-21.

43. Gao, W., R.H. Fang, S. Thamphiwatana, B.T. Luk, J. Li, P. Angsantikul, Q. Zhang, C.M. Hu, and L. Zhang, *Modulating antibacterial immunity via bacterial membrane-coated nanoparticles.* Nano Lett, 2015. **15**(2): p. 1403-9.

3.2 *In Situ* Multiantigenic Nanotoxoid for Antivirulence Vaccination

3.2.1 Introduction

The continued rise of antibiotic-resistant bacteria poses a significant threat to public health, yet the development of new small-molecule antibiotics remains slow [1]. An increasing number of lives will be at risk as time progresses, and thus finding new and innovative ways to combat these potentially lethal pathogens is of extremely high importance [2-6]. Along these lines, antivirulence therapy is a promising strategy for addressing bacterial infection that focuses on removing the offensive weapons used by bacteria to successfully colonize a host [7-9]. Examples of such factors include protein-based toxins, which can be used to attack host cells via physical disruption, biochemical degradation, or signaling interruption, thereby preventing immune clearance and providing the nutrients necessary for proliferation [10, 11]. Neutralization of these bacterial virulence factors can have a marked impact on bacteria survivability [12]. One major advantage of employing antivirulence therapy is that, unlike with antibiotics, the treatment itself does not exert direct selective pressure on individual bacterium; by focusing instead on blocking pathogen-to-host interactions, this strategy can ultimately translate into a reduced likelihood of developing resistance [13]. Implementation of this strategy

has varied, ranging from traditional antibody neutralization [14, 15], to novel nanotechnology-based complexation [16-19]. While antivirulence can be effective in therapeutic settings, arguably the most impactful applications center around prophylactic vaccination. In fact, commonly used vaccines in the clinic against diphtheria and tetanus are targeted against their respective virulence factors [20], underscoring the usefulness of this strategy.

While the immunity generated through antivirulence vaccination can be used to effectively prevent some bacterial infections, others have proven much more difficult to address [21]. A major challenge for creating vaccines against biological toxins is the balance that must be struck between safety and immunogenicity, which often exhibit an inverse relationship [22]. Toxicity can be attenuated via several different approaches, including heat treatment and chemical modification [23]; however, not all toxins are heat-labile, and denaturation has the potential to compromise vaccine efficacy due to the modified presentation of epitopic target s[24]. Subunit engineering can eliminate virulence, but requires significant upfront investment of resources and is only applicable towards well-characterized targets [25]. Vaccine potency is further challenged by the varying secretion profiles of different bacterial species and strains. As many bacteria produce a wide variety of toxins and other factors [26, 27], it can be difficult to pinpoint which of these are major contributors to pathogenesis. In some cases, vaccination approaches based on multiple known toxins have been shown to carry great utility [28], but these are hard to pursue given the significant time required for identification and

confirmation of new virulence factors. While such approaches will undoubtedly be aided by advances in genomic and proteomic technologies, the history of some well-known toxins, such as streptolysin S secreted by group A streptococcus, underscores the gap that often exists between knowledge and application [29].

To circumvent the need for identification of individual virulence factors, direct derivation from bacterial protein secretions should represent an attractive method to obtain the material needed for generating antivirulence vaccines. However, this strategy has seldom been studied [30, 31], likely also due to issues in balancing safety and immunogenicity, with the added challenge of having to manage the presence of irrelevant proteins that dilute immune focus. In this work, we report on a facile approach for generating on-demand nanotoxoids from naturally derived bacterial protein preparations by leveraging the near universal natural affinity of virulence factors for cellular membranes [16, 32] (Figure 3.2.1). Virulent proteins are biomimetically entrapped using a membrane-coated nanosponge construct [17], effectively modulating the surface material composition for custom vaccine applications. Following a generalizable workflow that does not require prior knowledge of secreted constituents, pathogen-specific formulations that are safe, potentially multiantigenic, and epitopically faithful can be fabricated. The feasibility of this approach is demonstrated using methicillin-resistant *Staphylococcus aureus* (MRSA), which employs multiple well-characterized toxins [26, 33], as the model pathogen, along with red blood cell (RBC) membrane-coated nanosponges as the model vector.

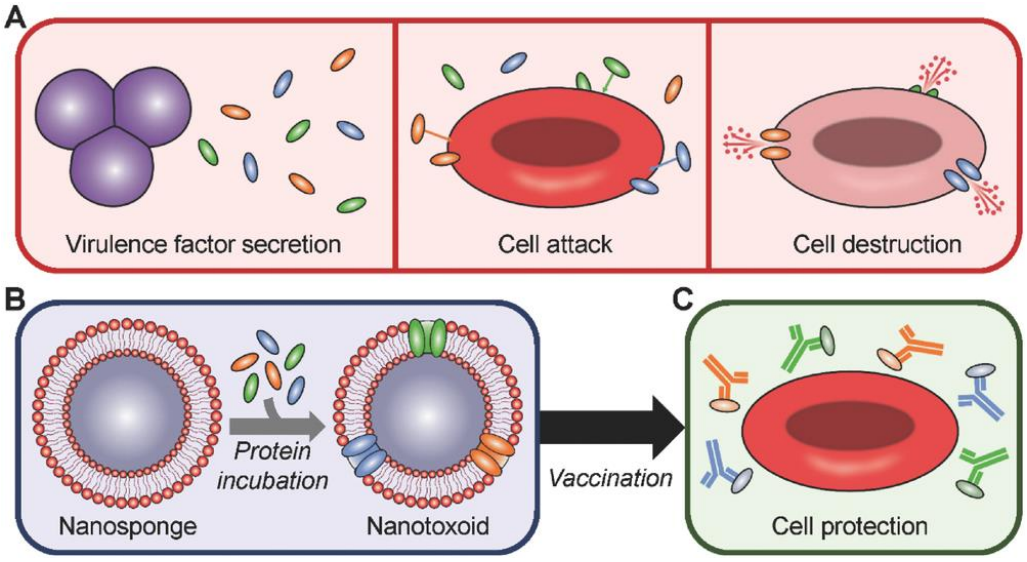

Figure 3.2.1: Schematic depicting on-demand fabrication of a pathogen-specific nanotoxoid and its vaccination benefits. A) Pathogens secrete virulence factors, which are capable of inserting into target cells and causing their destruction. B) Using nanosponges prepared with the membrane of target cells and incubating the particles with a bacterial supernatant-derived protein fraction, it is possible to generate a nanotoxoid carrying pathogen-specific virulence factors. C) After vaccination using the nanotoxoid, antibodies against the incorporated virulence factors are elicited and can prevent their toxic effects, leaving the intended targets unharmed.

3.2.2 Experimental Methods

3.2.2.1 Preparation of Hemolytic Secreted Protein Fraction

The MRSA strain USA300 (BAA-1717; American Type Culture Collection) was first plated onto a tryptic soy agar (Sigma Aldrich) plate overnight at 37 °C. A single colony was cultured in 5 mL of tryptic soy broth (TSB; Sigma Aldrich) for 24 h at 37 °C, and 1 mL was then transferred to another 100 mL of TSB and cultured for 24 h. The media were collected after spinning down the bacteria at 3 000 × *g* for 20 min. Saturated ammonium sulfate (Sigma Aldrich)

solution was added slowly to the media in a glass beaker while stirring at 4 °C up to a 25% volume ratio. After stirring for 1 h, the solution was centrifuged at 3 000 × *g* for 20 min to pellet the first fraction. Fractions at 50% and 75% volume ratios were collected in the same manner. Finally, solid ammonium sulfate was added to obtain the equivalent of a 95% saturated solution volume ratio and stirred overnight before collection of the last fraction. All precipitated protein pellets were dissolved in water and desalted using columns packed with fine G-25 Sephadex (GE Healthcare). Only the first protein fraction to pass through each column was collected, ultimately yielding concentrated samples free from most other nonprotein contaminants. Hemolytic activity was assessed by adjusting protein solutions to 1× phosphate buffered saline (PBS) and incubating at 1 mg $mL^{-1}$with an equal volume of 2.5% purified RBCs collected from male ICR mice (Envigo). All animal experiments were performed in accordance with NIH guidelines and approved by the Institutional Animal Care and Use Committee (IACUC) of the University of California, San Diego. After 30 min of incubation, the samples were spun down at 2 000 × g for 5 min. Hemolysis was determined by measuring the absorbance of the supernatant at 540 nm using a Tecan Infinite M200 plate reader. Fractions demonstrating considerable signal were combined together for further use as the hSP fraction.

3.2.2.2 Preparation and Physicochemical Characterization of Nanosponges and Nanotoxoid(hSP)

RBC-membrane-coated nanosponges were prepared by a previously reported method[34]. Membrane vesicles collected from male ICR mice were coated by a sonication process onto preformed polymeric cores prepared with carboxyl-terminated poly(lactic-*co*-glycolic acid) (0.67 dL g^{-1}, 50:50 monomer ratio; LACTEL Absorbable Polymers). To assess the ability of nanosponge preincubation to prevent hemolysis by the hSP fraction, 400 μg of the nanosponges was incubated with varying amounts of protein ranging from 1 to 50 μg in 10 wt% sucrose at 37 °C for 30 min. The mixtures in a volume of 100 μL were added to an equal volume of 2.5% mouse RBCs in PBS. Equivalent amounts of free hSP in the absence of nanosponges were used for comparison. After another 30 min of incubation at 37 °C, samples were spun down at 2 000 × *g* for 5 min. Hemolysis was determined by measuring the absorbance of the supernatant at 540 nm using a Tecan Infinite M200 plate reader. A 100% lysis control was prepared by treating the RBCs with Triton X-100 (Sigma Aldrich). Subsequent studies were carried out using a ratio of 400 μg nanosponges incubated directly with 15 μg of hSP, the product of which was referred to as the nanotoxoid(hSP) formulation. The size and the surface zeta potential of the nanoformulations were measured by dynamic light scattering using a Malvern ZEN 3600 Zetasizer. The structure of the nanotoxoid(hSP) was examined after negative staining with 1 wt% uranyl acetate (Electron Microscopy Sciences) on a carbon-coated 400-mesh copper grid (Electron Microscopy Sciences) using a Zeiss Libra 120 PLUS EF-TEM transmission electron microscope.

3.2.2.3 Protein Characterization

To visually confirm the presence of bacterial virulence factors on the resulting nanotoxoid(hSP), dot blots were performed to probe for three known toxins secreted by MRSA (α-toxin, PVL, and γ-toxin). In addition to hSP, nanosponge, and nanotoxoid(hSP), a washed nanotoxoid(hSP) sample was obtained by centrifugation at 21 100 × *g* to separate out unbound proteins. Nanoparticle samples were run at equivalent nanosponge concentrations, and hSP was run at the same concentration as inputted into the nanotoxoid(hSP) formulation. The samples were prepared using lithium dodecyl sulfate sample loading buffer (Invitrogen), heated at 70 °C for 15 min, and 5 μL of each was dropped onto a nitrocellulose membrane (Thermo Scientific) followed by drying under vacuum. Membranes were probed using either a polyclonal rabbit anti-staphylococcal α-toxin (Sigma Aldrich), polyclonal rabbit anti-PVL LukS subunit (IBT Bioservices), or polyclonal rabbit anti-staphylococcal γ-toxin B (IBT Bioservices) as the primary antibody along with an HRP-conjugated anti-rabbit IgG (Biolegend) as the secondary antibody. Blots were developed with ECL western blotting substrate (Pierce) using an ImageWorks Mini-Medical/90 Developer.

Western blotting was carried out to quantitatively determine the amount of toxins that remained bound to the nanoparticles. Nanotoxoid(hSP) and washed nanotoxoid(hSP) were prepared in the same manner as above and run on NuPAGE Novex 4%–12% Bis-Tris minigels (Invitrogen) in MOPS running buffer

(Invitrogen). After transferring onto nitrocellulose membranes, the blots were probed for α-toxin, PVL LukS subunit, or γ-toxin B. Band intensities were measured using Adobe Photoshop and normalized to the average values of the no wash nanotoxoid(hSP) sample for each toxin. To determine the composition of the final hSP preparation, different dilutions of the hSP protein, alongside purified α-toxin (Sigma Aldrich), PVL LukS subunit (IBT Bioservices), and γ-toxin B (IBT Bioservices), were subjected to western blot analysis. Linear standard curves were generated using the hSP dilutions upon probing for each toxin. Composition percentages were determined as the concentration of each purified toxin divided by the interpolated hSP concentration based on the band intensities measured for that specific toxin (n = 3; mean ± SD). To perform the release study, nanotoxoid(hSP) at a concentration of 2 mg mL^{-1} was placed into a 300 kDa MWCO Float-A-Lyzer G2 (Spectrum Laboratories) and dialyzed against 2 L of 1× PBS. Samples were collected at 0 and 48 h and probed for α-toxin, PVL LukS subunit, or γ-toxin B by western blotting. Values were normalized to the average band intensities of the 0 h samples for each toxin.

3.2.2.4 *In Vitro* Safety

To assess hemolytic activity, hSP (15 μg), heat-treated hSP (15 μg heated for 4 h at 100 °C), nanosponge (400 μg), and nanotoxoid(hSP) (400 μg of nanosponge incubated with 15 μg of hSP for 30 min) were added in 150 μL of solution to an equal volume of 2.5% mouse RBCs in PBS. Note that the

nanoparticle concentration employed was near the maximum feasible value allowed by the nanotoxoid fabrication process. After 30 min of incubation at 37 °C, each sample was spun down and the absorbance of hemoglobin in the supernatant was measured at 540 nm using a Tecan Infinite M200 plate reader. Bone marrow-derived dendritic cells were isolated from ICR mice and cultured as reported before[35]. To assess cytotoxicity, the cells were plated into 96-well plates and incubated with hSP (7.5 μg), heat-treated hSP (7.5 μg), nanosponge (200 μg), or nanotoxoid(hSP) (200 μg nanosponge with 7.5 μg hSP). After 24 h of incubation with the different samples, the cells were cultured for another 48 h in fresh media. Cell viability was assayed using an MTT reagent (Invitrogen) following the manufacturer's instructions. Untreated cells were used as the 100% viability control.

3.2.2.5 *In Vivo* Safety

Male ICR mice were first shaved to remove the hair on their back. Subsequently, 150 μL of blank solution, hSP (22.5 μg), heat-treated hSP (22.5 μg), nanosponge (600 μg), or nanotoxoid(hSP) (600 μg nanosponge with 22.5 μg hSP) was injected subcutaneously. After 48 h, the mice were euthanized, and skin samples at the site of injection, where most of the nanoparticles were expected to remain, were collected for histological processing. Sections were stained either by hematoxylin and eosin (H&E) using SelecTech reagents (Leica Biosystems) or by TUNEL using an ApopTag peroxidase *in situ* apoptosis detection kit (EMD

Millipore). Bright-field images were acquired using a Hamamatsu Nanozoomer slide scanning system.

3.2.2.6 Germinal Center Formation

Six-week-old male ICR mice were administered with blank solution, heat-treated hSP (7.5 μg), nanosponge (200 μg), or nanotoxoid(hSP) (200 μg nanosponge with 7.5 μg hSP) by hock injection. On day 21 after immunization, the draining popliteal lymph nodes were collected for analysis. For immunohistochemistry, the lymph nodes were cryosectioned and stained with Pacific Blue-labeled anti-mouse/human B220 (Clone: RA3-6B2; Biolegend), Alexa488-labeled anti-mouse IgD (Clone: 11-26c.2a; Biolegend), and Alexa647-labeled anti-mouse/human GL-7 (Clone GL7; Biolegend). Fluorescence imaging was conducted on a Keyence BZ-9000 microscope. For flow cytometric analysis, the popliteal lymph nodes were dissociated into single cell suspensions using 1 mg mL^{-1} collagenase D (Roche) and 1 mg mL^{-1} DNAse I (Roche). The cells were then stained with the above antibodies followed by data collection on a BD FACSCanto-II flow cytometer. Analysis was performed using Flowjo software.

3.2.2.7 Antibody Titer Responses

Six-week-old male ICR mice were vaccinated by subcutaneous injections at the neck region with blank solution, heat-treated hSP (75 μg), or nanotoxoid(hSP) (2 mg of nanosponge with 75 μg hSP) on days 0, 7, and 14. On

day 21, the blood of each mouse was collected, and the serum was subsequently derived by centrifugation at 700 × *g*. Antibody titers were assessed by an indirect ELISA using plates coated with purified α-toxin, PVL LukS subunit, or γ-toxin A (IBT Bioservices) following a previously reported protocol [12].

3.2.2.8 Protective Efficacy against MRSA Infection

Six-week-old male ICR mice were immunized using the same formulations and schedule as above. For the subcutaneous model, 1×10^9 CFU of MRSA USA300 was inoculated into the shaved back region away from the site of vaccination on day 35. The lesion on the skin of each mouse was monitored daily and reported as the width multiplied by the length of the visibly affected area. For the systemic model, 2×10^6 CFU of MRSA USA300 was injected via the tail vein. On day 3 after challenge, the blood was first collected prior to euthanasia. The mice were then perfused with PBS, and the liver, spleen, heart, lungs, and kidneys of each mouse were collected and processed for bacterial enumeration following a previously published protocol [12]. To obtain the total bacteria count, the values from all collected organs for each individual mouse were summed.

3.2.3 Results and Discussion

We first confirmed that RBC nanosponges could be used to effectively neutralize the harmful biological activity of proteins secreted by MRSA strain

USA300. Using a hemolytic secreted protein (hSP) fraction collected from bacterial culture supernatant via ammonium sulfate precipitation, it was demonstrated that preincubation with a sufficient amount of RBC nanosponges could effectively eliminate the hSP's lytic effects on RBCs (Figure 3.2.2A). From the data, ≈400 μg of nanosponges could be used to neutralize 15 μg of the protein, and this ratio was used to fabricate an hSP-loaded nanosponge vaccine formulation, termed nanotoxoid(hSP), for further study. According to dynamic light scattering measurements, the size of the nanotoxoid(hSP) was slightly larger and the surface zeta potential was less negative when compared to the blank nanosponges without hSP loading, both suggesting the association of the hSP with the membrane-coated nanoparticle substrate (Figure 3.2.2B,C). Transmission electron microscopy confirmed that, after protein loading, nanotoxoid(hSP) still exhibited a characteristic core–shell structure [36, 37], with a membrane layer surrounding the polymeric core (Figure 3.2.2D).

While previous versions of nanotoxoids have worked with individual, purified toxins [12, 38], the advantage of the present approach is its ability to entrap and neutralize pathogen-specific virulence factors from a protein preparation with unknown composition. To validate this concept, we probed the nanotoxoid(hSP) formulation for the presence of known virulence factors by immunoblotting (Figure 3.2.2E). Of the three different antigens that were analyzed, all were easily detectable on the nanotoxoid(hSP). These included α-toxin, a major MRSA virulence factor that has previously been successfully neutralized using RBC

nanosponges [17], as well as Panton–Valentine leukocidin (PVL), a white blood cell attacking toxin expressed in most community-acquired MRSA variants [39, 40], and γ-toxin, a bicomponent toxin formed from combinations of three different monomers [41]. Quantitative western blot analysis demonstrated that α-toxin, PVL, and γ-toxin contributed to 11.0% ± 0.7%, 8.7% ± 0.8%, and 5.6% ± 0.2% of the total bacterial protein, respectively (see Experimental Section). After subjecting the nanotoxoid(hSP) to a wash step, the three toxins remained strongly present (Figure 3.2.2F). Additionally, the toxins remained mostly bound to the nanoparticles even after dialyzing against physiological buffer for 48 h (Figure 3.2.2G), which suggested stable and efficient complexation and explained the ability of the nanoparticles to neutralize the toxins' hemolytic activity.

Given the robust binding of the toxins with the nanosponges, we further sought to evaluate the safety of the nanotoxoid(hSP) formulation in various settings. First, we compared the hemolytic capacity of hSP in its native form, when subjected to rigorous heat denaturation, and when in nanotoxoid(hSP) form (Figure 3.2.3A,B). Native hSP demonstrated complete lysis while nanotoxoid(hSP) fabricated with an equivalent amount of hSP had almost no activity; this neutralization effect has previously been shown to be exclusive to membrane-coated nanoparticles [17]. As expected, blank nanosponges were not hemolytic, but it was striking that, even after boiling the hSP for 4 h, 40% of its hemolytic activity was still preserved. While specific toxins secreted by MRSA are known to be heat-labile [38], the results demonstrated that the more complex hSP preparation

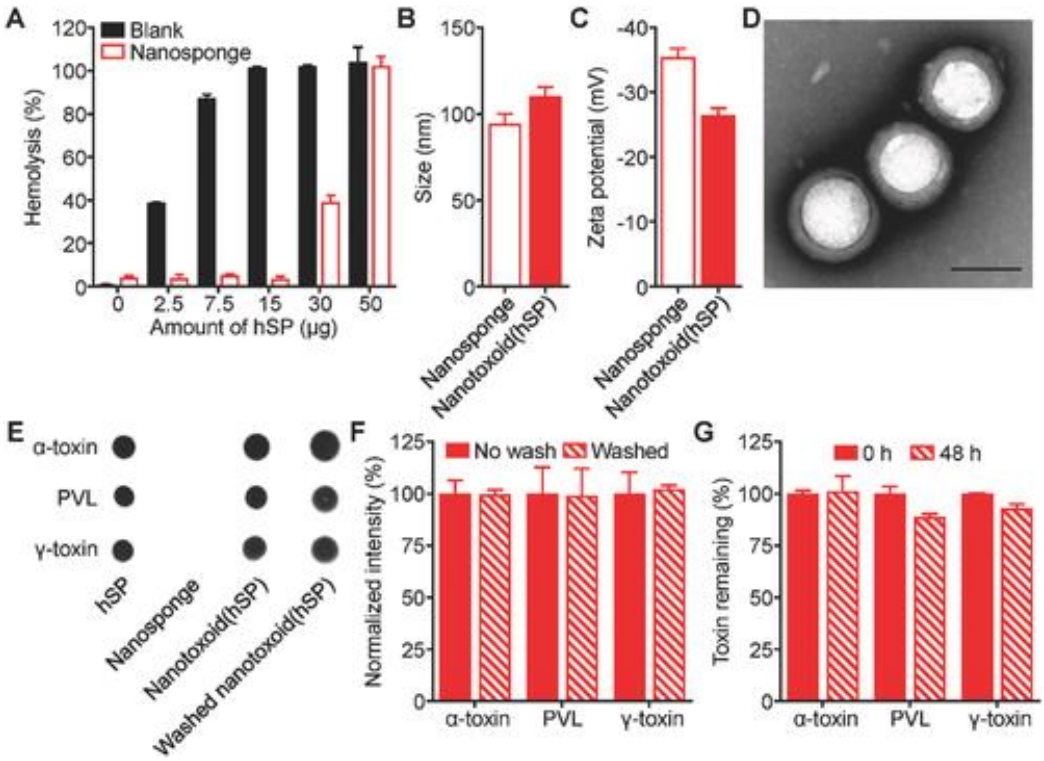

Figure 3.2.2: Synthesis and characterization of hemolytic-secreted-protein (hSP)-loaded nanotoxoid, denoted nanotoxoid(hSP). A) Hemolysis of RBCs when incubated with varying amounts of hSP in the absence or presence of 400 μg of RBC nanosponges (n = 3; mean ± SD). B) Size of RBC nanosponges and nanotoxoid(hSP) as measured by dynamic light scattering (n = 3; mean ± SD). C) Surface zeta potential of nanosponges and nanotoxoid(hSP) (n = 3; mean ± SD). D) Transmission electron microscope image of nanotoxoid(hSP) negatively stained with uranyl acetate (scale bar = 100 nm). E) Dot blots probing for α-toxin, PVL, or γ-toxin in hSP, blank nanosponges, nanotoxoid(hSP), or nanotoxoid(hSP) subject to a wash step. F) Relative band intensities of western blots probing for α-toxin, PVL, or γ-toxin in nanotoxoid(hSP) or nanotoxoid(hSP) subject to a wash step (n = 3; mean ± SD). G) Retention of α-toxin, PVL, or γ-toxin on nanotoxoid(hSP) after dialyzing against 1 × PBS for 48 h (n = 3; mean ± SD).

contained elements that were not sensitive to temperature. The data also hint that nanosponge-based neutralization, despite its nondenaturing approach, may also be more universally applicable. The results were mirrored when the same formulations were incubated with bone-marrow-derived dendritic cells (Figure 3.2.3C). The hSP preparation completely killed the cells *in vitro*, and the heat-treated proteins also

had significant toxicity, leading to only 20% of the cells remaining viable. On the other hand, both the nanotoxoid(hSP) and blank nanosponges showed no signs of cytotoxicity, again demonstrating the ability of nanocomplexation to much more effectively eliminate the harmful biological effects of the toxins.

In vivo, we assessed potential toxicity by administering the different formulations subcutaneously followed by histological analysis after 48 h (Figure 3.2.3D). Hematoxylin and eosin (H&E) staining showed that native hSP induced significant atrophy in the squamous epithelium and scattered bleeding in the dermal as well as subcutaneous tissues. Disarrangement and degeneration of collagen fibers were also observed. The toxicity of the protein was further demonstrated by TUNEL staining, which revealed widespread apoptosis throughout. In contrast, there was no obvious skin damage in the other three samples; the structure of the skin remained intact and orderly with minimal signs of apoptosis. While the heated hSP displayed considerable toxicity *in vitro*, the *in vivo* results suggest that the partial attenuation afforded by the heat treatment was sufficient to prevent it from reaching the threshold required for inducing significant damage in a more complex biological setting. Given the relative safety of the heat-treated hSP demonstrated here, we elected to employ it as a control in subsequent functional studies as a comparison against nanotoxoid(hSP).

Following the safety evaluation, the ability of the nanotoxoid(hSP) formulation to elicit potent humoral immunity was studied. The induction of germinal centers within lymph nodes is one of the critical steps in the immune

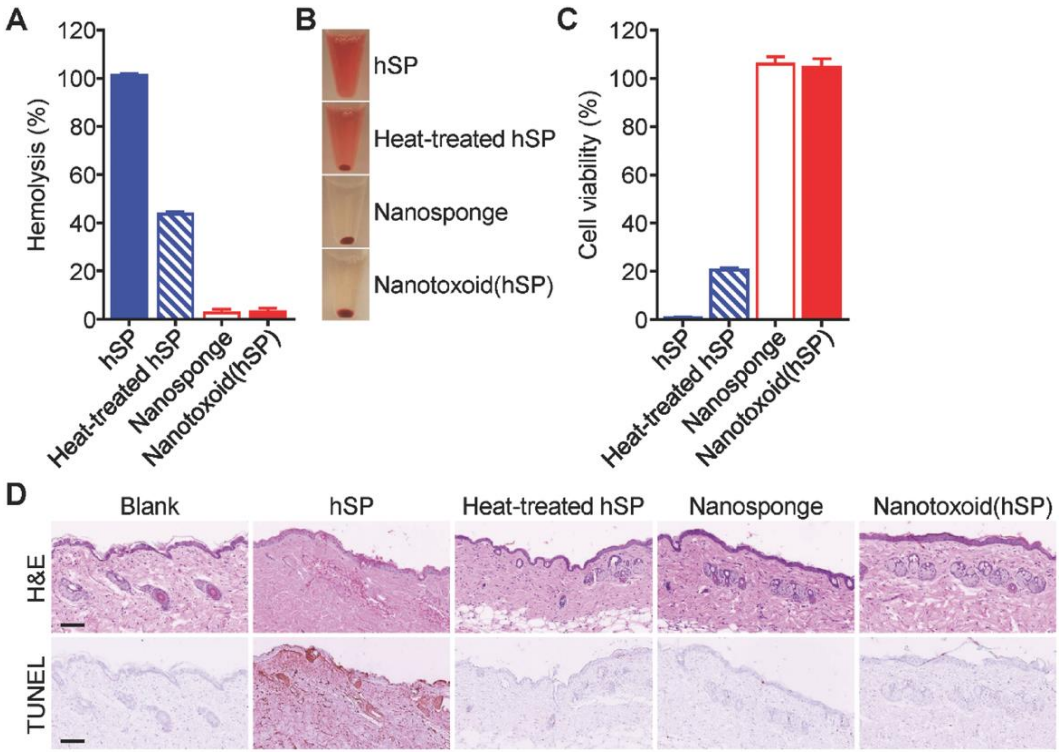

Figure 3.2.3: *In vitro* and *in vivo* safety studies. A) Comparison of hemolysis induced by hSP, heat-treated hSP, blank nanosponge, and nanotoxoid(hSP) (n = 3; mean ± SD). B) Representative images demonstrating the varying degrees of hemolysis in the samples from (A). C) Comparison of bone-marrow-derived dendritic cell viability after 24 h of incubation with hSP, heat-treated hSP, blank nanosponge, or nanotoxoid(hSP) followed by another 48 h of culture (n = 4; mean ± SD). D) Hematoxylin and eosin (H&E) and TUNEL staining of skin samples collected from untreated mice or from mice 48 h after subcutaneous injection of hSP, heat-treated hSP, blank nanosponge, or nanotoxoid(hSP) (scale bars = 100 µm).

response against infection, and it is in these regions where affinity-based maturation of B cells occurs [42]. To study the effect of the different formulations on this phenomenon, draining lymph nodes were collected 21 d after immunization and analyzed for the presence of B cells with the corresponding phenotype (Figure 3.2.4A,B). Flow cytometric analysis revealed that, of the different formulations, only the nanotoxoid(hSP) could significantly raise the percentage of B cells with the germinal center marker GL-7, with the value increasing to 44%

compared with 19% for the blank control. This was also evident by immunofluorescence staining of histological sections, which indicated the presence of several nodules with a high concentration of GL-7^+ cells in the lymph nodes of mice from the nanotoxoid(hSP) group. Of note, heat-treated hSP did not result in the formation of germinal centers despite delivering the same antigenic material. Additionally, blank nanosponges had no effect, precluding any adjuvanting contributions from the nanoparticle vector itself and suggesting a favorable biocompatibility profile [38]. From the data, it appears that the particulate delivery of undenatured bacterial hSP facilitates the generation of strong immune responses.

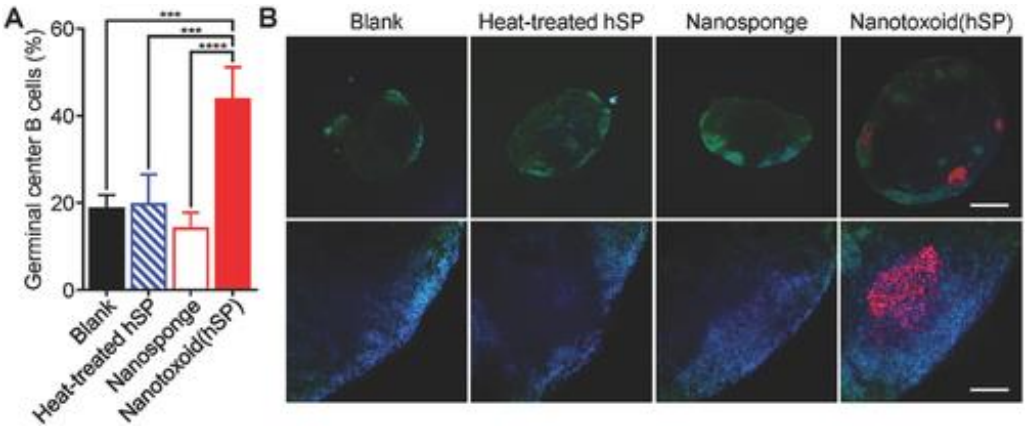

Figure 3.2.4: Germinal center formation. A) Flow cytometric analysis of cells at the draining lymph node 21 d after administration with blank solution, heat-treated hSP, blank nanosponge, or nanotoxoid(hSP) (n = 4; mean ± SD). Cells were first gated on the $B220^+IgD^{low}$ population and values are expressed as percentage GL-7^+. B) Fluorescent images of draining lymph node histological sections stained with antibodies against B220 (green), IgD (blue), and GL-7 (red) at different magnifications (top: 4× objective, scale bar = 500 µm; bottom: 20× objective, scale bar = 100 µm). ***$p < 0.001$, ****$p < 0.0001$, one-way ANOVA.

To test how the increased response to the nanoformulation would translate into antigen-specific immunity, we quantified the titers generated against known

constituents present on the nanotoxoid(hSP), including α-toxin, PVL, and γ-toxin (Figure 3.2.5A–C). To compare the different antigen-containing formulations, mice were vaccinated with a prime injection plus two boosts on days 7 and 14. On day 21, around the peak of IgG responses, the serum was sampled and titers analyzed by indirect enzyme-linked immunosorbent assays (ELISAs). For α-toxin, which is one of the most highly secreted by MRSA, there was an easily detectable difference in antibody production. This is consistent with previous reports on a nanotoxoid formulated with purified α-toxin [12, 38]. Heat-treated hSP was approximately two orders of magnitude less effective. For PVL, 57% of the mice exhibited highly elevated titers when vaccinated with the nanotoxoid(hSP), while the other portion were nonresponders. This represented a large improvement compared with the heat-treated hSP group, which had titer values near baseline. While the results for γ-toxin were less pronounced, the effect of nanotoxoid(hSP) vaccination still bordered on significance. It appeared that the trend in titer production reflected the relative amounts of each toxin in the hSP preparation. In total, the nanotoxoid(hSP) formulation was more adept at eliciting antitoxin immune responses compared with the heat-treated protein formulation, despite both delivering the same antigenic material.

Finally, we evaluated the effectiveness of nanotoxoid(hSP) vaccination in preventing live bacterial infection by employing MRSA strain USA300 in two

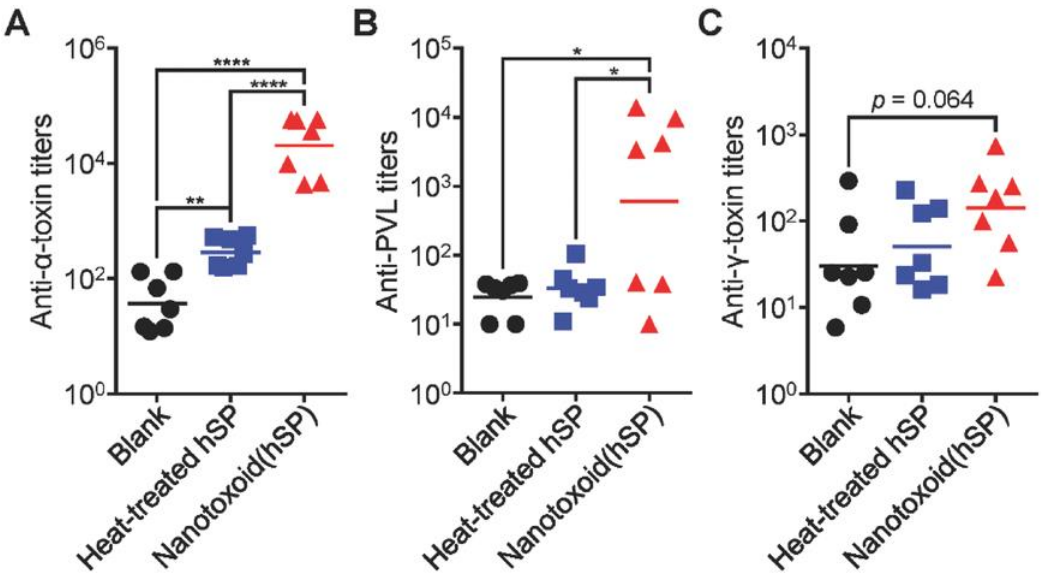

Figure 3.2.5: Multivalent antibody responses *in vivo*. Mice were vaccinated with blank solution, heat-treated hSP, or nanotoxoid(hSP) on day 0 with boosts on days 7 and 14. On day 21, the serum was sampled and analyzed for the presence of IgG antibody titers against A) α-toxin, B) PVL, and C) γ-toxin ($n = 7$; geometric mean). *$p < 0.05$, **$p < 0.01$, ****$p < 0.0001$, one-way ANOVA.

separate *in vivo* models reflective of how the disease presents in the clinic [43, 44]. For both studies, mice were vaccinated with a prime injection plus two boosts on days 7 and 14. On day 35 after the first administration, mice were challenged with bacteria, and the impact of antivirulence immunity on bacterial survival was assessed. In the subcutaneous model, which mimics the skin infections common to MRSA[45], the nanotoxoid(hSP) had a striking effect on skin lesion formation (Figure 3.2.6A). On the final day of the study, those receiving the nanotoxoid(hSP) had, on average, a threefold smaller affected area compared to mice vaccinated with heat-treated hSP. Similarly, the nanotoxoid(hSP) performed well in controlling bacterial growth upon intravenous injection, which was used to model potentially life-threatening systemic MRSA infections [46] (Figure 3.2.6B,C). Looking at the

total bacterial load 3 d after challenge, mice vaccinated with the nanotoxoid(hSP) were able to much more effectively clear out the MRSA bacteria compared to those receiving heat-treated hSP. At the organ level, the effect was most apparent in the heart, lungs, and especially the kidneys. Overall, the results are a reflection of the differences seen in titer production among the formulations and highlight the stronger immunity generated by the nanotoxoid(hSP) formulation, which inhibits the ability of the bacteria to survive over time.

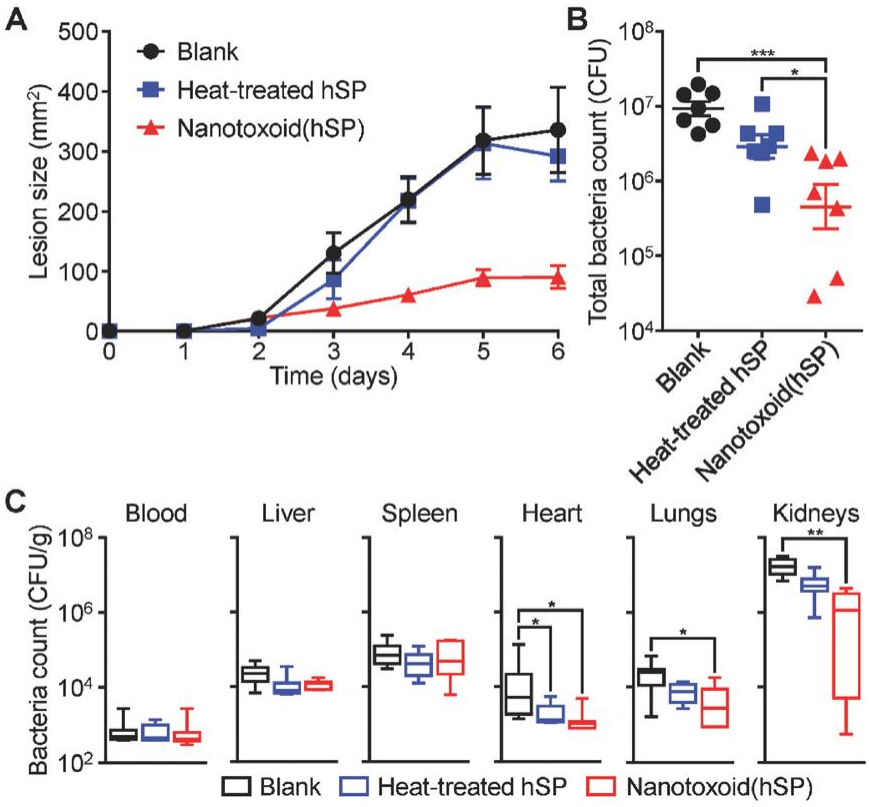

Figure 3.2.6: Protection against challenge with live bacteria. Mice were vaccinated with blank solution, heat-treated hSP, or nanotoxoid(hSP) on day 0 with boosts on days 7 and 14. A) Lesion size over time after subcutaneous challenge with MRSA USA300 on day 35 (n = 7; mean ± SEM). B) Total bacterial load summed from major organs 3 d after intravenous challenge with MRSA USA300 on day 35 (n = 7; geometric mean ± SEM). C) Individual, weight-normalized bacteria counts in major organs from (B) (n = 7; min to max). *p < 0.05, **p < 0.01, ***p < 0.001, one-way ANOVA.

3.2.4 Conclusion

In conclusion, we have reported on a method of fabricating on-demand nanotoxoids for use as vaccines against pathogenic bacteria. The nanoformulation was able to entrap virulence factors from protein preparations of unknown composition, was safe both *in vitro* and *in vivo*, and could elicit functional immunity capable of combating live bacterial infections. Despite containing the same bacterial antigens, the nanotoxoid(hSP) formulation consistently outperformed a denatured protein preparation in all of the metrics studied, which underscores the utility of biomimetic nanoparticle-based neutralization and delivery. Overall this strategy helps to address major hurdles in the design of antivirulence vaccines, enabling increased antigenic breadth while maintaining safety. Looking forward, the workflow presented here can easily be modified for application toward a variety of different pathogens. It may be possible to employ personalized culture isolates or to change culture conditions such that virulence factor production is modulated. Alternatively, nanotoxoid formulations can be screened to identify a broadly neutralizing option that is effective across multiple bacterial strains. Other purification or fractionation strategies can be tested to emphasize nonhemolytic virulence factors, and different membrane substrates derived from other cell types can be leveraged [47-49]. The inclusion of immunological adjuvants can also be considered to further boost efficacy [50-52]. Ultimately, the success of antivirulence vaccines may help to control the spread of many deadly diseases and abate the rising threat of antibiotic-resistant bacteria.

Chapter 3, in full, is a reprint of the material as it appears in *Advanced Functional Materials*, 2016, Fei Wang, Ronnie Fang, Brian Luk, Che-Ming Hu, Soracha Thamphiwatana, Diana Dehaini, Pavimol Angsantikul, Ashley Kroll, Zhiqing Pang, Weiwei Gao, Weiyue Lu and Liangfang Zhang, and *Advanced Materials*, 2017, Xiaoli Wei, Jie Gao, Fei Wang, Man Ying, Pavimol Angsantikul, Ashley Kroll, Jiarong Zhou, Weiwei Gao, Weiyue Lu, Ronnie Fang and Liangfang Zhang. The dissertation author was a major contributor and co-author of these papers.

3.2.5 References

1. Lewis, K., *Platforms for antibiotic discovery.* Nat Rev Drug Discov, 2013. **12**(5): p. 371-87.

2. Arias, C.A. and B.E. Murray, *Antibiotic-resistant bugs in the 21st century--a clinical super-challenge.* N Engl J Med, 2009. **360**(5): p. 439-43.

3. Wright, G.D. and A.D. Sutherland, *New strategies for combating multidrug-resistant bacteria.* Trends Mol Med, 2007. **13**(6): p. 260-7.

4. Spellberg, B., J.G. Bartlett, and D.N. Gilbert, *The future of antibiotics and resistance.* N Engl J Med, 2013. **368**(4): p. 299-302.

5. Ng, V.W., X. Ke, A.L. Lee, J.L. Hedrick, and Y.Y. Yang, *Synergistic co-delivery of membrane-disrupting polymers with commercial antibiotics against highly opportunistic bacteria.* Adv Mater, 2013. **25**(46): p. 6730-6.

6. Xiong, M.H., Y.J. Li, Y. Bao, X.Z. Yang, B. Hu, and J. Wang, *Bacteria-responsive multifunctional nanogel for targeted antibiotic delivery.* Adv Mater, 2012. **24**(46): p. 6175-80.

7. Rasko, D.A. and V. Sperandio, *Anti-virulence strategies to combat bacteria-mediated disease.* Nat Rev Drug Discov, 2010. **9**(2): p. 117-28.

8. Cegelski, L., G.R. Marshall, G.R. Eldridge, and S.J. Hultgren, *The biology and future prospects of antivirulence therapies.* Nat Rev Microbiol, 2008. **6**(1): p. 17-27.

9. Clatworthy, A.E., E. Pierson, and D.T. Hung, *Targeting virulence: a new paradigm for antimicrobial therapy.* Nat Chem Biol, 2007. **3**(9): p. 541-8.

10. Henkel, J.S., M.R. Baldwin, and J.T. Barbieri, *Toxins from bacteria.* EXS, 2010. **100**: p. 1-29.

11. Lubran, M.M., *Bacterial toxins.* Ann Clin Lab Sci, 1988. **18**(1): p. 58-71.

12. Wang, F., R.H. Fang, B.T. Luk, C.J. Hu, S. Thamphiwatana, D. Dehaini, P. Angsantikul, A.V. Kroll, Z. Pang, W. Gao, W. Lu, and L. Zhang, *Nanoparticle-Based Antivirulence Vaccine for the Management of Methicillin-Resistant Staphylococcus aureus Skin Infection.* Advanced Functional Materials, 2016. **26**(10): p. 1628-1635.

13. Mellbye, B. and M. Schuster, *The sociomicrobiology of antivirulence drug resistance: a proof of concept.* MBio, 2011. **2**(5).

14. Hua, L., T.S. Cohen, Y. Shi, V. Datta, J.J. Hilliard, C. Tkaczyk, J. Suzich, C.K. Stover, and B.R. Sellman, *MEDI4893* Promotes Survival and Extends the Antibiotic Treatment Window in a Staphylococcus aureus Immunocompromised Pneumonia Model.* Antimicrob Agents Chemother, 2015. **59**(8): p. 4526-32.

15. DiGiandomenico, A., A.E. Keller, C. Gao, G.J. Rainey, P. Warrener, M.M. Camara, J. Bonnell, R. Fleming, B. Bezabeh, N. Dimasi, B.R. Sellman, J. Hilliard, C.M. Guenther, V. Datta, W. Zhao, C. Gao, X.Q. Yu, J.A. Suzich, and C.K. Stover, *A multifunctional bispecific antibody protects against Pseudomonas aeruginosa.* Sci Transl Med, 2014. **6**(262): p. 262ra155.

16. Fang, R.H., B.T. Luk, C.M. Hu, and L. Zhang, *Engineered nanoparticles mimicking cell membranes for toxin neutralization.* Adv Drug Deliv Rev, 2015. **90**: p. 69-80.

17. Hu, C.M., R.H. Fang, J. Copp, B.T. Luk, and L. Zhang, *A biomimetic nanosponge that absorbs pore-forming toxins.* Nat Nanotechnol, 2013. **8**(5): p. 336-40.

18. Hoshino, Y., H. Koide, T. Urakami, H. Kanazawa, T. Kodama, N. Oku, and K.J. Shea, *Recognition, neutralization, and clearance of target peptides in the bloodstream of living mice by molecularly imprinted polymer nanoparticles: a plastic antibody.* J Am Chem Soc, 2010. **132**(19): p. 6644-5.

19. Wang, F., W. Gao, S. Thamphiwatana, B.T. Luk, P. Angsantikul, Q. Zhang, C.M. Hu, R.H. Fang, J.A. Copp, D. Pornpattananangkul, W. Lu, and L. Zhang, *Hydrogel Retaining Toxin-Absorbing Nanosponges for Local Treatment of Methicillin-Resistant Staphylococcus aureus Infection.* Adv Mater, 2015. **27**(22): p. 3437-43.

20. Kitchin, N.R., *Review of diphtheria, tetanus and pertussis vaccines in clinical development.* Expert Rev Vaccines, 2011. **10**(5): p. 605-15.

21. Watkins, R.R., M.Z. David, and R.A. Salata, *Current concepts on the virulence mechanisms of meticillin-resistant Staphylococcus aureus.* J Med Microbiol, 2012. **61**(Pt 9): p. 1179-93.

22. Cryz, S.J., Jr., E. Furer, and R. Germanier, *Effect of chemical and heat inactivation on the antigenicity and immunogenicity of Vibrio cholerae.* Infect Immun, 1982. **38**(1): p. 21-6.

23. Fulthorpe, A.J. and R.O. Thomson, *Antigenic efficiency of tetanus toxoids modified by excess formalin or by heat and phenol.* Immunology, 1960. **3**: p. 126-34.

24. Metz, B., G.F. Kersten, P. Hoogerhout, H.F. Brugghe, H.A. Timmermans, A. de Jong, H. Meiring, J. ten Hove, W.E. Hennink, D.J. Crommelin, and W. Jiskoot, *Identification of formaldehyde-induced modifications in proteins: reactions with model peptides.* J Biol Chem, 2004. **279**(8): p. 6235-43.

25. Zhang, W. and D.A. Sack, *Current Progress in Developing Subunit Vaccines against Enterotoxigenic Escherichia coli-Associated Diarrhea.* Clin Vaccine Immunol, 2015. **22**(9): p. 983-91.

26. Gordon, R.J. and F.D. Lowy, *Pathogenesis of methicillin-resistant Staphylococcus aureus infection.* Clin Infect Dis, 2008. **46 Suppl 5**: p. S350-9.

27. Wannamaker, L.W., *Streptococcal toxins.* Rev Infect Dis, 1983. **5 Suppl 4**: p. S723-32.

28. Fujita, Y. and H. Taguchi, *Current status of multiple antigen-presenting peptide vaccine systems: Application of organic and inorganic nanoparticles.* Chemistry Central Journal, 2011. **5**.

29. Molloy, E.M., P.D. Cotter, C. Hill, D.A. Mitchell, and R.P. Ross, *Streptolysin S-like virulence factors: the continuing sagA.* Nat Rev Microbiol, 2011. **9**(9): p. 670-81.

30. Shewen, P.E. and B.N. Wilkie, *Vaccination of calves with leukotoxic culture supernatant from Pasteurella haemolytica.* Can J Vet Res, 1988. **52**(1): p. 30-6.

31. Ferreira, R.B., Y. Valdez, B.K. Coombes, S. Sad, J.W. Gouw, E.M. Brown, Y. Li, G.A. Grassl, L.C. Antunes, N. Gill, M. Truong, R. Scholz, L.A. Reynolds, L. Krishnan, A.A. Zafer, N. Sal-Man, M.J. Lowden, S.D. Auweter, L.J. Foster, and B.B. Finlay, *A Highly Effective Component Vaccine against Nontyphoidal Salmonella enterica Infections.* MBio, 2015. **6**(5): p. e01421-15.

32. Geny, B. and M.R. Popoff, *Bacterial protein toxins and lipids: pore formation or toxin entry into cells.* Biol Cell, 2006. **98**(11): p. 667-78.

33. Otto, M., *Staphylococcus aureus toxins.* Curr Opin Microbiol, 2014. **17**: p. 32-7.

34. Copp, J.A., R.H. Fang, B.T. Luk, C.M. Hu, W. Gao, K. Zhang, and L. Zhang, *Clearance of pathological antibodies using biomimetic nanoparticles.* Proc Natl Acad Sci U S A, 2014. **111**(37): p. 13481-6.

35. Fang, R.H., C.M. Hu, B.T. Luk, W. Gao, J.A. Copp, Y. Tai, D.E. O'Connor, and L. Zhang, *Cancer cell membrane-coated nanoparticles for anticancer vaccination and drug delivery.* Nano Lett, 2014. **14**(4): p. 2181-8.

36. Gao, W., C.M. Hu, R.H. Fang, B.T. Luk, J. Su, and L. Zhang, *Surface functionalization of gold nanoparticles with red blood cell membranes.* Adv Mater, 2013. **25**(26): p. 3549-53.

37. Hu, C.M., L. Zhang, S. Aryal, C. Cheung, R.H. Fang, and L. Zhang, *Erythrocyte membrane-camouflaged polymeric nanoparticles as a biomimetic delivery platform.* Proc Natl Acad Sci U S A, 2011. **108**(27): p. 10980-5.

38. Hu, C.M., R.H. Fang, B.T. Luk, and L. Zhang, *Nanoparticle-detained toxins for safe and effective vaccination.* Nat Nanotechnol, 2013. **8**(12): p. 933-8.

39. Shallcross, L.J., E. Fragaszy, A.M. Johnson, and A.C. Hayward, *The role of the Panton-Valentine leucocidin toxin in staphylococcal disease: a systematic review and meta-analysis.* Lancet Infect Dis, 2013. **13**(1): p. 43-54.

40. Voyich, J.M., M. Otto, B. Mathema, K.R. Braughton, A.R. Whitney, D. Welty, R.D. Long, D.W. Dorward, D.J. Gardner, G. Lina, B.N. Kreiswirth, and F.R. DeLeo, *Is Panton-Valentine leukocidin the major virulence determinant in community-associated methicillin-resistant Staphylococcus aureus disease?* J Infect Dis, 2006. **194**(12): p. 1761-70.

41. Cooney, J., Z. Kienle, T.J. Foster, and P.W. O'Toole, *The gamma-hemolysin locus of Staphylococcus aureus comprises three linked genes, two of which are identical to the genes for the F and S components of leukocidin.* Infect Immun, 1993. **61**(2): p. 768-71.

42. Victora, G.D. and M.C. Nussenzweig, *Germinal centers.* Annu Rev Immunol, 2012. **30**: p. 429-57.

43. Klevens, R.M., M.A. Morrison, J. Nadle, S. Petit, K. Gershman, S. Ray, L.H. Harrison, R. Lynfield, G. Dumyati, J.M. Townes, A.S. Craig, E.R. Zell, G.E. Fosheim, L.K. McDougal, R.B. Carey, S.K. Fridkin, and M.I. Active Bacterial Core surveillance, *Invasive methicillin-resistant Staphylococcus aureus infections in the United States.* JAMA, 2007. **298**(15): p. 1763-71.

44. Gorwitz, R.J., *A review of community-associated methicillin-resistant Staphylococcus aureus skin and soft tissue infections.* Pediatr Infect Dis J, 2008. **27**(1): p. 1-7.

45. Boucher, H., L.G. Miller, and R.R. Razonable, *Serious infections caused by methicillin-resistant Staphylococcus aureus.* Clin Infect Dis, 2010. **51 Suppl 2**: p. S183-97.

46. Gonzalez, B.E., G. Martinez-Aguilar, K.G. Hulten, W.A. Hammerman, J. Coss-Bu, A. Avalos-Mishaan, E.O. Mason, Jr., and S.L. Kaplan, *Severe Staphylococcal sepsis in adolescents in the era of community-acquired methicillin-resistant Staphylococcus aureus.* Pediatrics, 2005. **115**(3): p. 642-8.

47. Fang, R.H., Y. Jiang, J.C. Fang, and L.F. Zhang, *Cell membrane-derived nanomaterials for biomedical applications.* Biomaterials, 2017. **128**: p. 69-83.

48. Dehaini, D., X. Wei, R.H. Fang, S. Masson, P. Angsantikul, B.T. Luk, Y. Zhang, M. Ying, Y. Jiang, A.V. Kroll, W. Gao, and L. Zhang, *Erythrocyte-Platelet Hybrid Membrane Coating for Enhanced Nanoparticle Functionalization.* Adv Mater, 2017. **29**(16).

49. Hu, C.M., R.H. Fang, K.C. Wang, B.T. Luk, S. Thamphiwatana, D. Dehaini, P. Nguyen, P. Angsantikul, C.H. Wen, A.V. Kroll, C. Carpenter, M. Ramesh, V. Qu, S.H. Patel, J. Zhu, W. Shi, F.M. Hofman, T.C. Chen, W. Gao, K. Zhang, S. Chien, and L. Zhang, *Nanoparticle biointerfacing by platelet membrane cloaking.* Nature, 2015. **526**(7571): p. 118-21.

50. Zhang, Y., F.M. Wang, E.G. Ju, Z. Liu, Z.W. Chen, J.S. Ren, and X.G. Qu, *Metal-Organic-Framework-Based Vaccine Platforms for Enhanced Systemic Immune and Memory Response.* Advanced Functional Materials, 2016. **26**(35): p. 6454-6461.

51. Tao, Y., E.G. Ju, Z.H. Li, J.S. Ren, and X.G. Qu, *Engineered CpG- Antigen Conjugates Protected Gold Nanoclusters as Smart Self- Vaccines for Enhanced Immune Response and Cell Imaging.* Advanced Functional Materials, 2014. **24**(7): p. 1004-1010.

52. Li, Z., Z. Liu, M. Yin, X. Yang, J. Ren, and X. Qu, *Combination delivery of antigens and CpG by lanthanides-based core-shell nanoparticles for enhanced immune response and dual-mode imaging.* Adv Healthc Mater, 2013. **2**(10): p. 1309-13.

Chapter 4

Platelet Membrane-Coated Nanoparticles as "Nanosponges" for Autoantibody Clearance

4.1 Introduction

Platelets, also known as thrombocytes, are a blood component that is essential for maintaining hemostasis. One of their main functions is to stop bleeding via initiation and propagation of the coagulation cascade [1, 2]. Platelet count is universally regarded as the key indicator of bleeding risk, and the normal range in healthy people sits between 150,000 and 450,000 platelets per microliter of blood. A count under the normal range, termed thrombocytopenia, can be due to either decreased platelet production or increased platelet destruction. Clinically, the disease can manifest itself as purpura, a delay in the normal process of clotting, and spontaneous or excessive bleeding. When platelet counts drop substantially lower than normal values, internal hemorrhaging can occur, a severe condition that can potentially be fatal [3].

Immune thrombocytopenia purpura (ITP), which is oftentimes also referred to as idiopathic thrombocytopenic purpura, is an immune-mediated hematological disorder characterized by low level of platelets and easy or excessive bleeding due to the presence of anti-platelet autoantibodies [4, 5]. These pathological antibodies bind to specific antigens on the platelet surface, leading to sequestration and destruction by the reticuloendothelial system. The age-adjusted prevalence of ITP is estimated to be 9.5 per 100,000 persons in the United States [6]. While the condition may appear secondary to a known autoimmune condition or infection, oftentimes the underlying etiology is unclear [7-9]. Given this fact, chronic ITP is

classically treated using nonspecific therapies such as corticosteroids. While capable of eliciting a rebound in platelet levels in many patients, such treatments are susceptible to relapse and can cause unwanted side effects [5, 10]. For those that fail to respond to frontline treatments, invasive and irreversible splenectomy is a common intervention, but has the chance of postoperative complications such as infection, bleeding, and hospitalization [11, 12]. Other second- and third-line treatments include intravenous immunoglobulin (IVIg) [13], intravenous Rho immunoglobulin (RhIg) [14], rituximab (anti-CD20) [15], and thrombopoietin receptor agonists [16]. Most carry significant iatrogenic risk given their generally non-specific modes of action. With the probability of high side effects, treatment can ultimately be more burdensome than the original disease. With these considerations in mind, the development of a treatment modality that can specifically target the pathological moieties responsible for ITP is highly desirable.

Cell membrane-coated nanoparticles represent an increasingly popular platform for a variety of applications, including drug delivery [17], vaccination [18, 19], and detoxification [20, 21]. A significant factor behind their appeal is the ability to replicate the surface properties of different cell types faithfully on nanoparticle surfaces. Employing biological materials through a top-down coating approach bestows synthetic nanoparticles with native cell functionalities. For example, it has been shown that coating with red blood cell membrane actively modulates residence time in the bloodstream via the display of self-markers that are recognized by the immune system [22]. Functionalization with platelet membrane

enables biomimetic targeting by taking advantage of the natural interactions between platelet surface markers and different targets, including damaged vasculature and pathogens [23, 24]. Given the wide range of biological interactions that natural cell membranes participate in, the potential of cell membrane-coated nanoparticles extends far beyond traditional nanodelivery applications. One such area is biodetoxification where the membrane coating serves as an ideal substrate for interaction with biological toxins, enabling their neutralization and subsequent clearance. For example, red blood cell membrane-coated nanoparticles have previously been shown to bind and clear both bacterial toxins [20] as well as small molecule poisons [21].

Here, we demonstrated the use of platelet-derived membrane as a natural biomaterial for the design of nanoparticulate decoys that can effectively bind and clear the pathological antibodies responsible for ITP (Figure 4.1). The binding capacity and specificity of platelet membrane-coated nanoparticles (PNPs) were evaluated before studying the neutralization capacity of PNPs against anti-platelet antibodies both *in vitro* and *in vivo*. Finally, an antibody-induced murine model of ITP was employed in order to assess treatment efficacy. As a possible new treatment for ITP, PNP administration holds distinct advantages compared to current therapies. By using the natural substrate of the pathological agent, the treatment is highly specific, which may prevent the immune compromising side effects commonly seen with other treatments. Further, by diverting anti-platelet antibodies away from healthy platelets, PNPs directly act to preserve normal

hemostatic function. Ultimately, employing this biomimetic nanoparticle system for the specific treatment of ITP may serve to improve patient outcomes in the clinic.

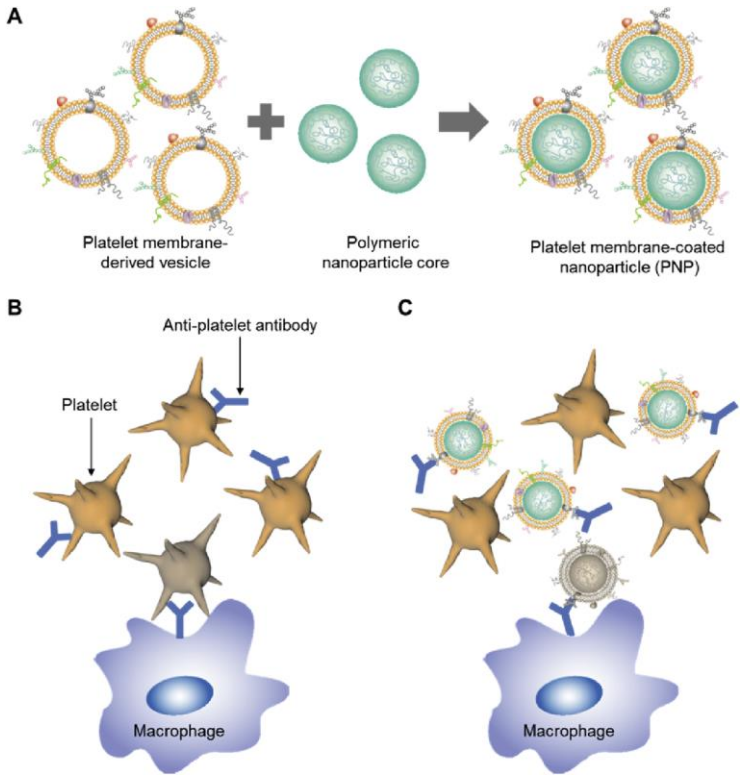

Figure 4.1: Schematic of platelet membrane-coated nanoparticles (PNPs) for the treatment of immune thrombocytopenia purpura (ITP). (A) To fabricate PNPs, the plasma membrane from fresh platelets is derived and then coated onto poly(lactic-co-glycolic acid) (PLGA) polymeric nanoparticle cores, transferring the surface antigenic material from the original cells onto the outside of the nanoparticles. (B) Without treatment, ITP is characterized by the binding of pathological autoantibodies to healthy platelets, resulting in their clearance by the reticuloendothelial system. (C) When PNPs are administered, they act as decoys that bind to the pathological autoantibodies, neutralizing them from circulation and enabling the survival of healthy platelets.

4.2 Experimental Methods

4.2.1 Animals

Male CD-1mice (6-week old; 20–24 g body weight) were purchased from Harlan Laboratories. All animal experiments were performed in accordance with NIH guidelines and approved by the Institutional Animal Care and Use Committee (IACUC) of the University of California, San Diego.

4.2.2 Platelet Isolation and Membrane Derivation

Whole blood was collected from male adult CD-1 mice (Harlan Laboratories) via puncture of the submandibular vein with ethylenediaminetetraacetic acid (EDTA; USB Corporation) as the anticoagulant. To isolate platelets, the blood was first centrifuged at 300*g* for 5 min at room temperature. The supernatant then was collected and spun at the same speed for another 5 min. The resulting supernatant, representing a platelet rich plasma, was then centrifuged at 2000*g* for 4 min in order to pellet down the platelets, which were resuspended in water, aliquoted, and stored at −80 °C for further use. Platelet membrane was derived by a repeated freeze-thaw process. A frozen aliquot of purified platelets was allowed to thaw at room temperature, centrifuged at 21,000*g* for 7 min, and the pellet was resuspended in water. The platelet suspension

was refrozen, and the process was repeated three times. The pellet was finally resuspended in water, and the membrane protein concentration was quantified using a commercial BCA assay (Pierce).

4.2.3 Preparation and Characterization of Platelet Membrane-Coated Nanoparticles (PNPs)

PNPs were prepared using a previously reported sonication method [24]. Polymeric nanoparticle cores were prepared using carboxyl acid-terminated 0.67 dL/g 50:50 poly($_{DL}$-lactic-*co*-glycolic acid) (PLGA; LACTEL Absorbable Polymers) in a nanoprecipitation process. A volume of 1 mL of a 10 mg/mL PLGA solution in acetone was added rapidly to 4 mL of water. The acetone was then allowed to evaporate under vacuum for 3 h. PNPs were prepared by fusing platelet membrane onto PLGA cores via sonication using a Fisher Scientific FS30D bath sonicator at a frequency of 42 kHz and a power of 100 W for 2 min. The size and zeta-potential of PNPs were measured by dynamic light scattering (DLS) using a Malvern ZEN 3600 Zetasizer. To study the morphology of PNPs by transmission electronic microscopy (TEM), samples were deposited onto a 400-mesh carbon-coated copper grid (Electron Microscopy Sciences) and negatively stained with vanadium (Abcam).

4.2.4 Platelet Membrane to Nanoparticle Ratio Optimization

To optimize the platelet membrane to PLGA core ratio, PNPs were synthesized at membrane-to-core weight ratios ranging from 0.125 to 2 at a final polymer concentration of 1 mg/mL. PLGA cores without membrane coating were included as a control. The sizes of each set of particles were first measured by DLS immediately after synthesis. Afterwards, the particle solutions were adjusted to 1 × PBS by adding an equal volume of 2 × PBS and the particle sizes were measured again. An increase in size upon introduction of PBS was used as an indicator of particle instability.

4.2.5 *In Vitro* Binding Capacity and Specificity Studies

To evaluate the *in vitro* binding capacity of PNPs, 10 μg of the nanoparticles was mixed with different amounts (2, 4, 8, 16, 32, 64, and 128 μg) of fluorescein isothiocyanate (FITC)-labeled polyclonal anti-mouse thrombocyte antibodies (Lifespan Biosciences). The precise antigen specificity of the antibodies was unknown. After mixing the PNPs with antibodies, the fluorescence intensity of the fluorescently labeled antibody was measured using a Tecan Infinite M200 plate reader. The mixtures were incubated for 10 min at 37 °C, then centrifuged at 21,000*g* for 8 min to pellet the PNP/anti-platelet complexes. The fluorescence intensity of the supernatant was measured and used to calculate the amount of

antibody that had bound to the PNPs. To evaluate binding specificity, either 10 μg of PNPs or 10 μg of polyethylene glycol-functionalized nanoparticles (PEG-NPs) [25] were mixed with 32 μg of FITC-labeled antibody. To test the binding capacity in serum, 10 μg of PNPs were incubated with 128 μg of FITC-labeled antibody in either PBS or 50 vol% mouse serum.

4.2.6 *In Vitro* Neutralization

For the pre-incubation study, 20 μg of FITC-labeled anti-platelet antibody was incubated with varying amounts of PNP (5, 10, 20, 50, and 100 μg) or PBS at 37 °C for 15 min. The mixture was then added to a solution containing the number of platelets equivalent to 40 μg worth of membrane material and incubated at 37 °C for 15 min. For competitive co-incubation study, the same amounts of PNPs and antibody were concurrently added to the platelets. All samples were then washed by centrifugation at 2000*g* three times with PBS. The amount of antibody binding to platelets was measured by flow cytometry on a Becton Dickinson FACSCanto II flow cytometer and analyzed using Treestar FlowJo.

4.2.7 *In Vivo* Binding Stability

To establish a mouse model of thrombocytopenia, 6-week old CD-1 mice were injected intraperitoneally with PBS or 50 μg of anti-thrombocyte antibody.

The mice were bled before injection as well as 4 h and 24 h after injection for platelet enumeration. Male 6-week old CD-1 mice were injected intraperitoneally with either 50 μg of anti-mouse thrombocyte antibody (Lifespan Biosciences) pre-incubated with 100 μg of PNPs, 50 μg of antibody alone, or PBS. Blood was sampled by submandibular vein puncture both before and 24 h after injection using EDTA as the anticoagulant. To enumerate the platelets, a 1 μL volume of blood was diluted 1000 times in 1% bovine serum albumin (Sigma Aldrich) in PBS. The diluted solution was then stained with FITC-labeled anti-mouse CD41 (Biolegend) for labeling of platelets, and flow cytometry was used to count the number of $FITC^+$ events per given volume.

4.2.8 *In Vivo* Treatment

Male 6-week old CD-1 mice were injected intraperitoneally with 50 μg of anti-thrombocyte antibody to induce thrombocytopenia. After 15 min, mice received either 400 μg of PNPs, 400 μg of PEG-NPs, or PBS via tail vein injection. Blood was sampled both before and 24 h after administration of antibody. To assess the effect of treatment on bleeding time, mice were first anesthetized 24 h after antibody administration with a cocktail of 150 mg/kg ketamine (Zoetis) and 10 mg/kg xylazine (Lloyd Laboratories). For the bleeding time assay, a tail segment 5 mm from the distal end was excised by a sterile blade, and the cut end of the tail was immediately placed into 37 °C saline solution in a 50 mL tube. The time from

amputation to complete cessation of bleeding was recorded for each mouse. Those mice bleeding longer than a pre-determined time limit of 20 min were euthanized immediately.

4.3 Results and Discussion

PNPs were prepared by fusing mouse platelet-derived membrane onto the surface of poly(lactic-*co*-glycolic acid) (PLGA) nanoparticle cores [24]. In brief, platelets collected from whole blood were subjected to repeated freeze-thaw cycles and centrifugation in order to obtain purified membrane. The membrane was then coated onto the surface of preformed PLGA nanoparticles by a sonication process. After the membrane coating, dynamic light scattering indicated an approximately 20 nm increase in the average hydrodynamic diameter over that of the bare PLGA cores (Figure 4.2A). Zeta potential measurements also suggested successful coating, as evidenced by the increase in surface charge of the coated nanoparticles to approximately the same level as a membrane vesicle only sample (Figure 4.2B). Moreover, transmission electron microscopy of negatively stained PNPs revealed a characteristic core-shell structure with a layer of membrane coated over the polymer core (Figure 4.2C). In order to optimize the membrane coating ratio, PNPs were prepared using different membrane to PLGA core weight ratios ranging from 0.125 to 2 (Figure 4.2D). After adjusting to 1 × phosphate buffered saline (PBS) solution, which represents physiological salt concentrations, bare PLGA cores with

no membrane coating aggregated immediately due to charge screening effects. With increasing amounts of membrane, there was a trend of decreasing aggregation. At a ratio of 1 to 1, no apparent size increase was observed, and this formulation was chosen for further studies. The particles also demonstrated little change in size and distribution when subjected to high shear conditions.

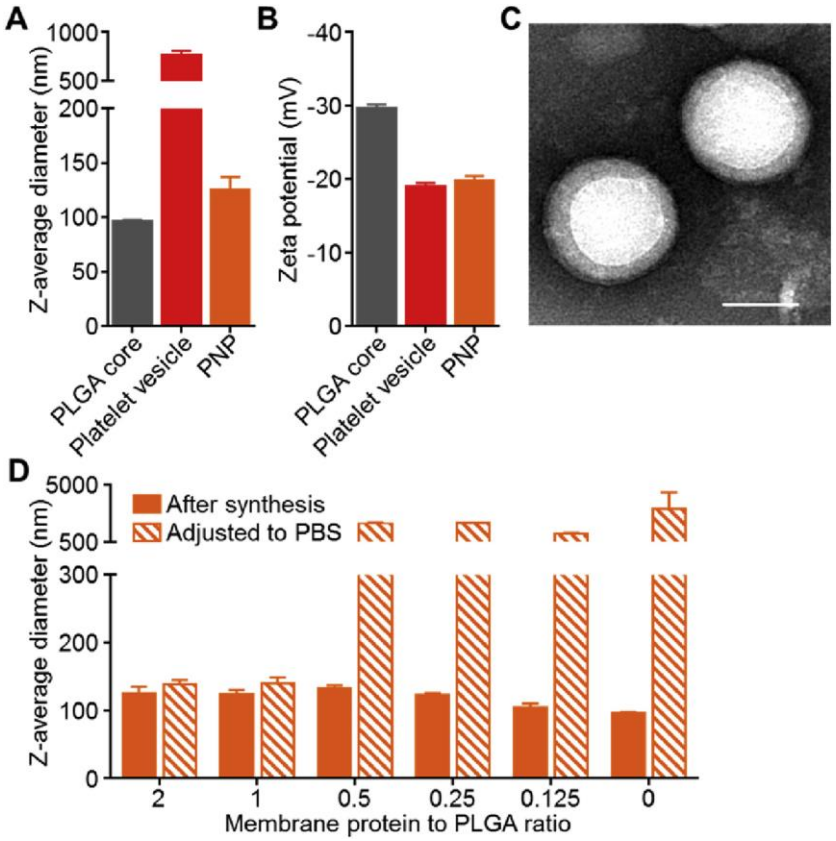

Figure 4.2: Characterization and optimization of PNPs. (A) Hydrodynamic size of bare PLGA cores, platelet vesicles, and PNPs as measured by dynamic light scattering (n = 3; mean ± SD). (B) Surface zeta potential of bare PLGA cores, platelet vesicles, and PNPs (n = 3; mean ± SD). (C) Transmission electron microscopy images of PNPs negatively stained with vanadium (scale bar = 75 nm). (D) Sizes of PNPs fabricated with varying membrane protein to PLGA weight ratios measured both immediately after synthesis in deionized water and after adjusting to 1 × PBS buffer solution (n = 3; mean ± SD).

To investigate the binding capability of PNPs to anti-platelet antibodies, 10 μg (polymer weight) of PNPs were incubated with different amounts of fluorescently labeled polyclonal anti-platelet antibodies ranging from 2 μg to 128 μg (Figure 4.3A). Quantification based on the fluorescent signal showed a linear increase in antibody binding at lower concentrations, after which the binding plateaued. From the plotted data, it was interpolated that 50% binding occurred at a polyclonal antibody input of approximately 25 μg. The experiment was also repeated keeping the amount of antibody constant while varying the PNP concentration. To assess the specificity of the PNP-antibody interaction, binding was compared to a control polyethylene glycol-functionalized lipid-polymer hybrid nanoparticle (PEG-NP) [25] (Figure 4.3B). Using an equivalent amount of either PNPs or PEG-NPs, it was demonstrated that, comparatively, the PEGylated nanoparticles exhibited the near absence of antibody binding. The different results observed between the two types of nanoparticles indicate that the platelet membrane bestows specific binding properties. Additionally, an isotype antibody not specific to platelet membrane also showed no binding to the PNPs. Furthermore, to evaluate the effect of the presence of other proteins, the binding of antibody to PNPs was tested in the presence of mouse serum (Figure 4.3C). Compared with binding in PBS, there was little difference observed for the sample tested in serum, indicating the potential of the nanoparticles retain their function within the complex biological environment found *in vivo*.

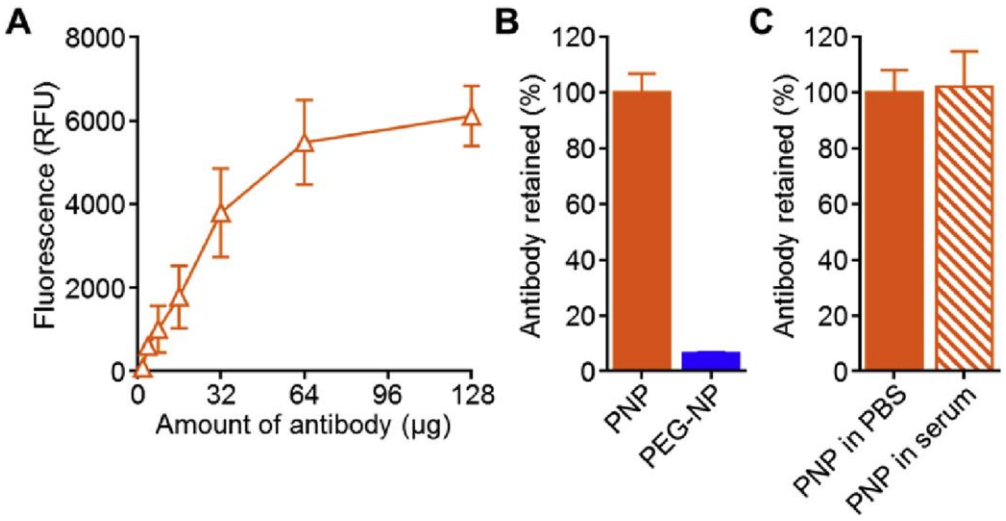

Figure 4.3: *In vitro* binding of anti-platelet antibodies to PNPs. (A) Fluorescent quantification of anti-platelet antibody binding to PNPs. A constant amount of PNPs (10 µg) was incubated with varying amounts of fluorescently labeled antibodies (n = 3; mean ± SEM). (B) Relative binding of anti-platelet antibodies to either PNPs or PEGylated nanoparticles (PEG-NPs) (n = 3; mean ± SD). (C) Relative binding of anti-platelet antibodies to PNPs in either PBS or mouse serum (n = 3; mean ± SD).

To characterize the ability of PNPs to neutralize anti-platelet antibodies *in vitro*, different amounts of PNPs ranging from 0 to 100 µg were pre-incubated with a constant amount of fluorescently labeled anti-platelet antibodies. This was followed by the addition of fresh platelets to the mixture and analysis of antibody binding to the platelets by flow cytometry (Figure 4.4A and B). It was shown that fluorescent signal sharply decreased with increasing amount of PNPs. Using 20 µg of polyclonal anti-platelet antibodies, it was observed that approximately 5–10 µg of PNPs were able to reduce mean fluorescence intensity by 50%, a ratio that was in line with what was observed from the antibody binding study. To evaluate the neutralization capacity in a competitive setting, both PNPs and fresh platelets were simultaneously incubated with the antibodies (Figure 4.4C

and D). In this scenario, mean fluorescence intensity was halved at approximately 20 μg of PNPs using 20 μg of antibodies. The antibody signal on the platelets decreased slower with increasing PNP concentration compared with the pre-incubation scenario, reflecting the increased challenge in neutralizing antibodies when both nanoparticle and fresh platelets compete for binding at the same time. Despite this fact, a great deal of neutralization capacity was still observed, indicating strong potential for therapeutic use.

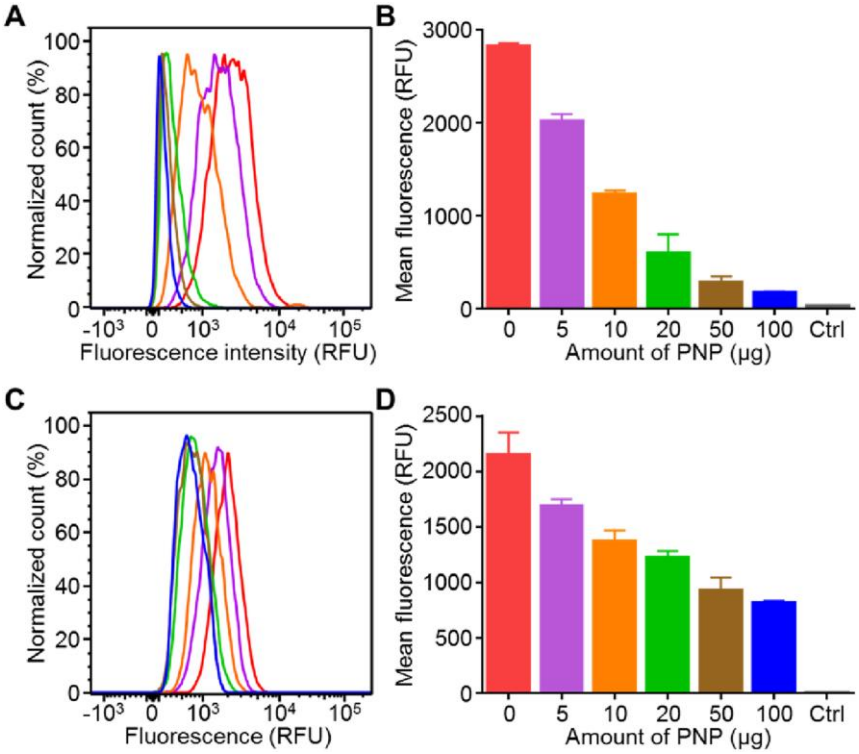

Figure 4.4: *In vitro* neutralization of anti-platelet antibodies by PNPs. (A) Representative flow cytometry histograms of platelets labeled with fluorescent anti-platelet antibodies pre-incubated with varying amounts of PNPs (from left to right: 100, 50, 20, 10, 5, and 0 μg). (B) Mean fluorescence intensity of the samples in (A) (n = 3, mean ± SD). Ctrl = no antibody. (C) Representative flow cytometry histograms of platelets labeled with fluorescent anti-platelet antibodies while concurrently incubated with varying amounts of PNPs (from left to right: 100, 50, 20, 10, 5, and 0 μg). (D) Mean fluorescence intensity of the samples in (C) (n = 3, mean ± SD). Ctrl = no antibody.

After confirming that PNPs could neutralize anti-platelet antibodies *in vitro*, their binding stability *in vivo* was assessed (Figure 4.5). To conduct the experiment, a previously established murine model of immune thrombocytopenia was employed [26]. When anti-platelet antibodies alone were administered intraperitoneally, their diffusion across the peritoneal membrane induced very obvious thrombocytopenia. Platelet counts dropped dramatically even 4 h post-injection and the challenged mice exhibited a more than 90% reduction in platelet counts 24 h post-injection. When the antibodies were pre-incubated with PNPs, followed by injection of the mixture, platelet counts were preserved to levels not statistically different from those of mice administered with only blank solution. The results suggest a strong binding interaction of the anti-platelet antibodies with the PNPs, which prevents the release of the pathological antibodies and thereby preventing their ability to cause the clearance of healthy platelets. The ability of the PNPs to maintain antibody neutralization within the complex *in vivo* biological environment was encouraging and motivated further study on the ability of the nanoparticles to perform this function *in situ* in a therapeutic setting.

Finally, the ability of PNPs to be used as a means for the therapeutic treatment of immune thrombocytopenia *in vivo* was assessed. Mice were first intraperitoneally administered a bolus dose of anti-platelet antibodies capable of causing a marked reduction of platelet counts. This was followed by intravenous administration of either blank solution, PEG-NPs, or PNPs. Blood was sampled both before and 24 h after challenge with anti-platelet antibodies, and platelet count

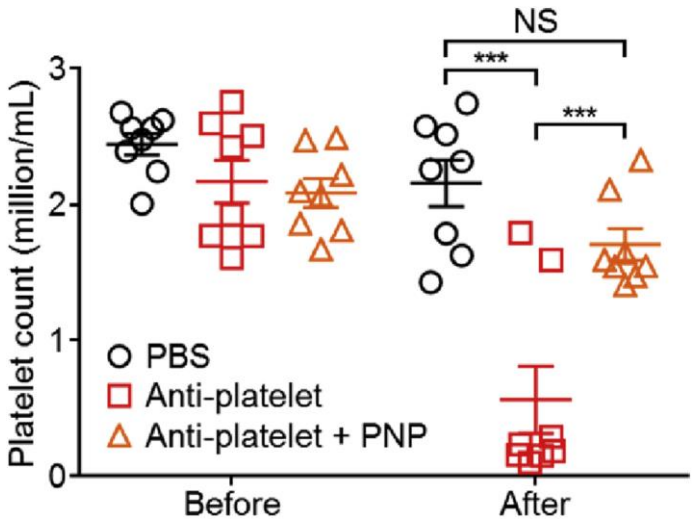

Figure 4.5: *In vivo* neutralization of anti-platelet antibody activity by PNPs. Mice were intraperitoneally administered with PBS, anti-platelet antibodies, or the antibodies pre-incubated with PNPs (n = 8; mean ± SEM). Blood was collected both before and 24 h after administration to quantify platelet counts. ***P < 0.001, NS = not significant, Student's t-test.

was determined (Figure 4.6A). Without any treatment, platelet counts dropped dramatically after 24 h and were approximately 10% of their original value. A similar drop was seen when mice were treated with PEG-NPs, which could not bind the antibodies and were unable to rescue platelet counts. In contrast, those mice treated with PNPs exhibited a marked increase in preservation of platelet number with final values at approximately 70% of pre-challenge values.

In order to demonstrate the importance of this platelet preservation on maintenance of hemostatic capacity, a bleeding time test, which is a commonly used *in vivo* assay for evaluating platelet function, was carried out (Figure 4.6B). After tail tip excision and immediate immersion into a warmed saline solution, the amount of time to bleeding cessation was recorded. For unchallenged mice, the

bleeding stopped on average between 1 and 2 min after excision, whereas those of anti-platelet antibody-challenged mice with no treatment exhibited increased bleeding times of at least 5 min; more than half of the untreated mice bled longer than a predetermined threshold of 20 min. The same level of bleeding was seen for those mice treated with PEG-NPs, whereas those treated with PNPs had bleeding times that were consistent with the unchallenged group. The results of the bleeding time assay correlate with the post-challenge platelet counts for each group and demonstrate that the amount of platelets retained in PNP-treated mice is sufficient to retain full hemostatic capabilities. This is in line with previous research that platelet counts need to decrease below a certain threshold in order to translate to increased bleeding times [27]. The treatment efficacy results here confirm the ability of PNPs to bind and neutralize pathological antibodies in circulation, thus preserving the function of healthy platelets.

ITP is a hematological disorder characterized by a decreased number of circulating platelets, which generally manifests as an increased tendency to bleed as well as susceptibility to bruising. While this can generally affect quality of life, severe cases can have serious consequences, such as the induction of intracranial hemorrhaging that carries with it a high mortality rate [28, 29]. The thrombocytopenic condition is very often acute and, in most cases, patients spontaneously recover platelet levels within a short period time without any specific treatment [30]. However, a small proportion may develop chronic ITP, which usually occurs in adults and is characterized by persistence of significantly low

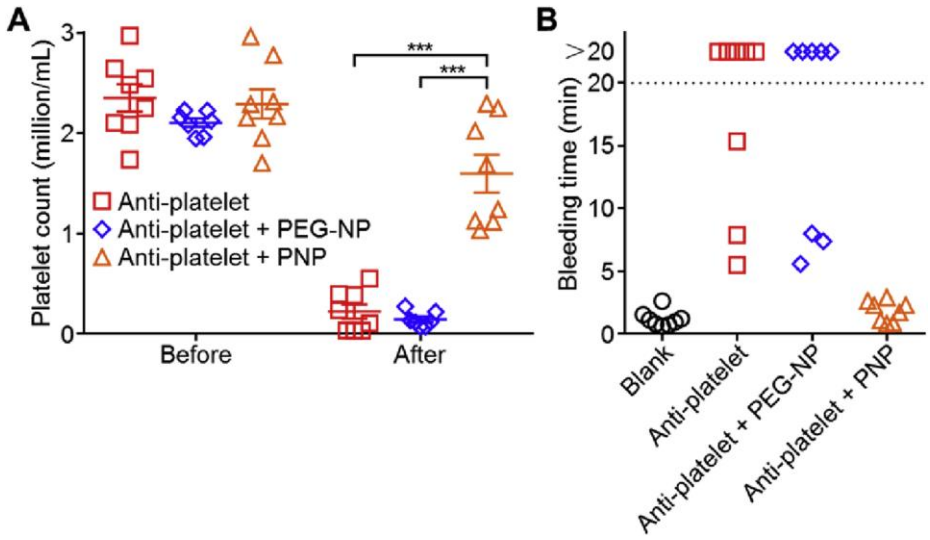

Figure 4.6: *In vivo* treatment of antibody-induced thrombocytopenia by PNPs. Mice were intraperitoneally administered with anti-platelet antibodies, followed 15 min later by intravenous injections of either blank solution, PNPs, or PEG-NPs via the tail vein. (A) Blood was collected both before and 24 h after administration to quantify platelet counts (n = 8; mean ± SEM). (B) Bleeding time from the tail vein into PBS. An upper time limit of 20 min was established prior to initiation of the study. ***P < 0.001, Student's t-test.

platelet counts for longer than 6–12 months. Unfortunately for patients suffering from chronic ITP, the disease commonly occurs in response to an unknown stimulus [31], making effective treatment a difficult task for clinicians. Drugs that either modulate or distract the immune system are generally employed, including the use of corticosteroids or IVIg as frontline therapies [32]. Splenectomy is the approach often taken after failure of initial treatment and can lead to the restoration of the platelet counts to a normal level by removing the organ responsible for both clearance of opsonized platelets and pathological antibody production [33]. The procedure, however, can be associated with infection, bleeding, hospitalization, and vascular complications [11, 12]. Moreover, a splenectomy is irreversible and can likely lead to long-term impairment of hematologic and immunological functions

[12, 34]. Other secondary or tertiary treatment options exist, including use of cytotoxic drugs, platelet transfusions, and thrombopoietin receptor agonists among others. To our knowledge, none of the current available therapies directly address the pathological moieties that contribute directly to the clearance of healthy platelets from circulation.

To create a platform capable of specific autoantibody depletion for the treatment of ITP, platelet membrane was directly employed in order to fabricate nanoparticles that mimic the surface properties of the original cell [17, 22]. One major advantage of this approach is that the nanoparticle surface serves as a natural substrate for autoantibodies against endogenous cellular targets [35]. Further, the nanoparticles present the relevant epitopic targets recognized by the antibodies without the need to identify antigen specificity, which can vary among patients [36]. Cell membrane-coated nanoparticles have previously demonstrated favorable safety profiles *in vivo* as well as lack of both acute and chronic anti-nanoparticle immune responses [19, 37]. Another advantage of the nanoparticulate platform is that storage after lyophilization is common practice [24], significantly extending shelf-life compared with whole platelets, which need to be carefully processed and expire within a week after collection [38].

In the present study, i*n vitro* binding of PNPs to anti-platelet antibodies was demonstrated to be both stable and specific. According to the information obtained from Figure 4.3A, the apparent weight binding ratio between PNPs and the anti-thrombocyte antibody was approximately 1:5. However, the antibody preparation

that we employed was polyclonal, and only about 15% of the antibody was actually specific to platelet membrane. Based on the information from these two pieces of data, we calculated that one PNP could sequester around 280 platelet membrane specific anti-thrombocyte antibodies. Pre-incubation and binding of antibodies to the nanoparticles appeared to preclude further interaction with platelets, a result that was confirmed *in vivo*. Impressively, the PNPs performed well in a competitive setting. As shown in Figures 4.4 C and D, 20 μg of PNPs, which contain 20 μg of platelet membrane material, was able to reduce binding of antibodies to platelets by half, despite the fact that they were in the presence of 40 μg worth of membrane material from the native platelets. This suggests that nanoparticulate membrane may have an inherent advantage in binding that can be exploited for other biodetoxification applications. Administration of PNPs in a therapeutic scenario demonstrated considerable efficacy, and a bleeding time assay was used to highlight the importance of preserving platelet counts. Compared with a 93% drop in platelet count for the PEG-NP treatment group, PNPs preserved 70% of the platelets, presumably due to their ability to bind the pathological antibodies and remove them from circulation. The results are not likely due to any thrombotic effect from the PNPs, as it has been demonstrated that the particles are absent most intracellular activating factors. Given the relative scarcity of platelets in the blood, it should be feasible to administer enough nanoparticles to significantly outnumber healthy circulating platelets. While the long-term consequences of administering cell membrane-derived antigenic material in a nanoparticulate format have yet to

be fully explored, it should be noted that platelet transfusion is a well-established clinical procedure; it can be reasonably expected that administration of membrane material only should be less burdensome given the lack of the biologically active components present in the intracellular compartment of intact platelets.

4.4 Conclusion

In conclusion, we have successfully demonstrated the application of PNPs towards the treatment of ITP. The nanoparticles showed the ability to specifically bind anti-platelet autoantibodies, which are directly responsible for reducing platelet counts. Upon binding, it was demonstrated that the interaction between the PNPs and the antibodies was strong, effectively neutralizing biological activity *in vivo*. In an antibody-induced thrombocytopenia animal model, mice treated with PNPs after challenge with antibodies were able to retain their platelet counts. Further, in a bleeding time assay, mice treated with PNPs exhibited normal hemostasis via effective clot formation, and average values were nearly identical to unchallenged controls. On the other hand, untreated mice or those administered with control nanoparticles bled excessively due to lowered platelets counts and impaired hemostasis capacity. The ability to specifically neutralize anti-platelet antibodies in ITP presents a new option in the current landscape of treatment for the disease. Currently, most therapies are non-specific and can significantly impair broad immune function. By targeting the pathological antibodies directly, it may be

possible to treat the disease while leaving the immunity intact, giving patients an increased opportunity for natural recovery of platelet counts without damaging and irreversible interventions. Alternatively, PNPs may also be used as an adjuvant therapy to either synergize with current treatments or enable a decrease in drug dosages to help limit unwanted side effects. Ultimately, PNPs represent a promising platform for the treatment of ITP and further study towards translation is warranted.

Chapter 4, in full, is a reprint of the material as it appears in *Biomaterials*, 2016, Xiaoli Wei, Jie Gao, Ronnie Fang, Brian Luk, Ashley Kroll, Diana Dehaini, Jiarong Zhou, Hyeon Woo Kim, Weiwei Gao, Weiyue Lu and Liangfang Zhang. The dissertation author was a major contributor and co-author of these papers.

4.5 References

1. Jurk, K., *Analysis of platelet function and dysfunction.* Hamostaseologie, 2015. **35**(1): p. 60-72.

2. Berger, S., *Platelet function: a review. I. Normal function.* Can Med Assoc J, 1970. **102**(12): p. 1271-4.

3. Psaila, B., A. Petrovic, L.K. Page, J. Menell, M. Schonholz, and J.B. Bussel, *Intracranial hemorrhage (ICH) in children with immune thrombocytopenia (ITP): study of 40 cases.* Blood, 2009. **114**(23): p. 4777-83.

4. Rodeghiero, F., R. Stasi, T. Gernsheimer, M. Michel, D. Provan, D.M. Arnold, J.B. Bussel, D.B. Cines, B.H. Chong, N. Cooper, B. Godeau, K. Lechner, M.G. Mazzucconi, R. McMillan, M.A. Sanz, P. Imbach, V. Blanchette, T. Kuhne, M. Ruggeri, and J.N. George, *Standardization of terminology, definitions and outcome criteria in immune thrombocytopenic purpura of adults and children: report from an international working group.* Blood, 2009. **113**(11): p. 2386-93.

5. Provan, D., R. Stasi, A.C. Newland, V.S. Blanchette, P. Bolton-Maggs, J.B. Bussel, B.H. Chong, D.B. Cines, T.B. Gernsheimer, B. Godeau, J. Grainger, I. Greer, B.J. Hunt, P.A. Imbach, G. Lyons, R. McMillan, F. Rodeghiero, M.A. Sanz, M. Tarantino, S. Watson, J. Young, and D.J. Kuter, *International consensus report on the investigation and management of primary immune thrombocytopenia.* Blood, 2010. **115**(2): p. 168-86.

6. Segal, J.B. and N.R. Powe, *Prevalence of immune thrombocytopenia: analyses of administrative data.* J Thromb Haemost, 2006. **4**(11): p. 2377-83.

7. Coopamah, M.D., M.B. Garvey, J. Freedman, and J.W. Semple, *Cellular immune mechanisms in autoimmune thrombocytopenic purpura: An update.* Transfus Med Rev, 2003. **17**(1): p. 69-80.

8. Gernsheimer, T., *Chronic idiopathic thrombocytopenic purpura: mechanisms of pathogenesis.* Oncologist, 2009. **14**(1): p. 12-21.

9. Thota, S., G. Kistangari, H. Daw, and T. Spiro, *Immune thrombocytopenia in adults: an update.* Cleve Clin J Med, 2012. **79**(9): p. 641-50.

10. Karpatkin, S., *Autoimmune thrombocytopenic purpura.* Blood, 1980. **56**(3): p. 329-43.

11. Kojouri, K., S.K. Vesely, D.R. Terrell, and J.N. George, *Splenectomy for adult patients with idiopathic thrombocytopenic purpura: a systematic review to assess long-term platelet count responses, prediction of response, and surgical complications.* Blood, 2004. **104**(9): p. 2623-34.

12. Ghanima, W., B. Godeau, D.B. Cines, and J.B. Bussel, *How I treat immune thrombocytopenia: the choice between splenectomy or a medical therapy as a second-line treatment.* Blood, 2012. **120**(5): p. 960-969.

13. Rowbotham, B. and R.L. Brearley, *High-dose intravenous IgG in adults with autoimmune thrombocytopenia.* Lancet, 1983. **1**(8321): p. 410.

14. Cardo, L.J., M. Strack, and J. Williams, *Anti-D for the Treatment of Splenectomized Patients with Immune Thrombocytopenic Purpura.* Blood, 1991. **78**(10): p. 2786-2787.

15. Cooper, N., R. Stasi, S.S. Cunningham-Rundles, M.A. Feuerstein, J.P. Leonard, S. Amadori, and J.B. Bussel, *The efficacy and safety of B-cell depletion with anti-CD20 monoclonal antibody in adults with chronic immune thrombocytopenic purpura.* British Journal of Haematology, 2004. **125**(2): p. 232-239.

16. Bussel, J.B., D.J. Kuter, J.N. George, R. McMillan, L.M. Aledort, G.T. Conklin, A.E. Lichtin, R.M. Lyons, J. Nieva, J.S. Wasser, I. Wiznitzer, R. Kelly, C.F. Chen, and J.L. Nichol, *AMG 531, a thrombopoiesis-stimulating protein, for chronic ITP.* New England Journal of Medicine, 2006. **355**(16): p. 1672-1681.

17. Hu, C.M.J., L. Zhang, S. Aryal, C. Cheung, R.H. Fang, and L.F. Zhang, *Erythrocyte membrane-camouflaged polymeric nanoparticles as a biomimetic delivery platform.* Proceedings of the National Academy of Sciences of the United States of America, 2011. **108**(27): p. 10980-10985.

18. Fang, R.H., C.M.J. Hu, B.T. Luk, W.W. Gao, J.A. Copp, Y.Y. Tai, D.E. O'Connor, and L.F. Zhang, *Cancer Cell Membrane-Coated Nanoparticles for Anticancer Vaccination and Drug Delivery.* Nano Letters, 2014. **14**(4): p. 2181-2188.

19. Hu, C.M.J., R.H. Fang, B.T. Luk, and L.F. Zhang, *Nanoparticle-detained toxins for safe and effective vaccination.* Nature Nanotechnology, 2013. **8**(12): p. 933-938.

20. Hu, C.M.J., R.H. Fang, J. Copp, B.T. Luk, and L.F. Zhang, *A biomimetic nanosponge that absorbs pore-forming toxins.* Nature Nanotechnology, 2013. **8**(5): p. 336-340.

21. Pang, Z.Q., C.M.J. Hu, R.H. Fang, B.T. Luk, W.W. Gao, F. Wang, E. Chuluun, P. Angsantikul, S. Thamphiwatana, W.Y. Lu, X.G. Jiang, and L.F. Zhang, *Detoxification of Organophosphate Poisoning Using Nanoparticle Bioscavengers.* Acs Nano, 2015. **9**(6): p. 6450-6458.

22. Hu, C.M.J., R.H. Fang, B.T. Luk, K.N.H. Chen, C. Carpenter, W.W. Gao, K. Zhang, and L.F. Zhang, *'Marker-of-self' functionalization of nanoscale particles through a top-down cellular membrane coating approach.* Nanoscale, 2013. **5**(7): p. 2664-2668.

23. Fang, R.H., B.T. Luk, C.M. Hu, and L. Zhang, *Engineered nanoparticles mimicking cell membranes for toxin neutralization.* Adv. Drug Deliv. Rev., 2015. **90**: p. 69-80.

24. Hu, C.M.J., R.H. Fang, K.C. Wang, B.T. Luk, S. Thamphiwatana, D. Dehaini, P. Nguyen, P. Angsantikul, C.H. Wen, A.V. Kroll, C. Carpenter, M. Ramesh, V. Qu, S.H. Patel, J. Zhu, W. Shi, F.M. Hofman, T.C. Chen, W.W. Gao, K. Zhang, S. Chien, and L.F. Zhang, *Nanoparticle biointerfacing by platelet membrane cloaking.* Nature, 2015. **526**(7571): p. 118-+.

25. Fang, R.H., S. Aryal, C.M.J. Hu, and L.F. Zhang, *Quick Synthesis of Lipid-Polymer Hybrid Nanoparticles with Low Polydispersity Using a Single-Step Sonication Method.* Langmuir, 2010. **26**(22): p. 16958-16962.

26. Alves-Rosa, F., C. Stanganelli, J. Cabrera, N. van Rooijen, M.S. Palermo, and M.A. Isturiz, *Treatment with liposome-encapsulated clodronate as a new strategic approach in the management of immune thrombocytopenic purpura in a mouse model.* Blood, 2000. **96**(8): p. 2834-2840.

27. Morowski, M., T. Vogtle, P. Kraft, C. Kleinschnitz, G. Stoll, and B. Nieswandt, *Only severe thrombocytopenia results in bleeding and defective thrombus formation in mice.* Blood, 2013. **121**(24): p. 4938-4947.

28. Butros, L.J. and J.B. Bussel, *Intracranial hemorrhage in immune thrombocytopenic purpura: A retrospective analysis.* Journal of Pediatric Hematology Oncology, 2003. **25**(8): p. 660-664.

29. Fogarty, P.F. and J.B. Segal, *The epidemiology of immune thrombocytopenic purpura.* Current Opinion in Hematology, 2007. **14**(5): p. 515-519.

30. George, J.N., S.H. Woolf, G.E. Raskob, J.S. Wasser, L.M. Aledort, P.J. Ballem, V.S. Blanchette, J.B. Bussel, D.B. Cines, J.G. Kelton, A.E. Lichtin, R. McMillan, J.A. Okerbloom, D.H. Regan, and I. Warrier, *Idiopathic*

thrombocytopenic purpura: A practice guideline developed by explicit methods for the American Society of Hematology. Blood, 1996. **88**(1): p. 3-40.

31. Cooper, N. and J. Bussel, *The pathogenesis of immune thrombocytopaenic purpura.* British Journal of Haematology, 2006. **133**(4): p. 364-374.

32. Pels, S.G., *Current Therapies in Primary Immune Thrombocytopenia.* Seminars in Thrombosis and Hemostasis, 2011. **37**(6): p. 621-630.

33. Mcmillan, R., R.L. Longmire, M. Tavassoli, S. Armstrong, and R. Yelenosky, *In-Vitro Platelet Phagocytosis by Splenic Leukocytes in Idiopathic Thrombocytopenic Purpura.* New England Journal of Medicine, 1974. **290**(5): p. 249-251.

34. Chadburn, A., *The spleen: Anatomy and anatomical function.* Seminars in Hematology, 2000. **37**(1): p. 13-21.

35. Copp, J.A., R.H. Fang, B.T. Luk, C.M.J. Hu, W.W. Gao, K. Zhang, and L.F. Zhang, *Clearance of pathological antibodies using biomimetic nanoparticles.* Proceedings of the National Academy of Sciences of the United States of America, 2014. **111**(37): p. 13481-13486.

36. He, R.Y., D.M. Reid, C.E. Jones, and N.R. Shulman, *Extracellular Epitopes of Platelet Glycoprotein Ib-Alpha Reactive with Serum Antibodies from Patients with Chronic Idiopathic Thrombocytopenic Purpura.* Blood, 1995. **86**(10): p. 3789-3796.

37. Luk, B.T., R.H. Fang, C.M.J. Hu, J.A. Copp, S. Thamphiwatana, D. Dehaini, W.W. Gao, K. Zhang, S.L. Li, and L.F. Zhang, *Safe and Immunocompatible Nanocarriers Cloaked in RBC Membranes for Drug Delivery to Treat Solid Tumors.* Theranostics, 2016. **6**(7): p. 1004-1011.

38. Kelsey, P., M.F. Murphy, M. Brown, P. Carrington, G. Hall, R.R. Jeffrey, S. Machin, C. Taylor, D. Thomas, F. Boulton, M. Bruce, H. Cohen, J. Duguid, S.M. Knowles, M.F. Murphy, G. Poole, L.M. Williamson, and B.T.T. Force, *Guidelines for the use of platelet transfusions.* British Journal of Haematology, 2003. **122**(1): p. 10-23.

Chapter 5

Conclusions

5.1 Cancer Cell Membrane-Coated Nanoparticles for Anticancer Vaccination

This chapter reported on the fabrication of a biomimetic, nanoparticulate anticancer vaccine that is capable of codelivering autologously derived tumor antigen material together with a highly immunostimulatory adjuvant. The nanovaccine was rationally designed to present the two major components, the tumor antigens and the adjuvant, in a way that enhances their ability to promote efficient antigen presentation and activation of downstream immune responses. The formulation takes advantage of the small size of nanoparticles for lymphatic drainage and uptake into antigen presenting cells, and the endosomal uptake route was complemented by choosing an adjuvant with an endosomal receptor. Further, the cancer cell membrane coating allows for the delivery of multiple tumor antigens to drive a multi-antigenic immune response as a strategy to overcome the tumor heterogeneity that is often responsible for partial treatment responses or recurrence. Ultimately, it is demonstrated that the nanovaccine can elicit potent antitumor immune responses *in vivo*, including dendritic cell maturation and T cell expansion. When combined with additional immunotherapies such as checkpoint blockades, the formulation demonstrates substantial therapeutic effect. Overall, the work exemplifies using nano-immunoengineering to create a novel anticancer vaccine that can later be extrapolated for the development of personalized, autologous anticancer vaccines with broad applicability.

5.2 Development of Red Blood Cell Membrane-Coated Nanoparticles as "Nanotoxoid" Antivirulence Vaccines

Red blood cell membrane-coated nanoparticles (RBCNP or "nanotoxoid") have great potential as a nanotoxoid vaccine by improving the deactivation and delivery of pore forming toxins for effective antivirulence immune responses. By mimicking the surface of red blood cells, the RBCNP serves as a decoy to absorb pore-forming toxins that are commonly secreted by pathogenic bacteria as a mechanism to cause cellular damage and increase virulence. Within the nanotoxoid formulation, the toxins are detained to reduce damage to the host while also being presented to the immune system in an undenatured form as antigens

In the chapter's first example, the efficacy of a biomimetic nanoparticle-based antivirulence vaccine is examined in a mouse model of methicillin-resistant *Staphylococcus aureus* (MRSA) skin infection. Vaccination with nanoparticle-detained staphylococcal α-hemolysin (Hla) caused strong *in vivo* immune responses including germinal center formation and high anti-Hla serum titers. This immune response provided protection against MRSA skin infection through both reduced lesion size and reduced bacterial load.

This concept was then extended in the second example of the chapter by using MRSA supernatant, which contains a multitude of pore-forming toxins, to make the nanotoxoid (nanotoxoid(hSP)). Using this *in situ* strategy, a multiantigenic nanotoxoid was made to improve vaccine potency by introducing a breadth of antigenic targets for more complete immunity formation. Compared to

a traditional anti-toxin vaccination consisting of heat-denatured MRSA supernatant, the nanotoxoid(hSP) caused the formation of higher anti-toxin titers for multiple different toxins. The improved immune response led to superior protection in both a MRSA skin infection model and an intravenous model. Importantly, no significant damage was caused by the nanotoxoid *in vitro* or *in vivo.* Overall, both examples show the utility of using the red blood cell membrane-coated nanoparticle for concurrent entrapment of toxins as the antigenic vaccine component in a manner that is both safe and highly immunogenic. Notably, this novel vaccination system is a way to combat bacteria without the use of antibiotics, which is important when antibiotic resistance is an increasing global concern.

5.3 Platelet Membrane-Coated Nanoparticles as "Nanosponges" for Autoantibody Clearance

In the fourth chapter, platelet membrane-coated nanoparticles are used as an immunomodulatory treatment for immune thrombocytopenia purpura (ITP). Pathological anti-platelet autoantibodies characteristic of ITP cause a reduction in platelet counts that can lead to uncontrolled bleeding which can be fatal. In the study, the use of platelet membrane-coated nanoparticles (PNPs) is explored as a therapy to specifically clear anti-platelet antibodies. The platelet membrane coating confers the nanoparticles with an outer surface displaying the full array of native platelet surface protein. In this way, it acts as a decoy to strongly bind the pathological antibodies that are specific to the platelet surface proteins. The ability of the nanoparticles to neutralize the autoantibody activity was shown both *in vitro* and *in vivo*. Ultimately, we leverage the antibody binding of PNPs to therapeutically treat a mouse model of antibody-induced thrombocytopenia. Treatment with the PNPs was efficacious in reducing antibody-mediated destruction of actual platelets, which allow for reduced bleeding in a bleeding time assay. The platelet membrane-coated nanoparticles exemplify a promising platform for specifically treating antibody-mediated immune thrombocytopenia by acting as a decoy for anti-platelet antibodies and preserving circulating platelets while leaving general immune functions intact. This platform can also potentially be expanded to address other autoimmune disorders that involve autoantibodies against specific host cells.